

**WATER HAMMER MODELING AND ANALYSIS FOR
KHOBAR-DAMMAM WATER TRANSMISSION RING LINE**

HUSSAIN TALEB AMMAR

CIVIL AND ENVIRONMENTAL ENGINEERING

MAY 2014

**WATER HAMMER MODELING AND ANALYSIS FOR
KHOBAR-DAMMAM WATER TRANSMISSION RING LINE**

BY
HUSSAIN TALEB AMMAR

A Thesis Presented to the
DEANSHIP OF GRADUATE STUDIES

KING FAHD UNIVERSITY OF PETROLEUM & MINERALS

DHAHRAN, SAUDI ARABIA

In Partial Fulfillment of the
Requirements for the Degree of

MASTER OF SCIENCE

In

CIVIL ENGINEERING

MAY, 2014


KING FAHD UNIVERSITY OF PETROLEUM & MINERALS

DHAHRAN- 31261, SAUDI ARABIA

DEANSHIP OF GRADUATE STUDIES

This thesis, written by HUSSAIN TALEB AMMAR under the direction his thesis advisor and approved by his thesis committee, has been presented and accepted by the Dean of Graduate Studies, in partial fulfillment of the requirements for the degree of **MASTER OF SCIENCE IN CIVIL ENGINEERING**.

19 MAY 2014



Dr. Nedal T. Ratrout
Department Chairman



Dr. Salam A. Zummo
Dean of Graduate Studies

22/5/14

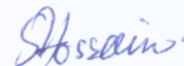
Date



Dr. Muhammed Al-Zahrani
(Advisor)



Dr. Mohammed S. Al-Suwaiyan
(Member)



Dr. Shakhawat Chowdhury
(Member)

© Hussain Taleb Ammar

2014

To My Parents, Wife, Brothers and Sister.

ACKNOWLEDGMENTS

In the name of Allah, the Most Merciful, the Most Compassionate

I would like to express my sincere appreciation and gratitude to the chairman of my thesis committee Dr. Muhammad Al-Zahrani for his valuable guidance, support and encouragement throughout this work. I highly acknowledge the encouragement and valuable suggestions from thesis committee members Dr. Shakhwat Choudhury and Dr. Mohammad Al-Suwian.

I am deeply grateful to the Civil and Environmental Engineering Department at King Fahd University of Petroleum & Minerals and Al Khobar branch of the General Directorate of Water in Eastern Region for providing the necessary support to conduct this study. Special thank goes to Eng. Faleh Al-Faleh, Eng. Mohammed Al-Abbad, and Eng. Suhail Al-Moamen for providing the necessary data for this research study and for facilitating the access to the KDRL facilities.

I would like to extend my thanks to Dr. Adel Abu-Jouda for his constructive suggestion with the hammer analysis and to Eng. Mohammed Hisham for his assistance with the surge protection analysis. My thanks also go to Mr. Adnan Al-Hajji and Dr. Amin Abo-Monaser for his support and valuable technical suggestions. I am also thankful to Eng. Khalid and Eng. Ashraf of Aramoon International Company, Eng. Abbas and Eng. Mohammed Hamza of the CWC for helping me with data collection.

A special gratitude and dedication of this work is due to my parents, my wife, brothers, sister, grandmothers, uncles and aunts for their support and encouragement throughout this period.

TABLE OF CONTENTS

ACKNOWLEDGMENTS	V
TABLE OF CONTENTS.....	VI
LIST OF TABLES.....	VIII
LIST OF FIGURES.....	IX
LIST OF ABBREVIATIONS.....	XI
ABSTRACT	XII
ARABIC ABSTRACT	XIV
CHAPTER 1 INTRODUCTION.....	1
1.1 Background	1
1.2 Problem Statement.....	4
1.3 Objectives of the Research.....	6
1.4 Research Methodology	8
CHAPTER 2 LITERATURE REVIEW	10
2.1 Introduction.....	10
2.2 Water Distribution System Hydraulics	11
2.3 Water Hammer Governing Equations.....	13
2.4 Modeling and Analysis of the Water System	16
2.5 Water Hammer Protections	17
2.6 Previous Researches	19
CHAPTER 3 KHOBAR-DAMMAM WATER RING LINE	23
3.1 Characteristics of KDRL	23
3.2 Flow and Pressure Measurements	35

CHAPTER 4 HYDRAULIC MODELING OF KDRL	42
4.1 Model Construction and Execution	42
4.2 Model Calibration	52
CHAPTER 5 WATER HAMMER MODELING & ANALYSIS	58
5.1 Background	58
5.2 Scenario 1: Power Failure and Pump Sudden Shutdown	64
5.3 Scenario 2: Sudden Closure of All Valves.....	69
5.3.1 Sudden Closure of KFUPM Valve	69
5.3.2 Sudden Closure of Doha3 Valve.....	71
5.3.3 Sudden Closure of All Valves	74
CHAPTER 6 WATER HAMMER CONTROL	76
6.1 Background	76
6.2 Isolating Branched Pipes from KDRL	76
6.3 Power Failure Protection	83
6.4 All Valves Sudden Closure Protection.....	86
CHAPTER 7 CONCLUSION AND RECOMMENDATIONS.....	89
REFERENCES.....	92
APPENDICES.....	95
Appendix A	96
Appendix B.....	100
Appendix C.....	103
Appendix D	113
VITAE	118

LIST OF TABLES

Table 1-1 Ground level variations along KDRL in meters from sea level	6
Table 2-1 Common surge protection devices	18
Table 3-1 KDRL summary of piping elements.....	27
Table 3-2 KDRL inventory	28
Table 3-3 Data for tanks/branches from KDRL	29
Table 3-4 Summary of flow meter readings at different locations along the KDRL	41
Table 4-1 Yarmouk-pump specifications.....	43
Table 4-2 KDRL operation controls	46
Table 4-3 List of metering device and their corresponding junction/pipe.....	48
Table 4-4 Common used Roughness Value	50
Table 4-5 Totalizing flow meter resulted from WaterGEMS calculations	52
Table 5-1 Physical pipe characteristics	63

LIST OF FIGURES

Figure 1-1 Schematic drawing showing KDRL.....	5
Figure 2-1 Wave characteristics in x-t plan to express the MOC [5]	15
Figure 3-1 Daily water supply from KDRL for the month of October, 2013.....	24
Figure 3-2 GIS map of the layout of KDRL	25
Figure 3-3 Ground elevation and locations of branched pipelines along the KDRL.....	26
Figure 3-4 Sample washout valve in KDRL.....	30
Figure 3-5 Sample air valves installed in KDRL.....	31
Figure 3-6 Sample branching connection in KDRL	32
Figure 3-7 Types of flow/pressure meters installed in KDRL.....	34
Figure 3-8 Installed flow/pressure meters on-site.....	34
Figure 3-9 Location of flow/pressure meter.	36
Figure 3-10 Flow and pressure readings at KFUPM collected on 1 st and 2 nd May13	38
Figure 3-11 Flow and pressure readings at Dana collected on 1 st and 2 nd May13.....	38
Figure 3-12 Flow and pressure readings at Khaleej collected on 1 st and 2 nd May13.....	38
Figure 3-13 Flow and pressure readings at Yarmouk from 18 th to 23 rd August13	39
Figure 3-14 Flow and pressure readings at KFUPM from 18 th to 23 rd August13	39
Figure 3-15 Flow and pressure readings at Doha-3 from 18 th to 23 rd August13	40
Figure 3-16 Flow and pressure readings at Dana from 18 th to 23 rd August13.....	40
Figure 4-1 KDRL schematic from WaterGEMS	44
Figure 4-2 Representation of Yarmouk tank station in the network.....	45
Figure 4-3 Details schematic of a branch from KDRL.....	47
Figure 4-4 HGL over KDRL (Steady-State Analysis).....	51
Figure 4-5 water level variation calculated over the period 28-30 Oct 2013	53
Figure 4-6 Pumped flow during 28-30 October 2013.....	53
Figure 4-7 Sub-model calibration correlation results	55
Figure 4-8 KDRL model calibration correlation results	55
Figure 4-9 Comparison of water level variation at Yarmouk tank	56
Figure 4-10 Comparison of the pumped flow	56
Figure 4-11 HGL at Yarmouk flow meter (28-30 Oct) based on the calibrated model....	57
Figure 5-1 Pressure/surge wave split from small to larger pipe	61

Figure 5-2 Pressure/surge wave split from large to smaller pipe, with a dead end	61
Figure 5-3 Pressure/surge wave movement and reflection through a pipe segments	62
Figure 5-4 Sample effects of water hammer	65
Figure 5-5 Surge wave effect along KDRL due to pump sudden shut down	67
Figure 5-6 Surge wave effect along KFUPM branch due to pump sudden shut down	67
Figure 5-7 Surge wave effect along Doha3 branch due to pump sudden shut down.....	68
Figure 5-8 Surge wave effect along Doha1 branch due to pump sudden shut down.....	68
Figure 5-9 Surge wave variation along KDRL due to sudden valve closure at KFUPM.	70
Figure 5-10 Surge wave variation along KFUPM due sudden valve closure at KFUPM	70
Figure 5-11 Surge wave variation at Doha3 due to sudden valve closure at KFUPM	71
Figure 5-12 Surge wave variation along KDRL due to sudden valve closure at Doha3 ..	72
Figure 5-13 Surge wave variation at KFUPM due to sudden valve closure at Doha3	72
Figure 5-14 Surge wave variation at Doah3 due to sudden valve closure at Doha3	73
Figure 5-15 Surge wave variation along DKRL due to sudden closure of all valves.....	74
Figure 5-16 Surge wave variation at KFUPM due to sudden closure of all valves.....	75
Figure 5-17 Surge wave variation at Doah3 due to sudden closure of all valves	75
Figure 6-1 Existing setup, tank valve and check valve in the upstream (case A).....	77
Figure 6-2 Proposed setup, tank valve upstream and check valve downstream (case B)	77
Figure 6-3 Proposed setup, tank valve and check valve downstream the pipe (case C).	77
Figure 6-4 Hammer analysis results comparison for cases A, B, and C– main pipeline..	79
Figure 6-5 Hammer analysis results comparison for cases A, B, and C – KFUPM	81
Figure 6-6 Water hammer analysis comparison for cases A, B, and C – Doha3.....	82
Figure 6-7 Surge protection using surge vessel – main pipeline	84
Figure 6-8 Surge protection using surge vessel – KFUPM	84
Figure 6-9 Surge protection using surge vessel – Doha3	85
Figure 6-10 Optimized protection at sudden closure of all pipes – main pipeline	88
Figure 6-11 Optimized protection considering sudden closure of all pipes – KFUPM ...	88

LIST OF ABBREVIATIONS

KDRL	:	Khobar-Dammam Ring Line
MOC	:	Method of Characteristics
WCM	:	Wave Characteristics Method
GIS	:	Geographic Information Systems
EPA	:	Environmental Protection Agency (USA)
DI	:	Ductile Iron Pipe
FRP	:	Fiber Reinforced Polymer Pipe
UPVC	:	Un-plasticized polyvinylchloride Pipe
CCP	:	Circular Concrete Pipe
PRV	:	Pressure Relief Valve – Surge Control
FCV	:	Flow Control Valve
P3	:	Pressure Sensor and Logger (continues logging)
FM	:	Flow Meter
HGL	:	Hydraulic Grade Line
WaterGEMS	:	Water Modeling Program with GIS capabilities (Bentley)

ABSTRACT

Full Name : HUSSAIN TALEB AMMAR
Thesis Title : Water Hammer Modeling and Analysis for Khobar-Dammam Water Transmission Ring Line
Major Field : Civil & Environmental Engineering - Water Resources and Environmental Engineering
Date of Degree : May 2014

Water hammer or hydraulic transient is a common problem in water distribution systems especially for water transmission pipelines. Hydraulic transient events in water distribution system can cause significant damage and disruption in the system, thus, it has been a subject of many research studies. One major pipeline that connects the water supply of two major cities (Khobar and Dammam) in the Eastern Province of Saudi Arabia is the Khobar-Dammam Ring Line (KDRL). This transmission line is vulnerable to a potential water hammer problem as it is controlled by the water level in two main tanks at its both ends. In addition, six other sub tanks along the KDRL are expected to increase the probability of water hammer occurrences in the system.

In this research, two widely used hydraulic simulation models were adapted to model and analyze the hydraulic and transient (water hammer) behavior in the KDRL. The two hydraulic programs were WaterGEMS and HAMMER. The WaterGEMS was used to simulate the hydraulics of the transmission pipeline under normal conditions, while the

HAMMER was used to analyze the occurrence of the water hammer and simulate different water hammer protection scenarios.

Based on the analysis, several water hammer protection devices were tested and approved to provide a complete protection against the water hammer for the system. Moreover, appropriate operational control measures were proposed to be adopted by the Water Authority to minimize the probability of water hammer occurrence and to protect the KDRL from the water hammer.

ملخص الرسالة

الاسم الكامل: حسين طالب أحمد بن عمار

عنوان الرسالة: النمذجة والتحليل لمطرقة المياه للخط الحلقي الناقل للمياه بين مدينتي الدمام والخبر.

التخصص: الهندسة المدنية و البيئة - هندسة مصادر المياه و البيئة

تاريخ الدرجة العلمية: مايو 2014

تعتبر مطرقة المياه أحد المشاكل الشائعة في أنظمة توزيع المياه وبالأخص في الخطوط الناقلة. لذلك كان هذا الموضوع محل إهتمام الباحثين. إن عملية التشغيل للخط الحلقي الناقل للمياه بين مدينتي الدمام و الخبر تعتمد على مستوى المياه بخزان اليرموك في الخبر و خزان 55 في الدمام بالإضافة إلى الخزانات المتصلة بالخط الحلقي الناقل و الواقعه على إمتداده، وهذا ما يجعل من عملية التشغيل معقدة مما يزيد من إحتمالية تعرض الخط الناقل للمطرقة المائيه بشكل متكرر.

في هذا البحث تم استخدام اثنين من نماذج المحاكاة الهيدروليكية واسعي الانتشار لنمذجة وتحليل مطرقة الماء في أنبوب الماء (KDRL). البرنامجان الهيدروليكيان المستخدمان هما WaterGEMS و HAMMER. وقد تم استخدام WaterGEMS للمحاكاة الهيدروليكية لخط أنابيب الماء في ظل ظروف طبيعية، في حين تم استخدام HAMMER لتحليل حدوث المطرقة المائية ومحاكاة حلول مختلفة لحماية أنبوب الماء عند حدوث المطرقة المائية. استنادا إلى التحليل، تم اختيار مجموعة من مختلف أجهزة الحماية والتي تم اختبارها وأثبتت التحاليل الهيدروليكية جدراتها في توفير الحماية الكاملة من المطرقة المائية للأنبوب . وعلاوة على ذلك، تم اقتراح تدابير مناسبة ليتم اعتمادها من قبل مصلحة المياه للتقليل من احتمال حدوث المطرقة المائية وحماية أنبوب نقل المياه KDRL من المطرقة المائية.

CHAPTER 1

INTRODUCTION

1.1 Background

Water Hammer, which is known as a water surge, is a pressure wave caused when there is a sudden change in flow or pressure condition at a point in the system, e.g. sudden valve closure. These waves propagate throughout the system causing change in pressure and flow, positive transient waves called up-surge while negative transient waves called down-surge.

Water hammer has been responsible for water distribution network component failure, pipeline breakage or collapse, loose at connections, and intrusion of dirty water into the water distribution system. Therefore, water hammer is considered to be a threat to the public in terms of cost, health and safety. Negative pressure in the system for example, represents a major risk of introducing unwanted and possibly hazardous species like bacteria into the water system. This will significantly affect water quality. Thus, the control of water hammer pressure in transmission pipelines is essential for economical and safe operation.

The following are some of the general causes of water hammer [1]:

- Pump startup/shutdown.
- Valve opening/closing.
- Rapid change in demand in certain location(s) (e.g. hydrant flushing).
- Change in transmission condition (e.g. pipe breakage).
- Pipe filling or draining (e.g. air release from pipe).
- Change in boundary condition (e.g. pressure change in tank).

One of following solutions can generally mitigate water hammer [1]:

- Altering piping system characteristics.
- Improvement of operational procedure and operational control conditions.
- Installation of surge protection system.

There has been significant research in the area to investigate and propose solutions to the water hammer phenomenon. The most widely accepted approximate equations to model the water hammer are:

- 1- Method of Characteristics (MOC).
- 2- Wave Characteristics Method (WCM).

A number of widely used computer codes based on MOC and WCM numerical solutions are currently available and have been successfully validated against field data and exact analytical solutions. However, water hammer analysis computer models can only be effective and reliable when used in conjunction with a properly constructed and well-calibrated hydraulic network model. System modeling can help to [2]:

- Have a better and easier representation of the real-world complexity of the system.
- Analyze more operational scenarios and test different alternative solutions.
- Save time and money and insure the data and model accuracy, which will provide better and more reliable decisions.

Once a model is constructed and validated, then it can be used as an assessment tool for future projects.

In order to validate the constructed hydraulic model, collected field data used to calibrate the constructed model to ensure that the model output match the filed data. Model calibration often reveals some of the hidden problems in the system that can easily solved and corrected, i.e. opening partially closed valves. Calibration can also help to identify bottleneck points in the system.

For the purpose of hydraulic modeling; especially for complex systems, a simplified representation of the hydraulic network usually used. A process called “Skeletonization” where selected pipes (main) chosen to represent original network while preserving the operational performance and integrity of the larger original system [2]. This a common practice in hydraulic modeling and analysis, but should be avoided in the water hammer analysis, as it would lead to wrong decisions, skelatel model is not capable of representing the origin model in case of hammer analysis, as the hammer analysis is strongly dependent on the system characteristics.

1.2 Problem Statement

In this research, the Dammam-Khobar Water Transmission Ring Line (KDRL) will be investigated for the water hammer problem. KDRL is an 18-kilometer water transmission pipeline with a diameter of 700 mm, connecting Yarmouk water tank in Khobar to tank-55 in Dammam. The pipeline was designed to operate for emergency conditions to ensure no water shortages will occur in any one of the two cities. Later, it was decided to use KDRL for delivering water directly to districts located along the pipeline. Currently, there are six additional sub tanks connected to the KDRL, and one direct connection to a sub network. Figure 1.1 shows a schematic drawing of the KDRL and all the sub tanks connected to it.

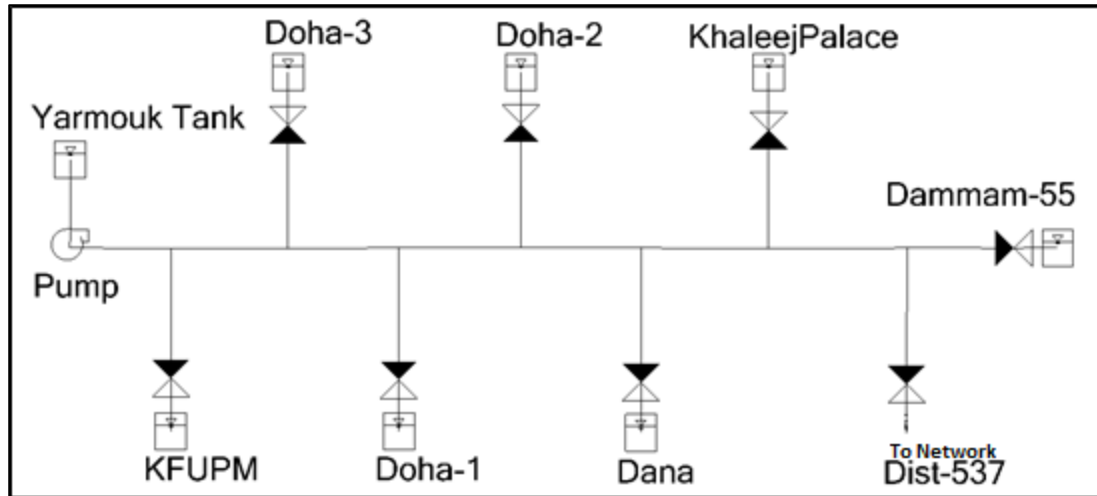


Figure 1-1 Schematic drawing showing KDRL

Dammam and Khobar are the two main cities in the eastern region of the Kingdom of Saudi Arabia with the highest population density in the region. Tank-55 is the only desalinated water source for Dammam city. This desalinated water is mixed with groundwater at blending stations before it is distributed to the city. On the other hand, Yarmouk Tank is the only desalinated water source for Khobar. Any failure in the KDRL will impact the desalinated water supply to districts along the KDRL, necessitating the use of backup raw water (groundwater) supply.

Moreover, the high-water pressure KDRL is laid along the highway with a high traffic density. Therefore, in case any sudden rupture occurs along the pipeline, then there will be a potential life-threatening incident to the highway users or to the people living close by. The layout of the pipeline and the water hydraulic regime create several high and low pressure points, which raise the risk of developing a water hammer phenomenon. Table 1.1

shows the ground level layout variations in the KDRL, which cause pressure variations along the pipeline which seriously impact and complicate the pipeline operation.

Table 1-1 Ground level variations along KDRL in meters from sea level

Start Level	Highest Level	Lowest Level	2nd High Level	End Level
29.5	52.5	26	51	33

KDRL is operated and controlled by the water levels of the eight different tanks along it. The water pressure along the pipeline is affected by the operation conditions of the valves (opening/closing) and the pumps (off/on), which could generate surge waves in the system. Therefore, it is recommended that the current daily KDRL operation be investigated to come up with an operational strategy that help controlling or minimizing the risk of water hammer.

1.3 Objectives of the Research

Water hammer causes a rapid change in the pressure that creates a wave of large magnitude fluctuating along the pipeline, affecting the network components. In addition, high pressure could exceed the safe operational pressure of the system causing pipe rupture. Even if a safe operating pressure is not exceeded, the fatigue load of cyclic surge pressure will reduce the life span of the system component. On the other hand, low pressure can lead to cavitation, column separation, and can cause pipe collapse or promote intrusion of

outside water, air, or contaminants. Also, water hammer can cause a hydraulic vibration of the pipeline at its connections and supports, causing leak or connections loose. Therefore, water hammer analysis is more important than the conventional steady-state analysis carried out by piping system designers, and it should be considered in the structural design of the pipeline. “It has been reported that any optimized design that fails to properly account for water hammer effects is likely to be, at best, suboptimal and, at worst, completely inadequate” [3].

The main objectives of this study are:

- (a) Construct a reliable water hydraulic model for the water transmission ring-line connecting Dammam and Khobar (KDRL) to simulate the existing operation.
- (b) Use the model to investigate the water hammer phenomenon in the KDRL and simulate the effect of different protections in order to assist the Water Authority to control or reduce the risk associated with water hammer.
- (c) Identify existing major factors effecting the KDRL operation as well as revealing problems in existing operational policy based on field observations.
- (d) Recommend proper control devices that can help resolving or minimizing the occurrence of water hammer along KDRL transmission line.

1.4 Research Methodology

To achieve the objectives of the study, several operational scenarios and approaches will be analyzed using WaterGEM and HAMEER simulation programs. First hydraulic simulation of KDRL will be conducted using WaterGEM followed by a water hammer analysis using HAMMER simulation model. Following are the procedures to achieve the goals of this study:

- Collection of data relevant to operational procedure and control conditions of the KDRL.
- Field Survey to collect data about KDRL component and pipeline profile.
- Installation of flow/pressure meters at both ends of the KDRL and all branches from the main pipeline to the sub tanks.
- Construction of GIS model of the KDRL to be exported to the Hydraulic Modeling Program WaterGEMS.
- Initial runs of the model to simulate the operational conditions.
- Model analysis for the steady-state and extended-period simulation using WterGEMS.
- Data collection from all metering points.
- Model calibration using real-field operational data, including readings collected at the metering points.
- Correction of all field problems as revealed by the calibration process.
- Simplification of the model for the water hammer analysis after a reliable hydraulic model is obtained.

- Investigation of the water hammer in the KDRL using HAMMER.
- Simulation of the protection mechanism using surge protection device or combination of devices. Table 2.1 lists major protection devices under consideration.
- Recommendations to improve the current operational procedure to minimize the probability of the occurrence of the water hammer in the KDRL.

CHAPTER 2

LITERATURE REVIEW

2.1 Introduction

Delivery of sufficient and safe water is essential for the community. However, water delivery through a large pipeline network is usually associated with different problems such as water hammer or hydraulic transient. Water hammer usually occurred when the flow is caused to suddenly stop or change direction, leading to a surge of propagating wave. Several actions during pipe network operation can generate water hammer phenomena such as a sudden valve closure or during a water pump startup/shutdown. This phenomenon can cause major problems such as noise/vibration, or pipe rupture/collapse. In addition, the water transient flow during a water hammer event will have significant impact on the water quality and, therefore, health implications.

Water hammer has become one of the major research area in hydraulic studies due to its major impact on the process of water delivery. This chapter will cover the following:

- The basic fundamentals of water hydraulics.
- Causes of unsteady flow and the governing equations.
- Water hammer modeling programs adopted in this research.

- General mitigations and protections against water hammer.
- Previous studies.

2.2 Water Distribution System Hydraulics

Water distribution network consists of pipes connected to a water source such as a reservoir or a tank to transport water from a source to customers in the required quantity and within acceptable quality measures. The pipeline is equipped with valves, nodes or junctions, pumps, and other components like flow/pressure meters, and fittings. Analysis of water distribution involves the determination of nodal pressure (head) and pipe flow rates that satisfy the principles of mass and energy conservations. The mass conservation or continuity states that the algebraic sum of the flow rates in all the elements meeting at a junction, together with any external flows, is zero. The energy conservation, on the other hand, states that the algebraic sum of the headlosses in each element, combined with any head generated by pumps, around any closed loop formed by hydraulic components, is zero.

There are many alternative formulations for the system governing equations and techniques to solve these equations. The process of the water transmission within a close conduit is governed by the conservation of mass equation (Eq. 2.1), and the energy law presented (Eq. 2.2) [2, 4].

The general form of the continuity equation is as follows:

$$\sum Q_{IN} \Delta t = \sum Q_{OUT} \Delta t + \Delta V_s \quad (2.1)$$

Where,

Q_{IN} = Total flow into the node

Q_{OUT} = Total demand at the node

Z = Elevation

V_s = Change in storage volume

t = Change in time

The energy equation between any two points can be express as:

$$\frac{P_1}{\gamma} + Z_1 + \frac{V_1^2}{2g} + h_p = \frac{P_2}{\gamma} + Z_2 + \frac{V_2^2}{2g} + h_L \quad (2.2)$$

Where,

P = Pressure

γ = Specific weight

Z = Elevation

V = Velocity

h_p = Head gain

h_L = Combined head loss

The combined headloss in the above equation account for losses in the energy is due to friction and other minor losses such as at valves or fittings. Different equations are used to compute the friction losses in the water network distribution such as Hazen-William and Darcy-Weisbach.

2.3 Water Hammer Governing Equations

The general cause of the water hammer is a rapid change in the velocity of the fluid. Such event could occur if there is a sudden valve closure, pump startup/shutdown, or a sudden change in flow direction. This sudden change generates a pressure wave that propagates throughout the system at supersonic speed, causing a change in the flow and pressure.

The governing equations for the unsteady/transient flow (during the water hammer event) are derived from the basic laws of physics: the law of conservation of mass and the law of conservation of energy. The first law is presented as the continuity equation whereas the latter is presented as the momentum equation. Both equations are simplified to the case of one dimensional incompressible fluid flow, which matches the objective of this research study [1, 2, 5].

The simplified form of the Continuity Equation is as follows:

$$\frac{\partial H}{\partial t} + \frac{a^2}{g} \frac{\partial V}{\partial x} = 0 \quad (2.3)$$

Where

a = Pressure wave speed

V = Average velocity in the x direction

H = Hydraulic grade line (HGL)

The momentum equation, can be expressed as:

$$\frac{\partial V}{\partial t} + g \frac{\partial H}{\partial x} + \frac{f V |V|}{2D} = 0 \quad (2.4)$$

Where

a = Pressure wave speed

V = Average velocity in the direction of x

H = HGL

f = Darcy-Weisbach friction coefficient

D = Inside diameter of the pipe

The above equation is valid under the following assumptions:

- Fluid is homogeneous
- Fluid and pipe wall are linearly elastic
- Flow is one-dimensional
- Pipe flow is full
- Average velocity is used
- Viscous losses are similar to steady-state

The most widely used method, Method of Characteristics (MOC), solve these equations for the transient flow by transforming the two partial differential equations to a pair of equations to solve for H and V for every point and time step. Other available numerical solutions to express the behavior of the water hammer compute the change in head and velocity at the junctions, such as, at both ends of pipes or at valves.

Whereas, The MOC calculates the resulted change of head and velocity along the pipes.

The MOC is expressed mathematically as follows [5]:

$$\left. \begin{aligned} \frac{\partial V}{\partial t} + \frac{g}{a} \frac{\partial H}{\partial t} + \frac{f V |V|}{2D} &= 0 \\ \frac{\partial x}{\partial t} &= +a \end{aligned} \right\} \text{C+}$$

$$\left. \begin{aligned} \frac{\partial V}{\partial t} + \frac{g}{a} \frac{\partial H}{\partial t} + \frac{f V |V|}{2D} &= 0 \\ \frac{\partial x}{\partial t} &= -a \end{aligned} \right\} \text{C-}$$
(2.5)

The MOC cannot be solved analytically but can be expressed graphically as shown in

Figure 2.1. Detailed of the MOC can be found at (Larock et al, 2000) [5].

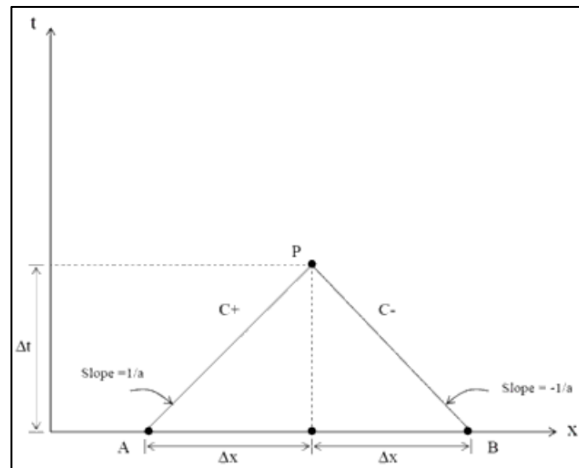


Figure 2-1 Wave characteristics in x-t plan to express the MOC [5]

2.4 Modeling and Analysis of the Water System

Modeling water hydraulics and transient problems to find practical solutions of the complex phenomenon has become easier with the availability of advanced modeling packages. The adopted programs: WaterGEMS and HAMMER in this research are product of Bentley Systems, Inc [2, 6, 7]. Both are widely trusted hydraulic simulation and analysis programs.

The WaterGEMS is a water network modeling and simulation program integrated with the Geographic Information System (GIS). The hydraulic computation and network solver used in the WaterGEMS is based on EPANET's computational engine [2, 7]. For complete and comprehensive engineering analysis, WaterGEMS is equipped with a different module such as the designer, optimized calibration, scheduler and skelebrator modules. In addition, Genetic Algorithm (GA) optimization engines are included in the program. These optimization engines were used in this study to perform calibration in order to minimize the difference between model output and collected field data. Both WaterGEMS and HAMMER programs contain all the commonly used water network components such as pipes, pumps, valves and tanks. The WaterGEMS is used for regular hydraulic analysis under normal operation and can be extended for emergency operations, e.g. hydrant flushing, while the HAMMER is specialized for transient analysis and simulation.

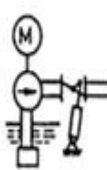

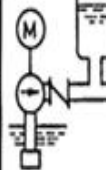
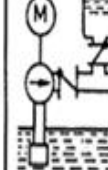

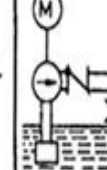

HAMMER was developed by collaboration between the Bentley's Haestad Methods Solution Center and Environmental Hydraulics Group (GENIVAR) of Toronto, Canada [7]. The hydraulic solver of the WaterGEMS is built-in the HAMMER to calculate the water system's initial steady-state condition, which will be elaborated in the water hammer analysis. The HAMMER program adopted an iterative procedure in conjunction with the MOC solver to advance the solution results of transient analysis. The HAMMER is equipped with several surge protection devices, including surge tank (open, spilling, one-way, orifice, variable area, differential), check valve, air valves, anticipator valve, and pressure relief valve, these are examples of available devices in the program. The HAMMER is also capable of simulating special transient events that include, for example, cavitation and column separation [7]. The HAMMER is a powerful decision support tool for hydraulic and environmental engineers.

2.5 Water Hammer Protections

The water system behavior during the water hammer transient flow, its major factors, and different protection methods has been extensively investigated in the literature. For a complete protection strategy, water hammer mitigation with improved operation, such as the enforcement of delayed valve closure, should be considered in the first place. Different protection devices are available to control and protect the piping system from undesired water hammer effect. Table 2.1 lists major protection devices under consideration in this research. As shown in the table, some surge devices

are designed to protect against up-surge, while others are used for down-surge protection. . The protection against water hammer will be discussed in more details in chapter six.

Table 2-1 Common surge protection devices [8]

Device	Controlled valve closure	Surge tank	Air chamber	One-way surge tank	Pressure relief valve	Bypass	Air valve
Schematic							
Principle of operation	Regulates discharge	Energy accumulator	Energy accumulator	Provides flow	Relieves pressure	Maintains flow, controls reverse flow	Air admission and release
Pipeline system/ effectiveness	Always useful	Very low head systems	Long pipelines, medium to high head systems	Long pipe with high points	High head systems	Low head systems, long suction line	Long pipelines with high points
Protection against	High pressures	High pressures and column separation	High pressures and column separation	Column separation	High pressures	Column separation	Column separation
Reliability	Moderate	Excellent	Good	Moderate	Poor	Poor	Poor
Frequency of application	Very often	Rarely	Very often	Rarely	Sometimes	Sometimes	Often
Cost	Low	High	Very high	Moderate	Moderate	Low	Low

2.6 Previous Researches

A reduced rate flow change, through a slower valve action is an effective and more economical satisfactory solution to many problems. The surge tank serves as a partial reflection point for the pressure waves, thereby protecting long tunnels from a short period pressure wave propagation. Air chambers and surge tanks are probably considered the safest and less long term cost solutions to the water hammer. Both could be used for the up-surge case as well as for the down-surge if placed properly and accordingly, while pressure relief valve is a common up-surge control device. Rapture disk is also an alternative to protect the system against up-surge but it causes a trouble when it needs replacement [9].

Thorley indicated the necessity of a check valve installation for water hammer protection using a surge tank. He also illustrates the sensitivity of the protection to valve response time [9].

With a proper design of the surge protection devices and enforcement of a proper operational procedures, water hammer will be generally controlled within allowable limits. Surge tanks are the recommended options, followed by other flow and pressure limiting devices, such as a pressure relief valve, check valves, and air valves [9].

Lohrasbi and Attarnejad [10] have developed a MOC-based computer solution for the water hammer effect that can be made public by numerically integrating the characteristic relations of the full equations. The program was called the “method of specified time intervals”.

The modeling and simulation of the water hammer phenomenon was investigated using GIS [11]. The authors compared the results with those from the MOC and the regression of the relationship between the dependent and independent variables from the lab experiments and concluded that using numerical MOC solution is more accurate. Also, the research pays attention to operational procedure suggesting that the slow valves closure should reduce the risk of system damage or failure due to hammering.

Anton and Arris [12] have studied the parameters affecting the shape and timing of the water hammer wave considering the unsteady friction, cavitation, and number of fluid-structure interaction (FSI). The authors used MOC for developing a mathematical model combining all three factors. The study concludes that cavitation, column separation, and FSI can cause hammer larger than classical water hammer theory.

The WCM (Wave Characteristics Method) modeling of water hammer was extended to model the water column separation in the water distribution networks [13].

The methodology was based on the physical concept that when a sub-atmospheric pressure is reached within the system, the vapor cavity forms and continue to grow while the sub-atmospheric pressure is maintained, and suddenly collapses at the instant the cavity volume is reduced to zero. This developed approach proved to be robust and straight-forward and producing results identical to those obtained from an Eulerian-based MOC implementation approach.

Dhandayudhapani et al. [14], contrasted the two popular transient modeling approaches: WCM and MOC by paying close attention to the computational efficiency and the numerical accuracy of the solutions. Although both methods solved the same governing equations using similar assumptions, they differed significantly in their approaches. The primary difference between both models was the way the pressure wave was tracked between the two boundaries of the pipeline segment. The MOC tracked a disturbance in the time–space grid using a numerical method based on characteristics whereas the WCM tracked the disturbance on the basis of wave-propagation mechanics. Compared with the WCM, the results indicated that the first- and the second-order MOC schemes needed a substantially greater number of segments within a pipeline for the same level of accuracy. The authors also explored the computational efforts for short, long pipelines, and a pipelines network associated with the first- and second-order MOC schemes and the WCM where the results highlighted the computational advantages of the WCM and the difference in computational effort could be several orders of magnitude, depending on the time step chosen.

The effect of the pipe slope on the water hammer was investigated and it was found that the slope of the water hydraulic grade line relative to the pipeline slope was an important factor controlling the formation of cavitation during the water hammer [15].

The water hammer protection of a water system considering two demand approaches: the pressure-sensitive demand and the nodal demand was investigated [16]. It was concluded that the nodal demand significantly overestimated the risk of the contaminant intrusion due to the down-surge pressure which lead to an increased protection cost but not necessarily provide better safety. The pressure-sensitive demand modeling is a must. This is because the nodal demand ignores the implicit relation between demand and pressure, does not account for the transient discharge dependency on the elevation at the point of demand, and exaggerates the surge wave leading to an overestimated negative pressure in the system. Therefore, WaterGEMS adopted a built-in pressure-dependent demand (PDD) model to effectively model the nodal demand as a function of pressure [17, 18].

Bong et al. [19], investigated water distribution model skeletonization for surge analysis. Study shows that unlike the steady-state analysis where the result obtained from a skeletonized model will have the same result as the complete system, surge analysis results are strongly affected by the level of skeletonization. Thus, surge analysis should only be performed on a detailed representative network model to determine, locate, and size the effective surge protection devices.

CHAPTER 3

KHOBAR-DAMMAM WATER RING LINE

3.1 Characteristics of KDRL

Khobar Dammam Ring Line (KDRL) is of great importance and a case sensitive water transmission pipeline for local water utility as it is the only source of desalinated water for five major communities namely:

- 1- KFUPM Campus
- 2- Doha District
- 3- Dana District
- 4- District No. 537
- 5- Khaleej Royal Palace

In addition, it is considered as a secondary or emergency water supply for the major water blending stations in Dammam.

The KDRL transmits approximately 40,000 m³ of desalinated water daily. Any failure in the system will deprive the five communities from the desalinated water supply and, therefore, they have to revert to raw groundwater supplies. Figure 3.1 shows the daily water supply of KDRL during the month of October, 2013.

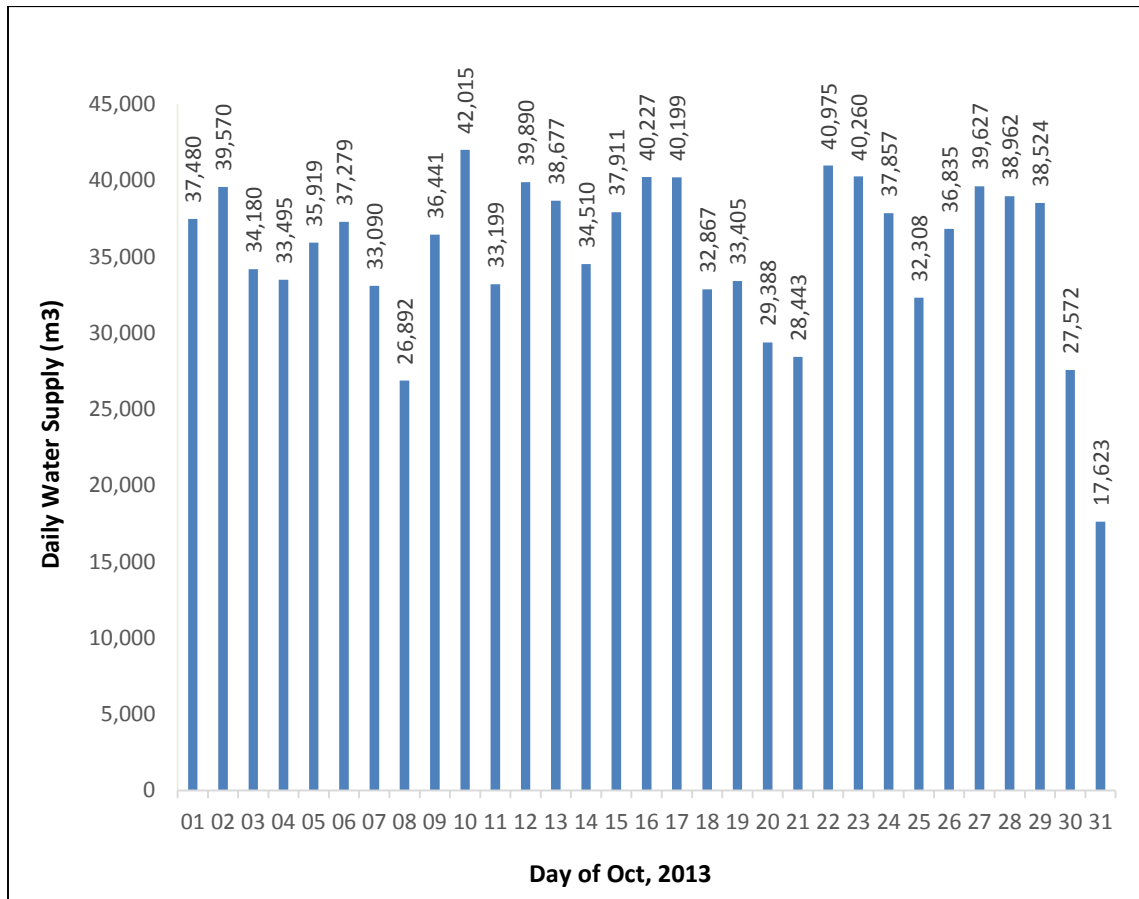


Figure 3-1 Daily water supply from KDRL for the month of October, 2013

The KDRL is running through a terrain of varying topographies, resulting in too many tops and bottoms at the pipeline. This makes the system's operation a challenging task to optimize. Figures 3.2 and 3.3 show the layout and the profile of KDRL, respectively. The figures highlight the branching point's stations, ground level, and the length of the branched pipeline from the station zero at Khobar pumping station.

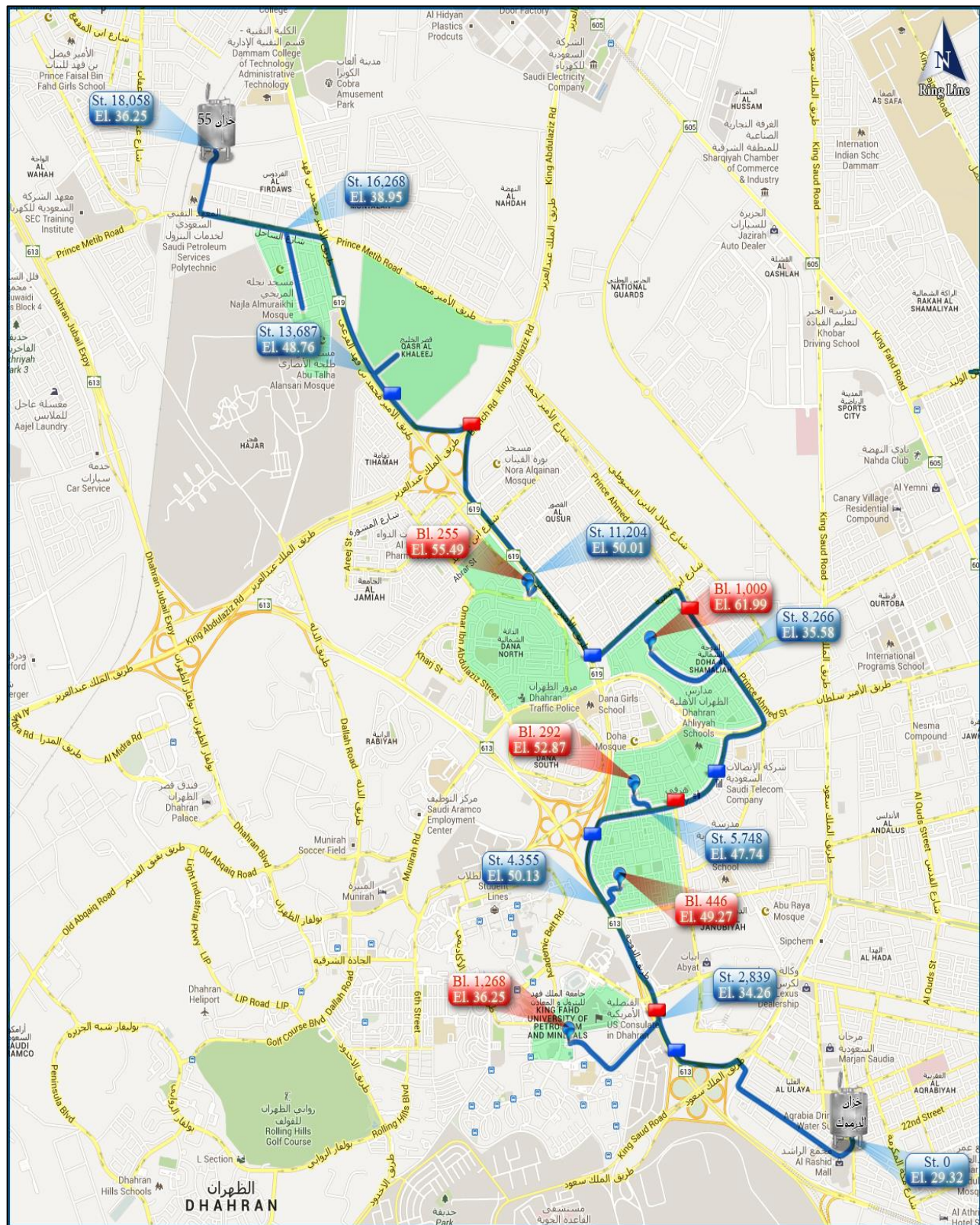


Figure 3-2 GIS map of the layout of KDRL

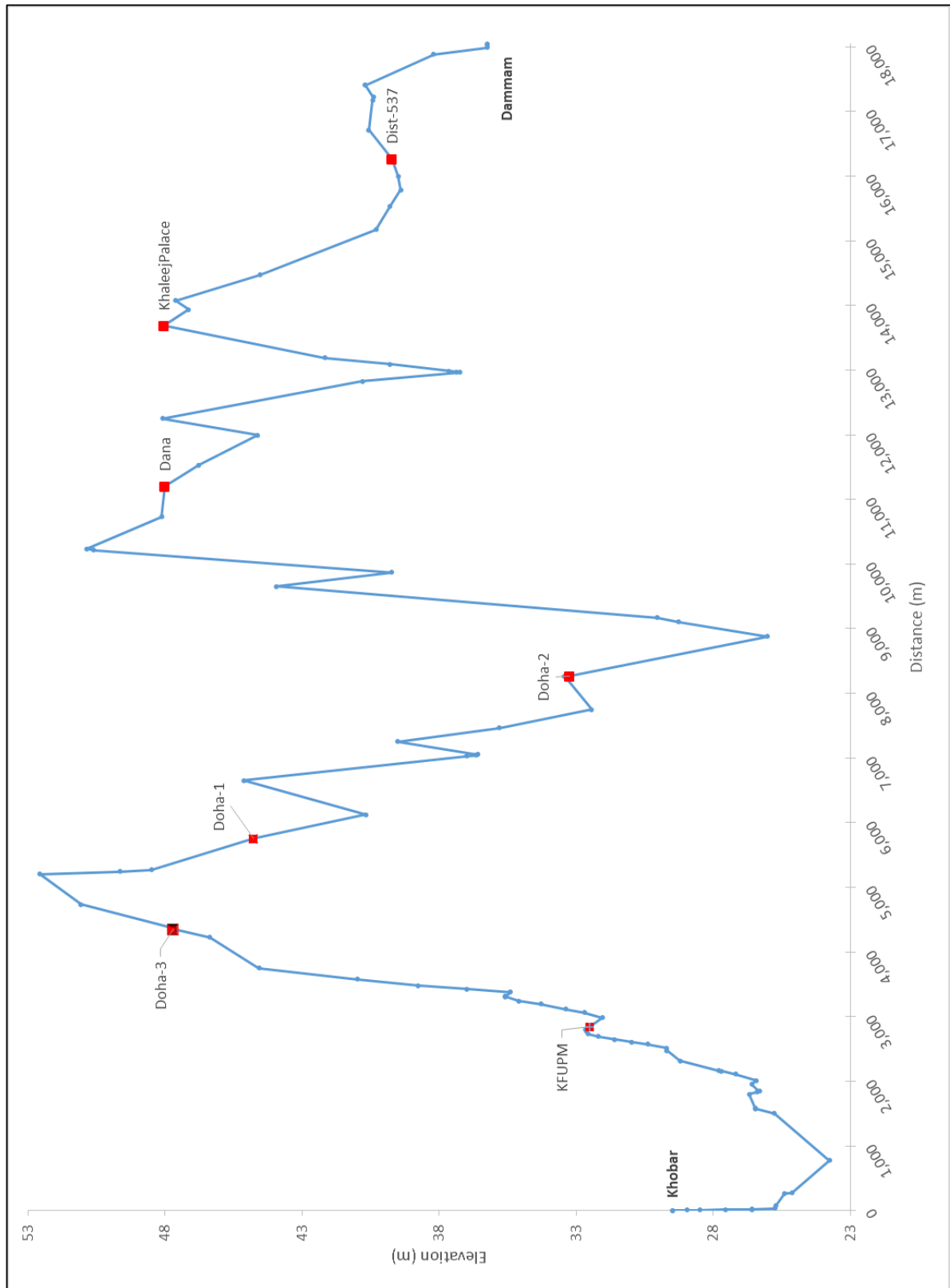


Figure 3-3 Ground elevation and locations of branched pipelines along the KDRL

A field survey was conducted to help constructing the pipeline contour to accurately evaluate the layout and topography of the KDRL. Figure 3.3 shows the ground level variations as well as the branching points along the KDRL. Detailed field data from all KDRL components was saved into a GIS Database. Tables 3.1 and 3.2 summarize the inventory and layout data of the KDRL in the GIS database, respectively. Table 3.3 summarizes information about the tanks connected to the KDRL. Figures 3.4, 3.5 and 3.6 show examples of KDRL components.

Table 3-1 KDRL summary of piping elements

Khobar PS Tank	Branching Point		Branch Pipe			Branch ending Level
	Station	Elevation	Diameter	Material	Length	
KFUPM	2,844	32.49	400	UPVC	1,268	56.35
Doha-3	4,361	47.7	200	UPVC	446	49.28
Doha-1	5,755	44.77	200	UPVC	292	49.87
Doha-2	8,272	33.24	300	FRP	1010	57.01
Dana	11,202	48.02	400	DI	255	55.58
Palace	13,692	48.05	300	FRP	285	/
Dist-537	16,270	39.72	300	FRP	740	/
Dam-55	18,055	/	700	CCP	18,055	36.25

Table 3-2 KDRL inventory

Pressure Pipes Inventory					
Diameter	CCP	FRP	DI	UPVC	All Materials
(mm)	(m)	(m)	(m)	(m)	(m)
200	0	0	0	738	738
300	0	2,045	0	0	2,045
400	0	0	255	1,268	1,523
600	0	0	85	0	85
700	18,086	0	0	0	18,076
All Dia.	18,086	2,045	340	2,006	22,477
Components Inventory					
Chambers	Discharge	Isolation Valve	Pressure reduce valve	Air Valves	Metering Point
31	27	58	3	14	11
Pipe Segments		Junctions/Pipe fittings			Pumps
212		201			1

Table 3-3 Data for tanks/branches from KDRL

Tank	Diameter (m)	Elevation (m)		Avg. % Flow of Total
		Height		
Yarmouk PS	40	Height	18	100.0%
		Ground level	29.5	
KFUPM	40	Height	10	6.6%
		Ground level	56.35	
Doha-3	18	Height	11	17.5%
		Ground level	49.28	
Doha-1	18	Height	11	14.0%
		Ground level	52.87	
Doha-2	11	Height	11	18.0%
		Ground level	65.99	
Dana	7	Height	11	30.0%
		Ground level	70.54	
Khaleej Palace	To network	Ground level	48.6	1.5%
District No. 537	To network	Ground level	44.23	10.6%
Dam-55 PS	40	Height	18	1.8%
		Ground level	36.25	



Figure 3-4 Sample washout valve in KDRL



Figure 3-5 Sample air valves installed in KDRL



Figure 3-6 Sample branching connection in KDRL

The detailed survey shows some discrepancy between the data collected by the surveyor's and the KDRL as-built drawings. Appendix A shows the difference between these data. In this study, the analysis was performed based on the surveyed data.

In order to achieve a robust model for the KDRL, operational and historical data related to KDRL were gathered and were entered into the GIS database. Moreover, eleven flow and pressure meters were installed along the KDRL. Figure 3.7 shows the types of the flow/pressure meter installed according to the site conditions. Two flow/pressure meters were installed at both Khobar and Dammam ends of the KDRL. Additional seven flow/pressure meters were installed at each branch connecting to the KDRL in order to measure the water flow and the pressure to the tanks at the metering point. These nine flow/pressure meters provide a reading of the pressure and flow every 15 minutes. Additionally, two on-line pressure meters that provide instantaneous and continues readings were installed at other points on the KDRL ends. Figure 3.8 shows sample of installed flow/pressure meter.

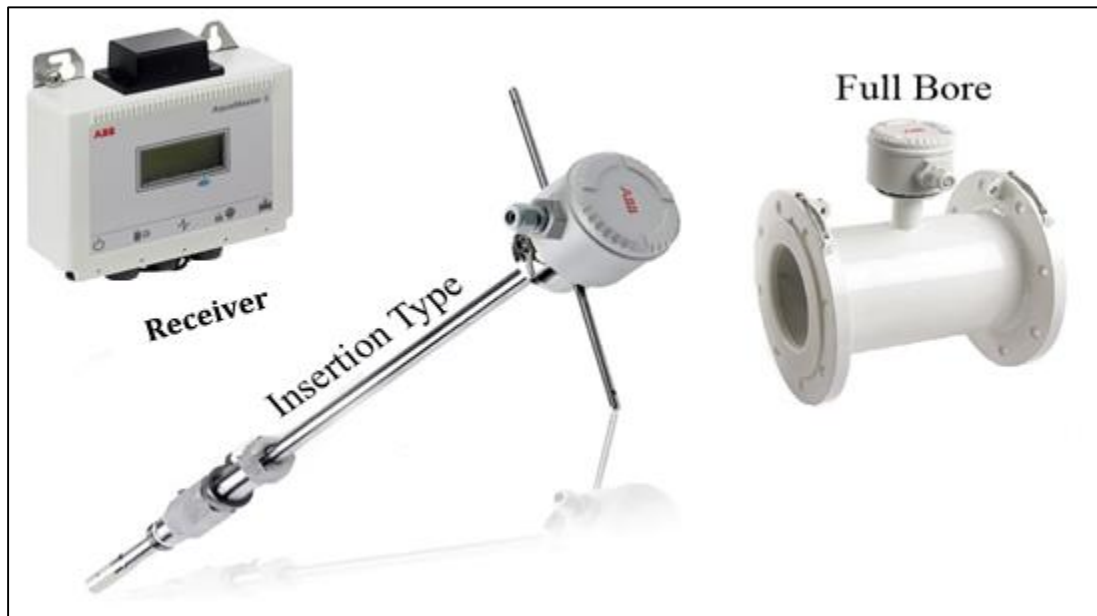


Figure 3-7 Types of flow/pressure meters installed in KDRL

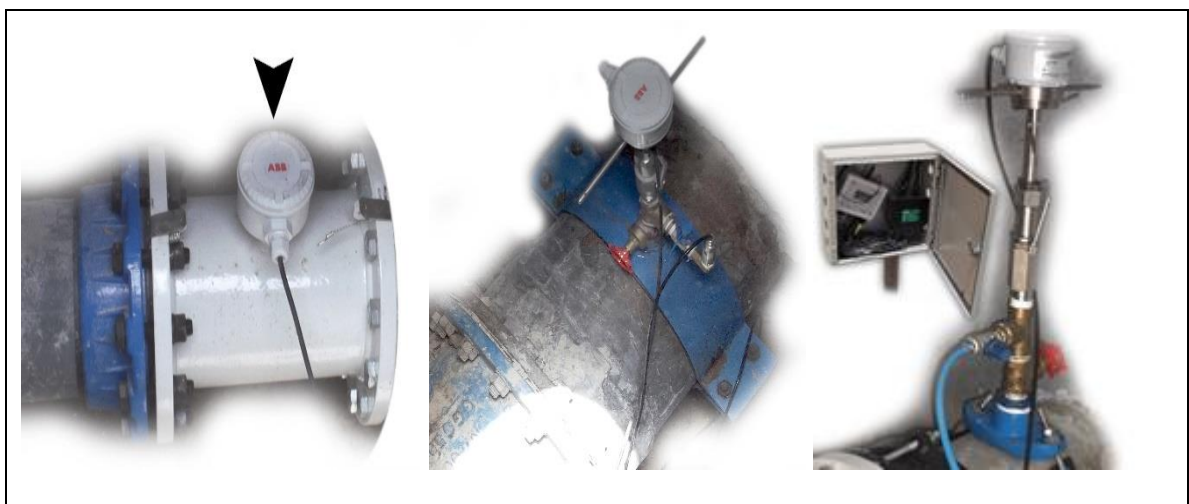


Figure 3-8 Installed flow/pressure meters on-site

3.2 Flow and Pressure Measurements

Flow/Pressure meters were installed in April 2013 along the KDRL to send log data every 15 minutes. Collected data were directed to the GIS database and linked to a corresponding element in the KDRL system. Figure 3.9 shows the location of flow/pressure meters. These flow/pressure meters were continually monitored for the water flow and pressure. Flow meter data indicated that there were some operational problems in the system as there was a non-working or defect element. For example, a flow meter installed prior to the non-return valve shows a reverse flow in the pipe which indicates that the non-return valve is defected. A major problem faced during data collection was related to the rapid pressure variation along the pipeline due to the development of the water hammer which damages three installed devices. All the operational problems were fixed prior to the start of KDRL hydraulic analysis.

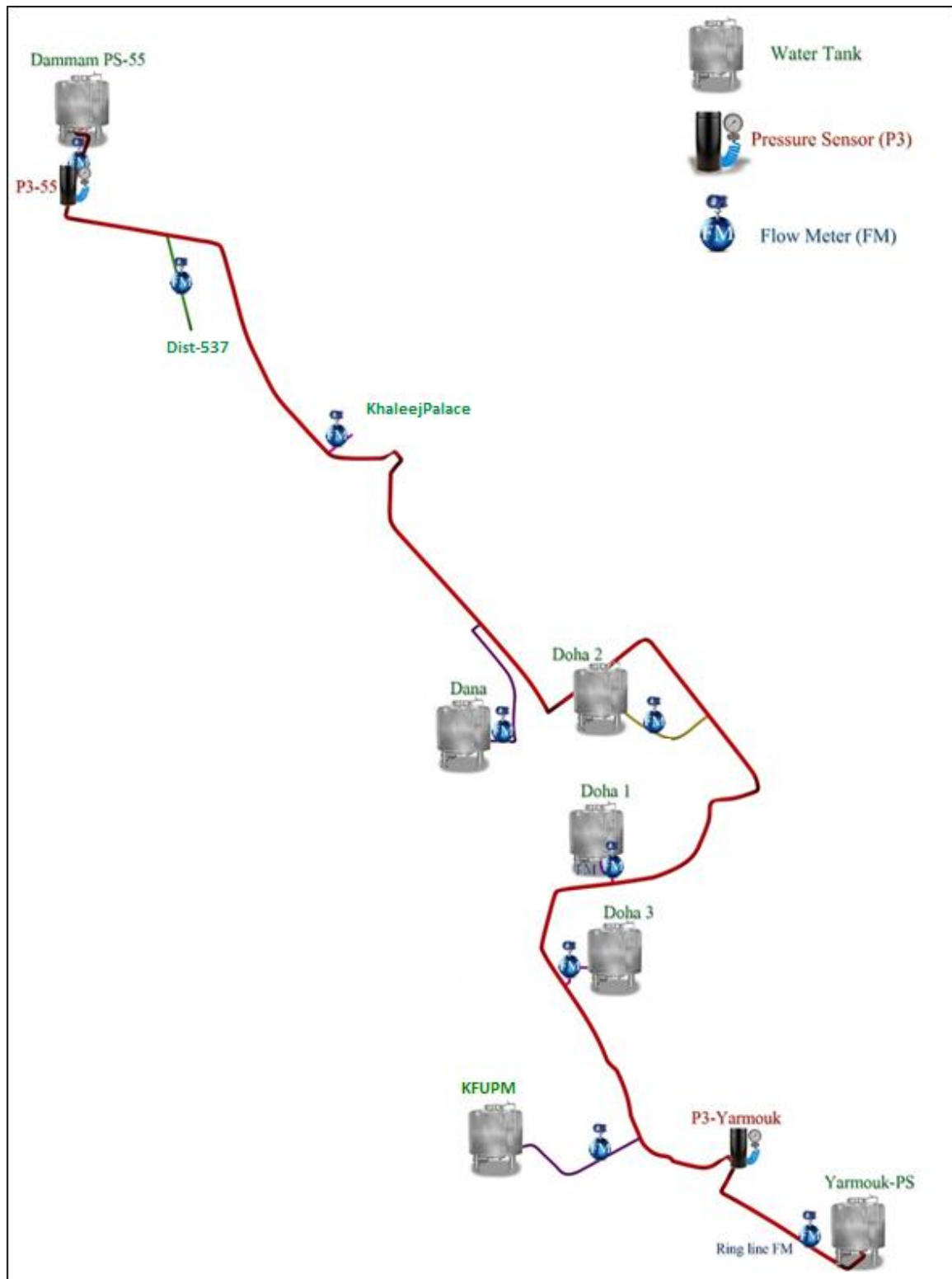


Figure 3-9 Location of flow/pressure meter.

Flow and pressure data using proper devices installed at different locations along the KDRL were collected over a period of six months (May 2013 to October 2013). The data indicated that an extreme water hammer has developed along the pipeline. Figure 3.10 shows the readings at the KFUPM branch after a sudden closure of the tank's valve. As a result, the flow became zero and a surge wave developed. The generated wave increased the pressure in the KFUPM branch pipeline to more than 16bars, causing a serious damage to the flow/pressure meter. The sudden closure of the valve at KFUPM tank was, most probably, not the only cause of this problem since the flow/pressure meter survived from similar previous incidents many times. Sudden closure of other valves at other branches might have contributed to this incident. Later in the analysis, it will be shown clearly that KFUPM branch was the part of KDRL that was the most affected during the water hammer event. Figure 3.11 shows the reading at Dana branch at the same time when the KFUPM pressure meter was damaged. The reading indicates that a suction pressure up to 3-bar was created. The behavior at Khaleej Palace where valves are open to fill tank for 2-hours in a day then closed suddenly is depicted in Figure 3.12.

During the period of 18th to 23rd of August 2013 there was a deviation from the normal operation due to an abnormal flow condition. This serious flow condition over long-period which affected all branch pipelines was most probably caused by a malfunctioning valve at the KFUPM tank as displayed in Figures 3.13, 3.14, 3.15 and 3.16.

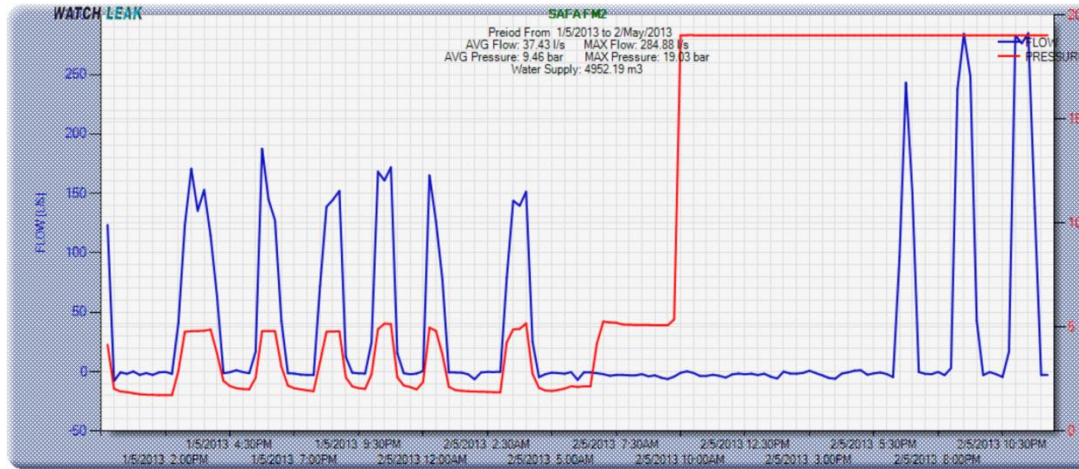


Figure 3-10 Flow and pressure readings at KFUPM branch collected on 1st and 2nd May, 2013

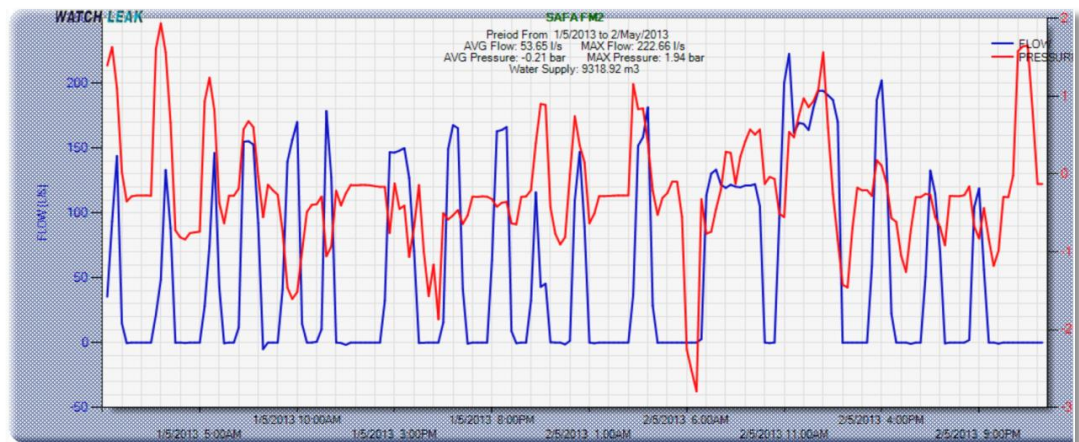


Figure 3-11 Flow and pressure readings at Dana branch collected on 1st and 2nd May, 2013

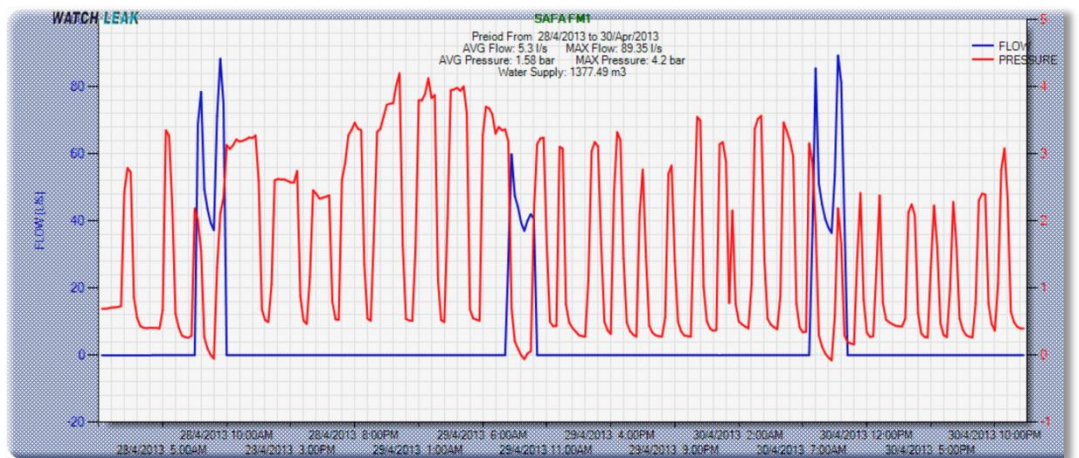


Figure 3-12 Flow and pressure readings at Khaleej branch collected on 1st and 2nd May, 2013

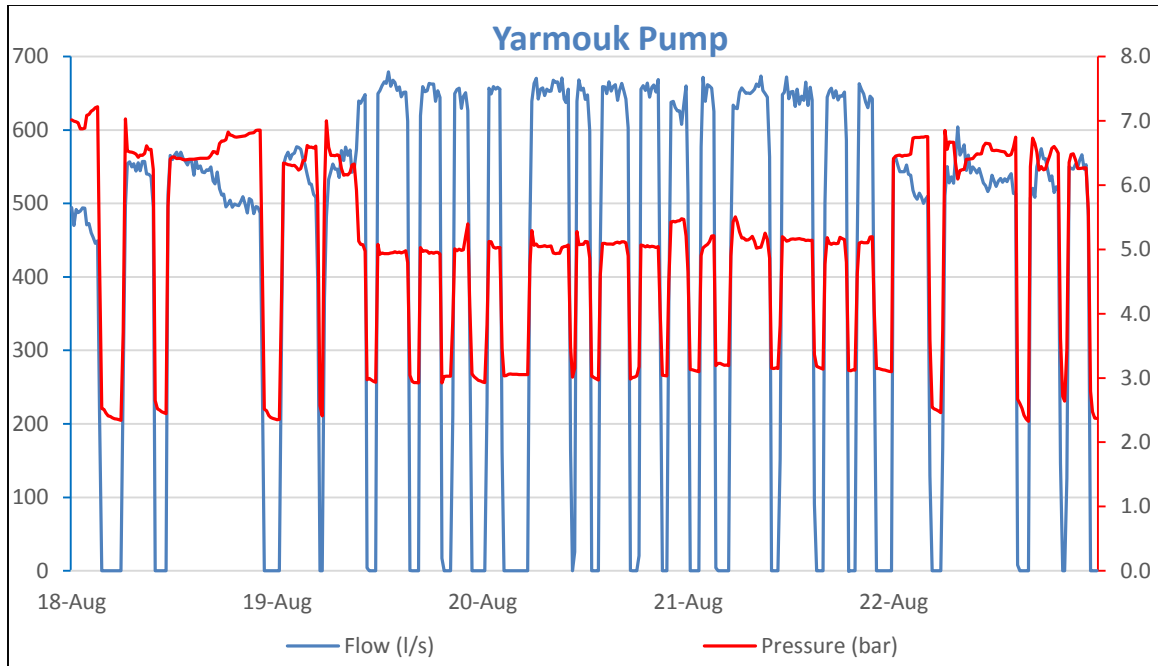


Figure 3-13 Flow and pressure readings at Yarmouk tank from 18th to 23rd August, 2013

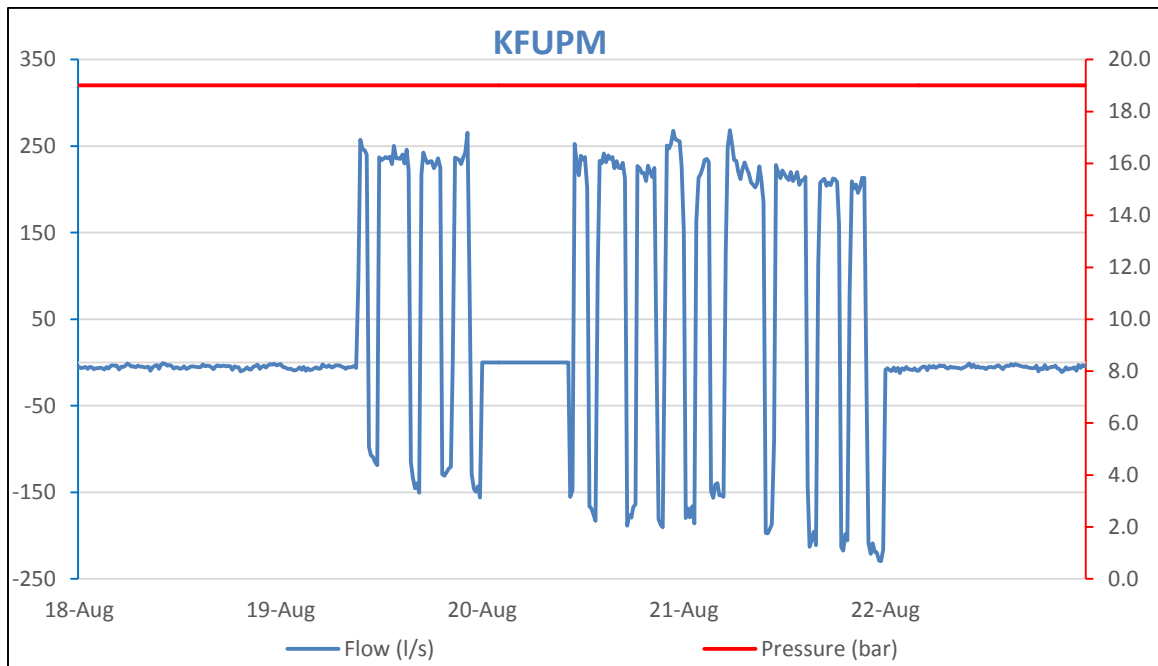


Figure 3-14 Flow and pressure readings at KFUPM tank from 18th to 23rd August, 2013

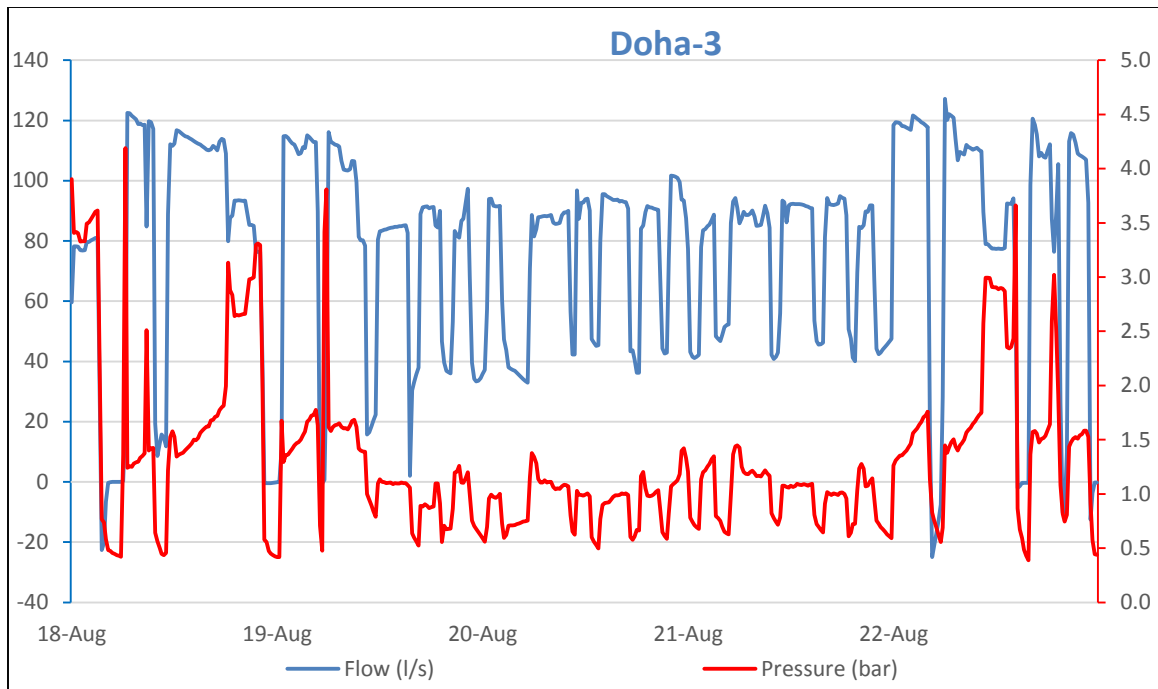


Figure 3-15 Flow and pressure readings at Doha-3 tank from 18th to 23rd August, 2013

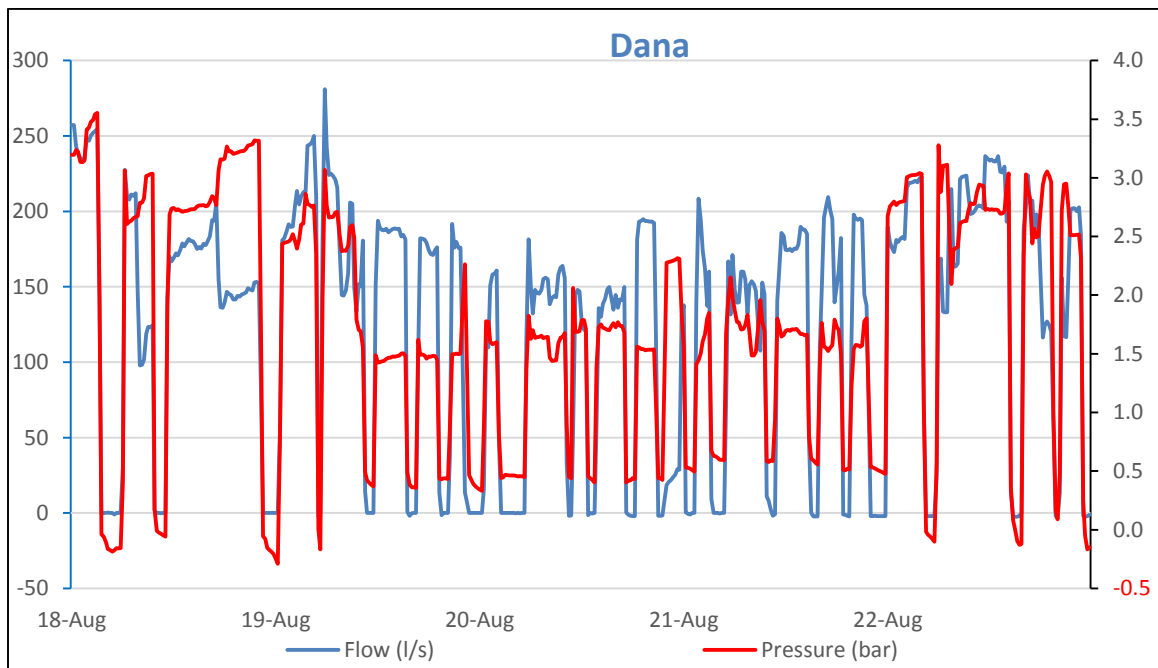


Figure 3-16 Flow and pressure readings at Dana tank from 18th to 23rd August, 2013

The total supply of the KDRL in one month (October, 2013) and the fluctuations in the flow and pressure during the same period in all branches are listed in Table 3.4.

Table 3-4 Summary of flow meter readings at different locations along the KDRL during October 2013

Flow Meter Location	Total Water Supply (m³)	Max Flow (l/s)	Avg Flow (l/s)	Max Pressure (bar)	Avg Pressure (bar)
Yarmouk	1,095,135	673.86	408.88	7.92	5.25
KFUPM	73,069	200.56	27.66	/	7.45
Doha3	192,449	124.66	71.83	4.42	1.39
Doha1	154,772	117.06	57.77	3.98	1.28
Doha2	197,969	189.37	73.89	3.95	0.86
Dana	349,862	273.41	130.62	4.81	1.85
Palace	15,681	88.78	6.14	5.62	2.67
Dist-537	115,661	100.66	43.17	2.5	1.74
Dam-55	19,836	58.81	7.41	1.95	1.21

The flow and pressure measurements collected during the six month period (May – October, 2013) indicate the need to perform a detailed water hydraulic analysis of the KDRL. This is an essential step that needs to be performed prior to the water hammer analysis. This is because the water hydraulic analysis will help enhance the performance of the KDRL by optimizing its operation, and identify critical points in the system.

CHAPTER 4

HYDRAULIC MODELING OF KDRL

4.1 Model Construction and Execution

Water hydraulic modeling of the KDRL has to be performed before the analysis of water hammer is conducted. Such modeling is essential to understand the behavior of the system under normal conditions and to validate the results from the model with the field data. In case there is a discrepancy between the model results and the field data, then the model will be calibrated and corrected accordingly. For the purpose of the water hydraulic modeling, two program packages, namely ESRI ArcMap GIS and WaterGEMS were used. ESRI ArcMap GIS program was used to construct the model and automate the elevation projection to the model using field survey data. On the other hand, WaterGEMS program, which is a widely known water hydraulic modeling and simulation package that enables integration with the GIS, was used for the water hydraulic analysis. Darwin Calibrator, which is an extension to WaterGEMS, was used to optimize the automatic calibration. The main goal of the water hydraulic analysis was to calibrate the model and assure its adequacy to represent the real condition in order to run water hammer analysis and simulate different protections for the KDRL from water hammer.

The Yarmouk station at Khobar receives water from two sources: desalinated water from the SWCC and raw groundwater from local water wells. The water, which is coming from

these sources, is blended in Yarmouk tank and then distributed to Khobar city. The average water supply to Yarmouk station is about 5,600 m³/h. Approximately 63% of this amount (3,500 m³/h) is supplied to Khobar Central station and to Makkah station. The water amount transported through the KDRL is approximately 2,100m³/h. KDRL is operated using one pump located at Yarmouk station (Yar-Pump). Table 4.1 shows the characteristic curve for this pump.

Table 4-1 Yarmouk-pump specifications

Yar-Pump	Shut-off	Design	Max		Inertia	Speed	Specific
Flow	0	500	1,000		(Kg.m²)	(rpm)	Speed
Head	89	67	0		19,000	1,171	76

Each of the six sub tanks that are connected to the KDRL is serving a large community. Therefore, each tank is connected to a local water well to make up for water supply shortages during the high water demand. KDRL also is feeding District No. 537 from a branching pipe connected directly to the district sub network.

Using GIS data, a model was built and exported to WaterGEMS. A schematic of the KDRL as imported from the WaterGEMS is depicted in Figure 4.1, showing the locations of each tanks, sub tanks, pump, and air valves.

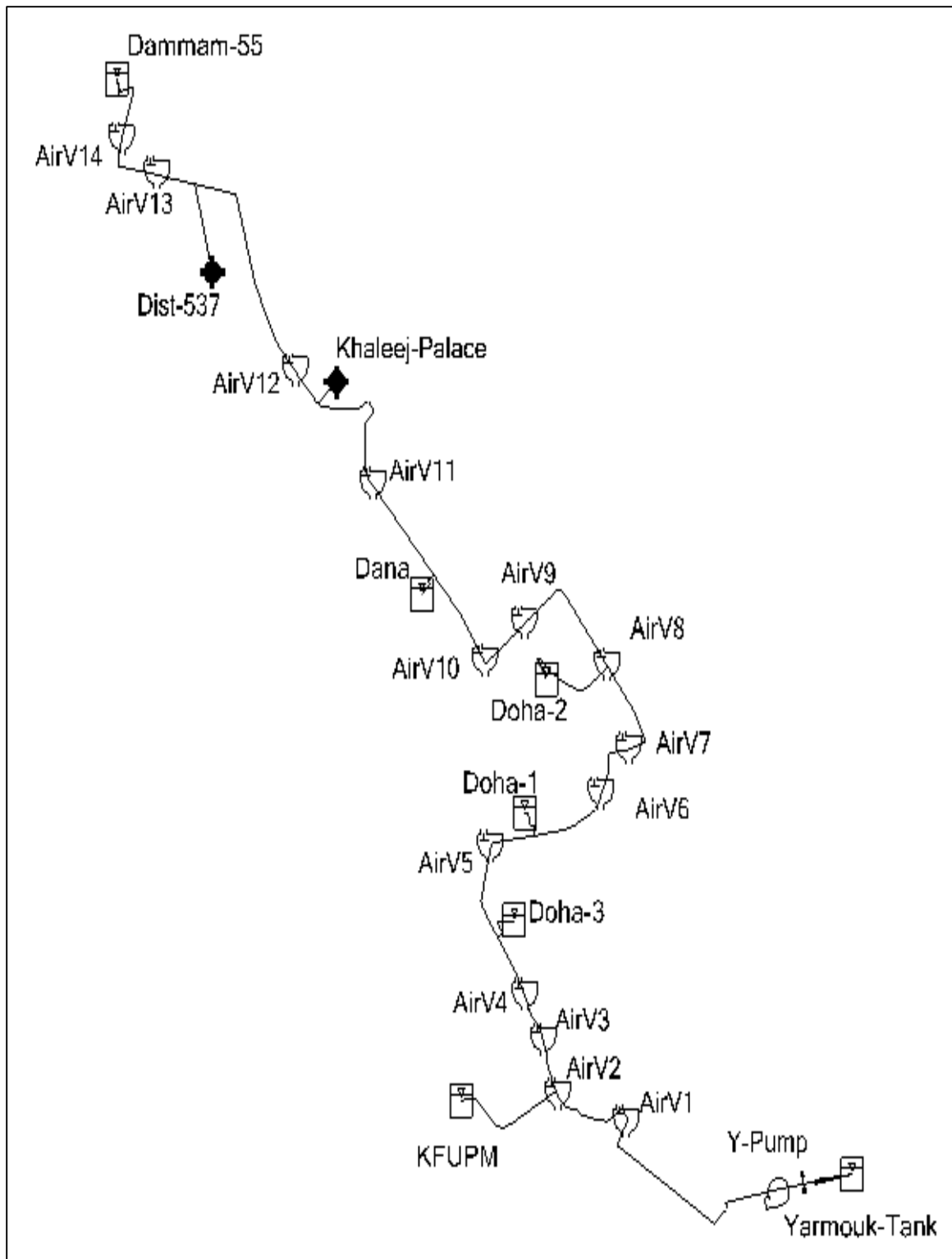


Figure 4-1 KDRL schematic from WaterGEMS

There are fourteen air valves installed in all crests of the main pipeline. In addition, actuator valves were installed upstream of each sub tank to control the water feeding to the tank from the KDRL. The desalinated water and the water from the water wells at Yarmouk blending station are represented as a junction with a negative demand connected to the tank, while all water demands to Khobar city are represented by a junction (KH-D) as shown in Figure 4.2.

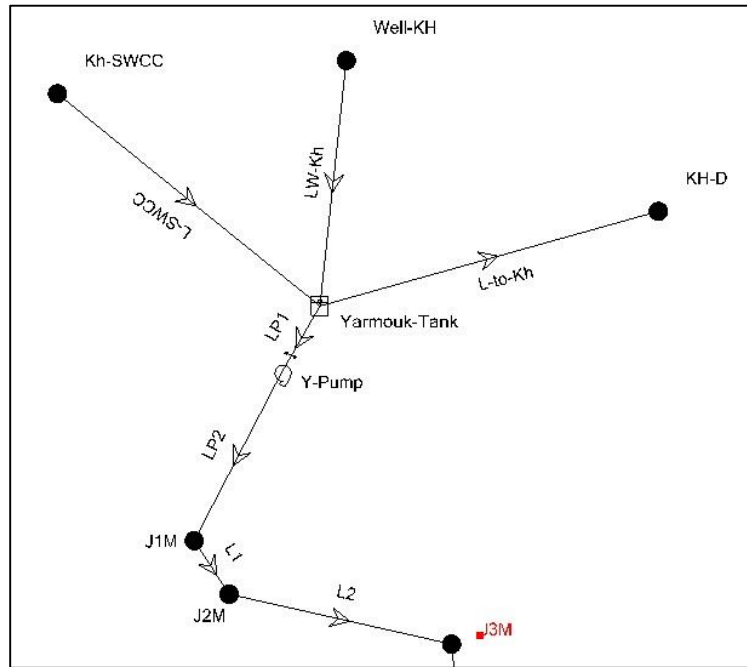


Figure 4-2 Representation of Yarmouk tank station in the network

The operation of KDRL is controlled by the water levels in the tanks, except Khaleej palace tank where the valve is manually operated to receive water from KDRL for 3 hours during the daytime. Thus, for the purpose of modeling, Khaleej palace tank is represented as a junction with a defined demand pattern. Summary of the KDRL operational controls are summarized in Table 4.2.

Table 4-2 KDRL operation controls

Action on Element	Controlling Condition	On/Open Level	Off/Close Level
Yar-Pump On/Off	Yar-Tank Level	12.5	14
KFUPM Valve 0/1	KFUPM Tank level	3	10
Doha-3 Valve 0/1	Doha-3 Tank level	8	11
Doha-1 Valve 0/1	Doha-1 Tank level	8	11
Doha-2 Valve 0/1	Doha-2 Tank level	8	11
Dana Valve 0/1	Dana Tank level	2	4

When constructing the water hydraulic model for KDRL, the community water demands as supplied from the tanks are modeled as a demand junctions located after the tank. For example, Figure 4.3 shows the schematic layout of the junction demand for Dana tank. The demands for the communities are estimated by collecting relevant data from the corresponding flow meter. A one-month long reading (every 15 min) from each flow meter is stored in the GIS database, averaged, and then assigned to the demand node after the tank. The flow meter readings used to create a pattern for the demand as well.

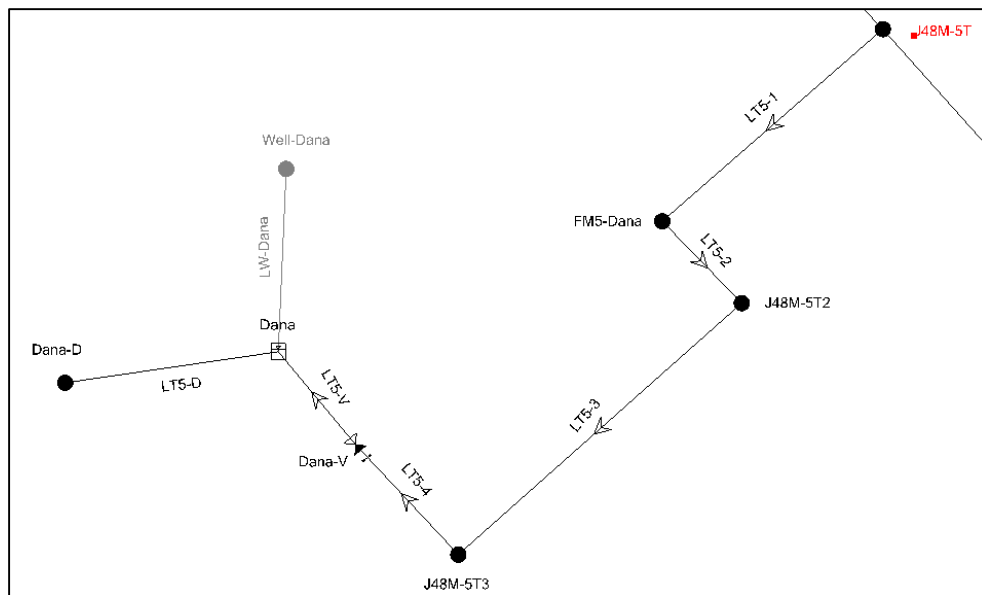


Figure 4-3 Details schematic of a branch from KDRL

Table 4.3 summarizes the data from the installed flow/pressure meters and their corresponding element to represent the reading during the calibration.

Table 4-3 List of metering device and their corresponding junction/pipe

Meter ID	ELEVATION	Junction @ Model	Flow @ Model
Khubar	27.002	FM-Yarmouk @ 27.5	L7
KFUPM	34.643	FM1-KFUPM @ 34.68	LT1-1
DOHA 3	49.288	FM2-Doha3 @ 49.29	LT2-3
DOHA 1	52.873	FM3-Doha1 @ 52.87	LT3-5
DOHA 2	60.814	FM4-Doha2 @ 60.81	LT4-2
Dana	55.650	FM5-Dana @ 55.66	LT5-3
Palace	49.388	FM6-Khaleej @ 48.74	LT6-1
Dist 537	41.220	FM7-p537 @ 42.25	LT7-1
TANK 55	39.601	AirV10 assumed to be @ FM-Tank55	L97
P3- YAR	27.214	AirV1 assume @ J9M	NON
P3-T55	36.25	@ Junction Dm55-P3	NON

Appendix B contains sample data of the junctions and pipes used to create this model, initial conditions, and all other input data to construct and run the model, along with the results of initial hydraulic analysis results in a tabular form.

Upon the completion of the model construction and data input, the model calculation option is chosen to be based on Hazen-Williams equation. The general form of H-W equation is [2, 4]:

$$Q = k \cdot A \cdot R^{0.63} \cdot S^{0.54} \quad (4.1)$$

Where,

Q = Discharge in the section

C = Hazen-Williams roughness coefficient

A = Flow area

R = Hydraulic radius

S = Friction slope

K = Constant (0.85 for SI units or 1.32 for US units)

The H-W roughness coefficient can be estimated from Table 4.4. Initially, all C -values are set to be 130. The adjusted values from the calibration process will be applied to each element at a later stage.

Initial run of the model was successful as presented by the WaterGEM output shown in Figure 4.4. The figure reveals that, under normal conditions, the HGL is decreasing in the direction of the flow along the KDRL and it is always above the ground level.

Table 4-4 Common used Roughness Value [2, 19]

Material	Manning's Coefficient n	Hazen- Williams C	Darcy-Weisbach Roughness Height	
			k (mm)	k (0.001 ft.)
Asbestos cement	0.011	140	0.0015	0.005
Brass	0.011	135	0.0015	0.005
Brick	0.015	100	0.6	2
Cast-iron, new	0.012	130	0.26	0.85
Concrete:				
Steel forms	0.011	140	0.18	0.6
Wooden forms	0.015	120	0.6	2
Centrifugally spun	0.013	135	0.36	1.2
Copper	0.011	135	0.0015	0.005
Corrugated metal	0.022	—	45	150
Galvanized iron	0.016	120	0.15	0.5
Glass	0.011	140	0.0015	0.005
Lead	0.011	135	0.0015	0.005
Plastic	0.009	150	0.0015	0.005
Steel				
Coal-tar enamel	0.010	148	0.0048	0.016
New unlined	0.011	145	0.045	0.15
Riveted	0.019	110	0.9	3
Wood stave	0.012	120	0.18	0.6

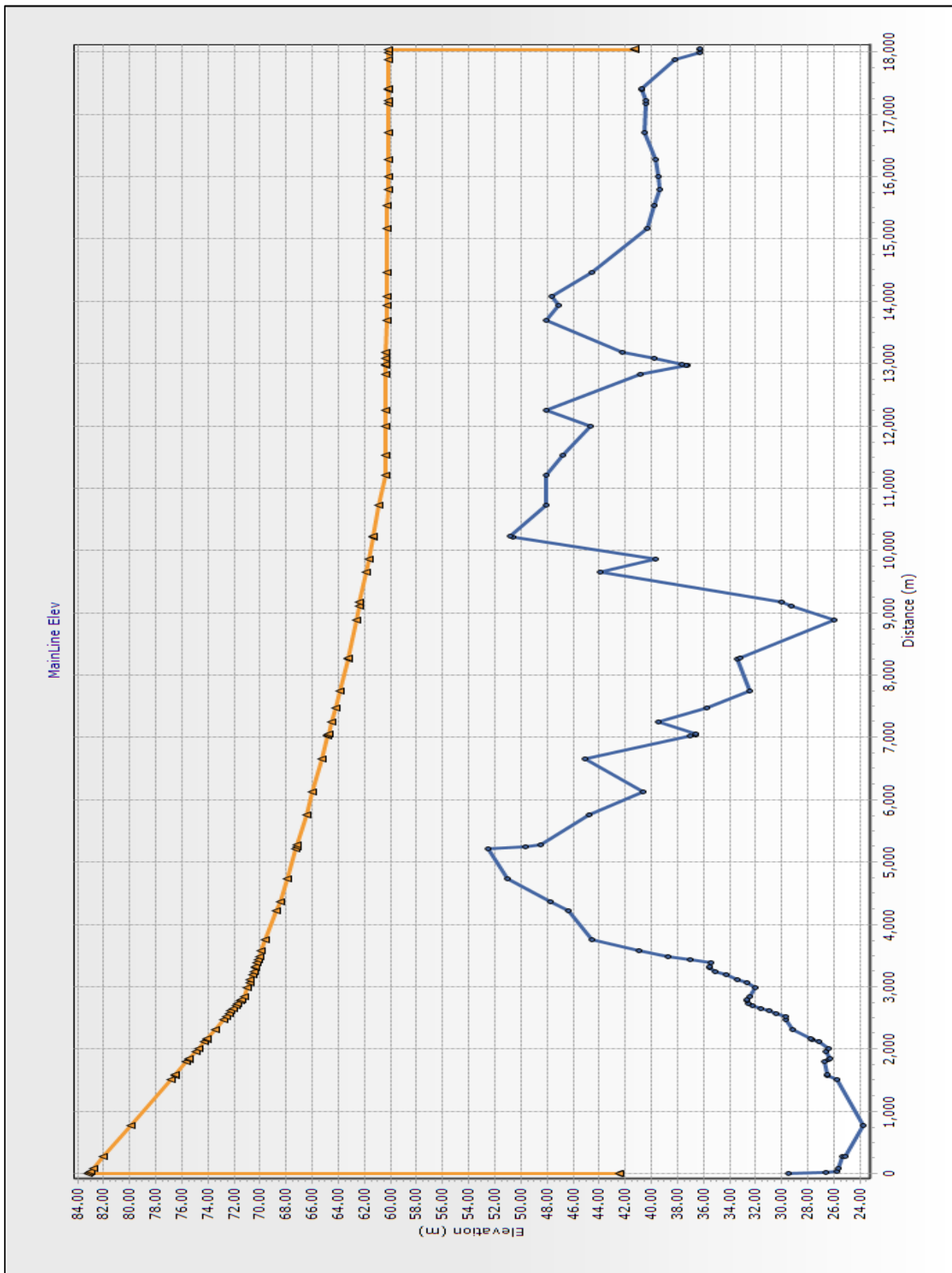


Figure 4-4 HGL over KDRL (Steady-State Analysis)

4.2 Model Calibration

After the model was constructed, it needed to be calibrated by comparing the model output with the field data. For this purpose, two day duration (28th-30th October 2013) was selected. Field data related to the flow and pressure at different locations along the KDRL were collected during the same period from 28th - 30th October, 2013. The first initial conditions of this period were used as input to the constructed model which was executed for a period of 48 hours with a time step of 15 minutes. The 15-minute time step was selected to match the time interval that was considered when the readings were collected using the flow/pressure meters. The total flow through the system based on the WaterGEM calculation is summarized in Table 4.5. Sample output of the WaterGEM model is in Appendix B. The water level variation in Yarmouk tank and the pumped flows for the testing period are presented in Figures 4.5 and 4.6, respectively.

Table 4-5 Totalizing flow meter resulted from WaterGEMS calculations

	Element Label	Net Volume (m³)	% of KDRL amount
Yar- Station	Kh-SWCC	-238,769.09	/
	Well-KH	-46,704.06	/
	KH-D	197,685.00	/
KDRL	KFUPM-D	8,059.90	9.18
	Doha3-D	13,074.12	14.89
	Doha1-D	10,105.50	11.51
	Doha2-D	14,614.21	16.65
	Dana-D	23,565.13	26.84
	Khaleej-Palace	1238.92	1.41
	Dist-537	7,587.09	8.64
	Dm55-D	3,837.47	4.37

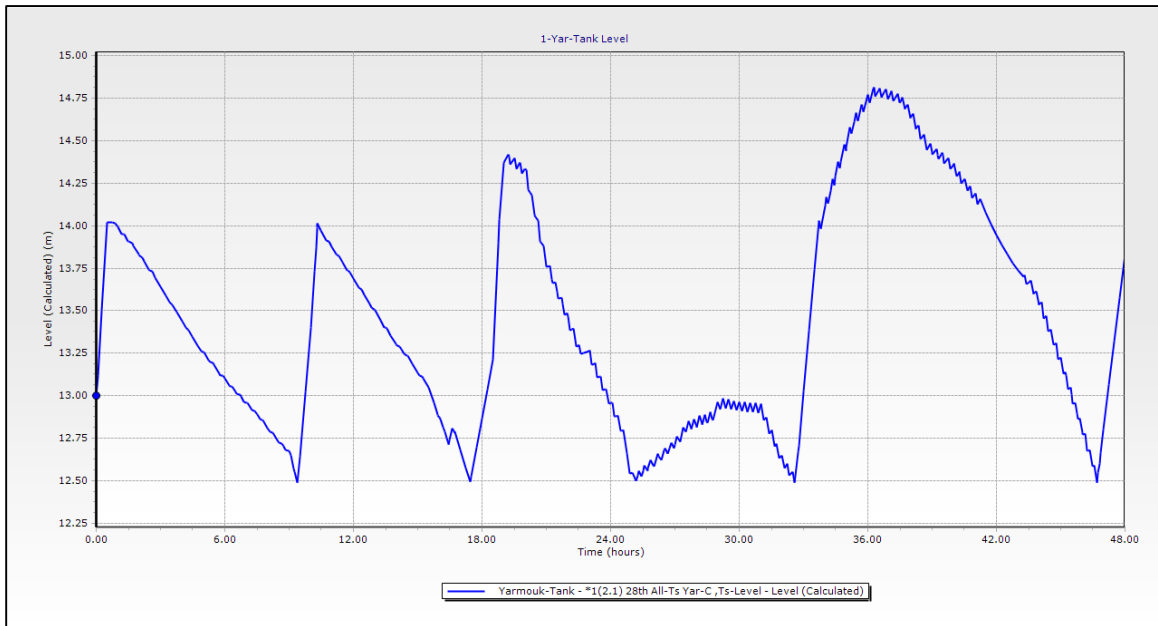


Figure 4-5 water level variation calculated over the period 28-30 Oct 2013

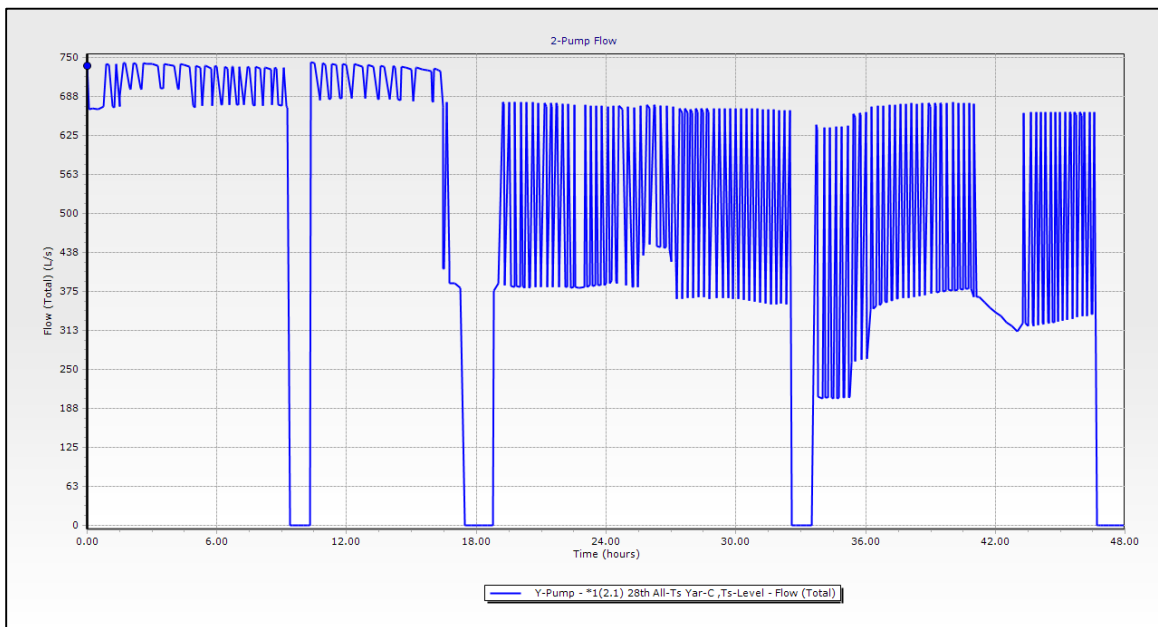


Figure 4-6 Pumped flow during 28-30 October 2013

For an optimized calibration, two stage processes were adopted. Firstly, a scenario was built considering a sub-model based on Yarmouk station up to the point of Yarmouk flow meter (Yarmouk FM) only. For this case, a demand value equals to the pumped quantity has been assigned to the junction at Yarmouk FM and a pattern demand similar to the total flow pumped to KDRL was adopted. Thus, a reading from only one meter (Yarmouk FM) is used for the sub-model calibration, while the reading from all eleven meters were used in calibrating the full model. Next “Darwin Calibrator” feature of the WaterGEM model used for calibration based on flow/pressure reading collected from filed (during the 28th to 30th October, 2013 period) and the WaterGEM calculation output. The calibration analysis shows a small fitness value (0.001) indicating that model output is very close to field data. Figures 4.7 and 4.8 show the correlation results for both sub-model and full model, respectively. Sample of the calibration results for both model and sub-model are presented in Appendix C along with the sample of observed field data.

Calibration process adjustment to both roughness coefficients and demands were applied to the model elements. A comparison between the water level variation obtained from the WaterGEM and that collected from the field is depicted in Figure 4.9. The Figure shows a strong match between the two calculated (after calibration) and the observed field data curves, indicating the capability of the model to simulate field conditions. Similar conclusion can also be drawn for the pumped flow as indicated form Figure 4.10. Both figures clearly show the added value to the calculation capability and its adjustment to ensure model output is similar to filed data.

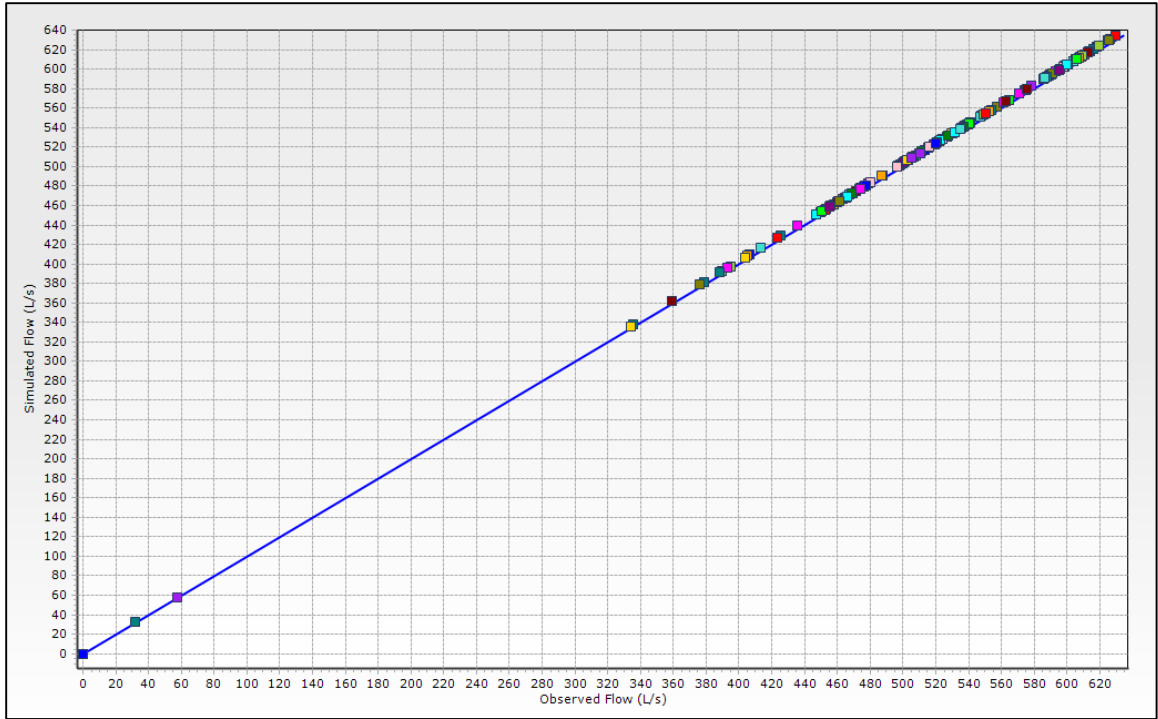


Figure 4-7 Sub-model calibration correlation results

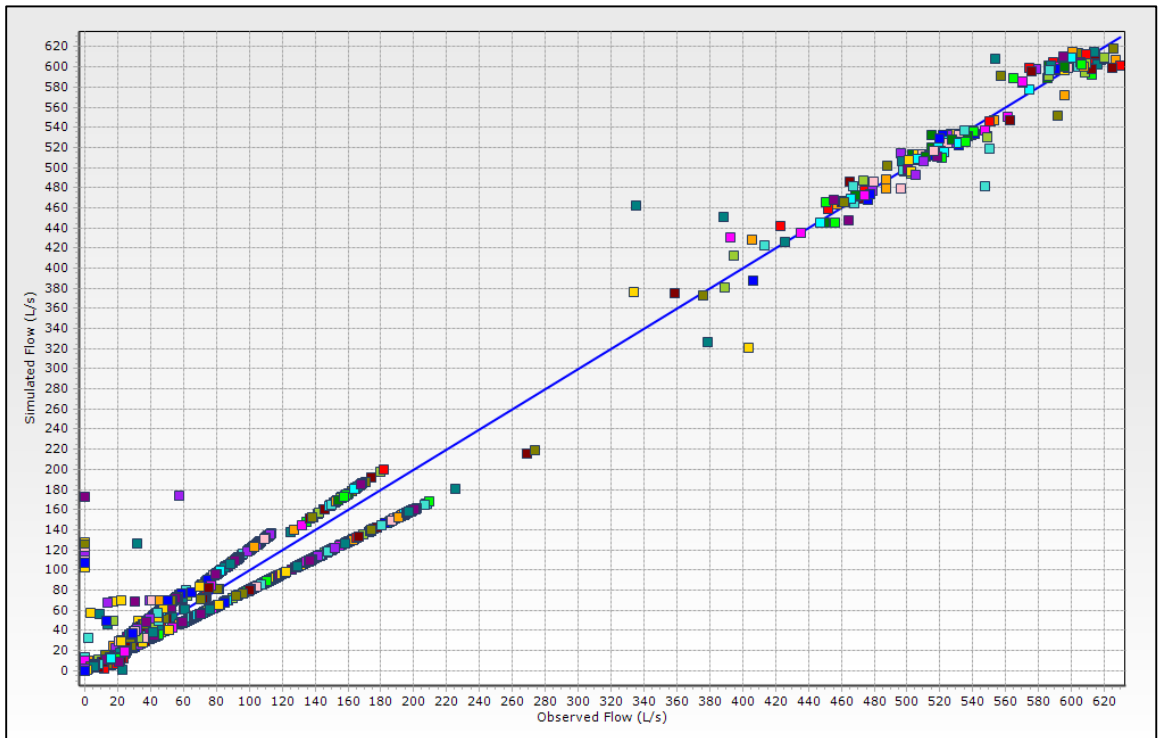


Figure 4-8 KDRL model calibration correlation results

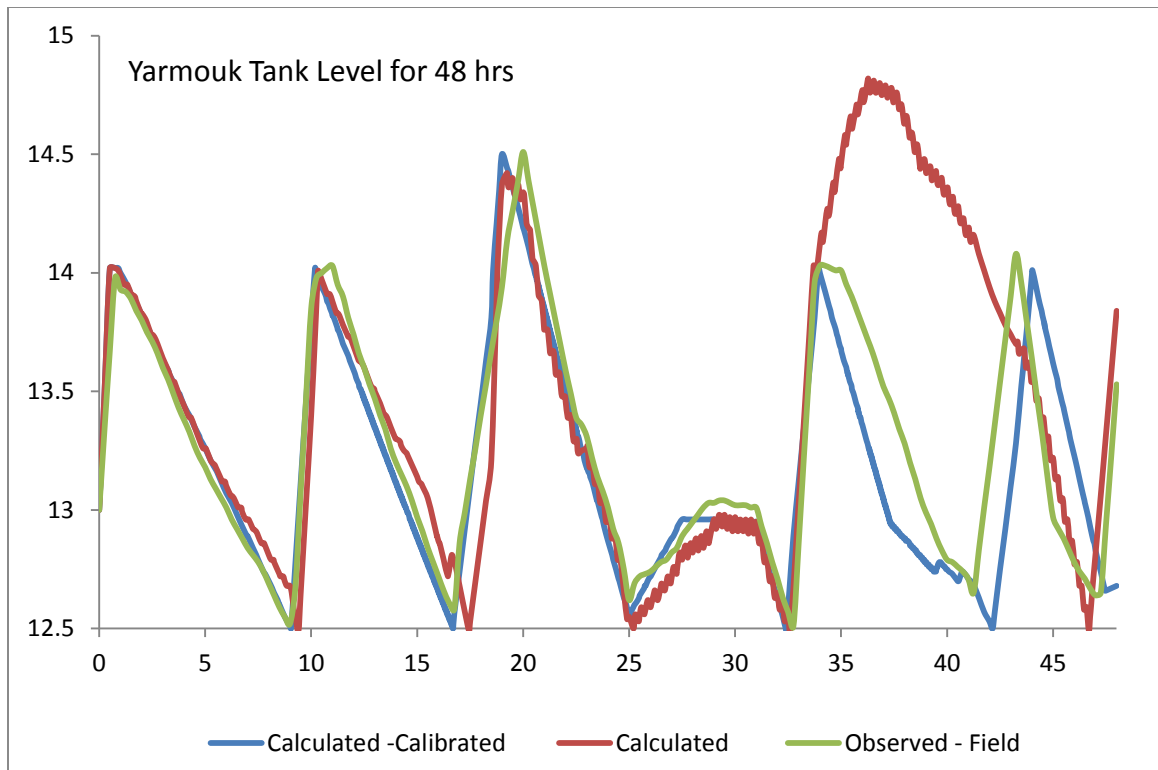


Figure 4-9 Comparison of water level variation at Yarmouk tank

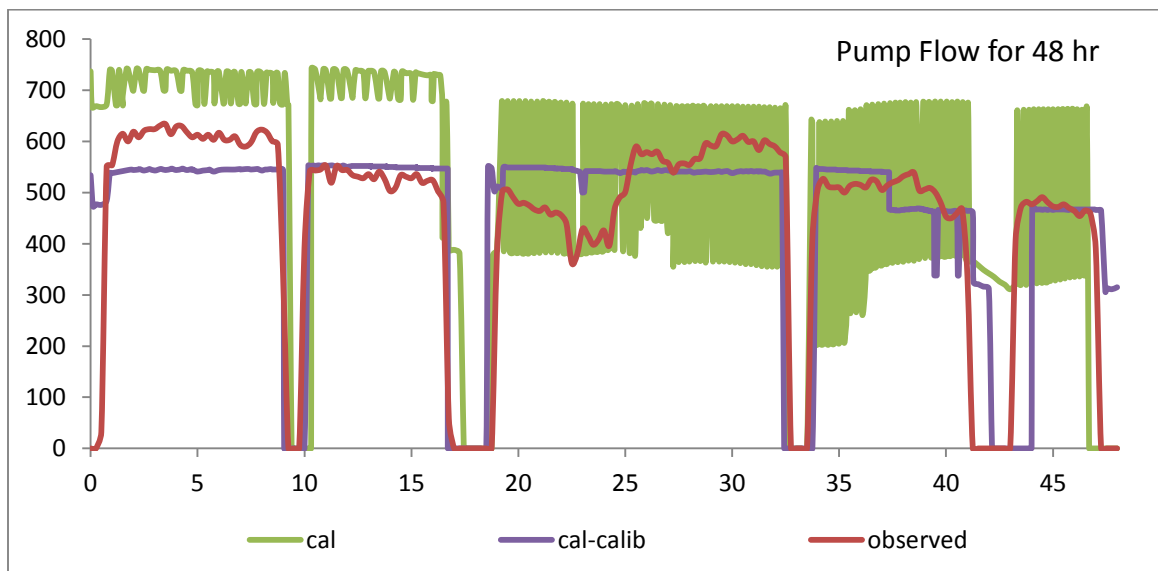


Figure 4-10 Comparison of the pumped flow

Results above indicate that the constructed hydraulic model using WaterGEM can accurately represent conditions likely to be experienced in the KDRL. The model is calibrated to adequately represent the actual field conditions using field measurements and observations.

The HGL at Yarmouk flow meter junction over a period of 48 hours (28-30 October 2013) based on the calibrated model is shown in Figure 4.11. The graph shows an extreme negative pressure at 42 hour. This indicates that close investigation is required as well as proper protection for such an incident is mandatory.

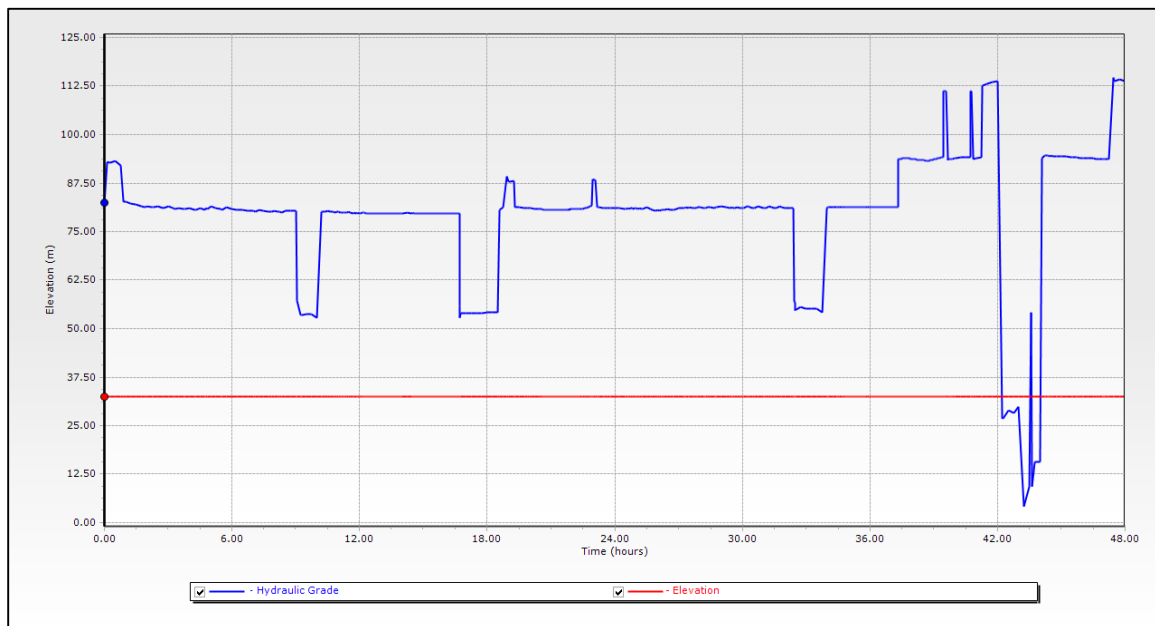


Figure 4-11 HGL at junction Yarmouk flow meter (28-30 Oct) based on the calibrated model

Once a hydraulic model for the KDRL was constructed and calibrated, the next step was to investigate the occurrence and control of a water hammer that might occur at any point along the pipeline.

CHAPTER 5

WATER HAMMER MODELING & ANALYSIS

5.1 Background

Water hammer or hydraulic transients in pipelines mainly occur due to the following:

- a) Water Pumps startup or shut down
- b) Main valves opening or closure.
- c) Sudden power failure, causing water pumps to shut down.

Pumps startup or shutdown usually does not cause major transient in the system if proper operational procedure has been adopted, such as soft starter or delayed shutdown. Currently the Water Authority of Khobar city is practicing operational control to prevent water hammer in KDRL, by enforcing gradual operation for the pump and all valves. This practice, however, is of no value in the case of power outage and/or pipe breaks. The worst case, for down-surge development, is after a power failure where a sudden pump shutdown takes place. Valves closure will have a minor effect if operated properly and not suddenly closed. However, human intervention in the system operation by unskilled operators can lead to a disaster. Thus, the study will consider the worst case scenarios. Accordingly, the following two scenarios will be investigated:

- 1) Power failure and a sudden pump shutdown at Yarmouk station, and
- 2) Simultaneous and sudden closure of all valves located prior to sub tanks.

To get a feeling of the pressure change during a water hammer, the *Joukowski Equation* [1, 2] for calculation was used. The equation states that the change in the head pressure (during water hammer) equal to the change in the fluid velocity multiplied by the supersonic speed (c) divided by the specific gravity (g). Mathematically it can be expressed as:

$$\Delta H = c \cdot \Delta V / g \quad (5.1)$$

where,

ΔH = change in head

ΔV = change in fluid velocity

To compare this with a sample calculation at a specific location along the KDRL, consider the junction located at the Doha-2 branch, in the case of Doha-2 valve closure. Following are the conditions at this specific location:

- HGL at the point is 71 m
- Pipe wave speed is 702 m/s
- Change in Speed is from 3.24 m/s to zero = 3.24 m/s
- Change in head = $702 \cdot 3.24 / 9.81 = 231.8$ m
- Resulting Up-Surge Head = $71 + 231.8 = 302.8$ m!! 300% increment.

Moreover, pressure wave travel along the pipe in a supersonic speed, split at junctions to all branches' pipelines, and reflect back. The wave magnifies when it splits from a wider pipeline to a narrower pipeline and magnifies at the dead ends. This is the case in all branches of the KDRL. When two wave passes by each other, they change and magnify

the flow and pressure but don not effect each other, cancel each other, subtract from each other, or add to each other. For example, consider two waves *A* and *B*. If wave *A* is 5 bar and wave *B* is -3 bar when they meet the change in magnitude will be 2 bar but after they pass each other, wave *A* and *B* will be intact (*A* is 5 bar and *B* is -3 bar). The schematic of the wave behavior at a splitting point from a wider to a narrower pipeline or vice versa with sample values is depicted in Figures 5.1, 5.2 and 5.3 [7].

To investigate the occurrence of the water hammer, Bentley HAMMER program, will be used. Table 5.1 summarizes the calculated wave speed based on the characteristics of the pipeline materials and the liquid using HAMMER.

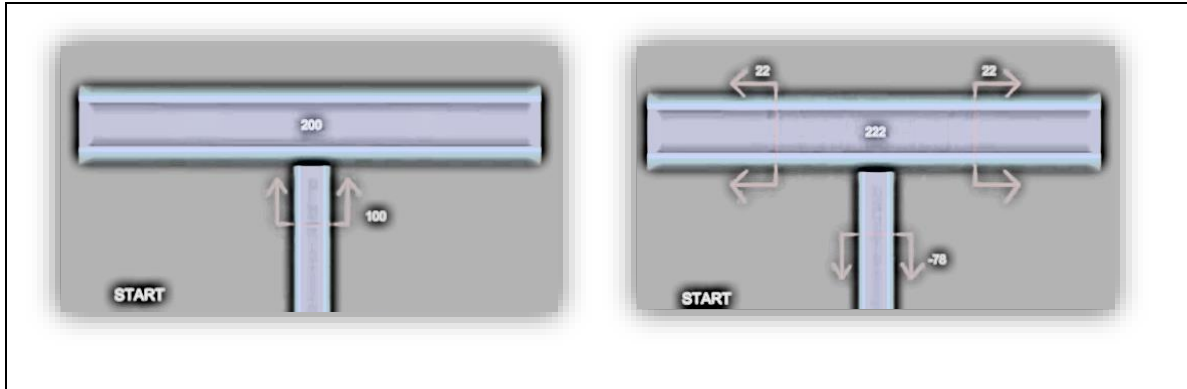


Figure 5-1 Pressure/surge wave split from small to larger pipe [20]

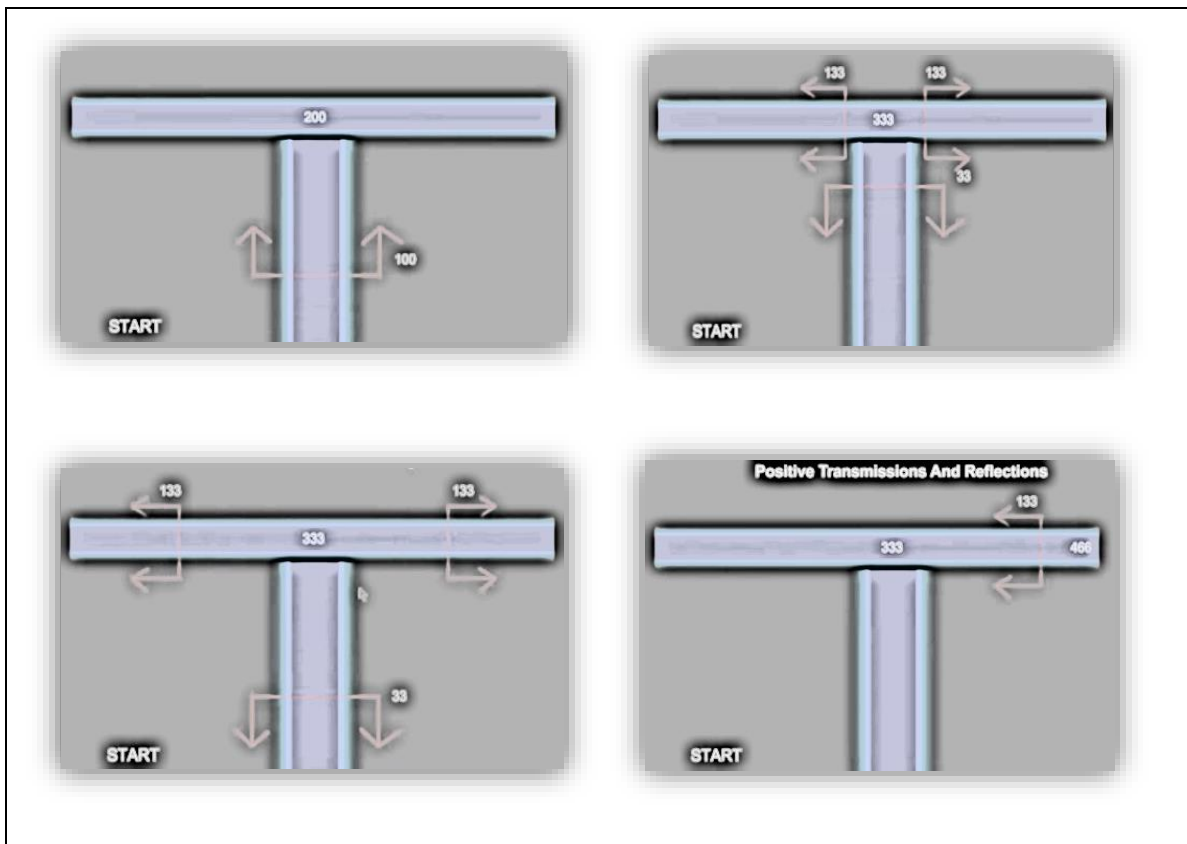


Figure 5-2 Pressure/surge wave split from large to smaller pipe, with a dead end [20]

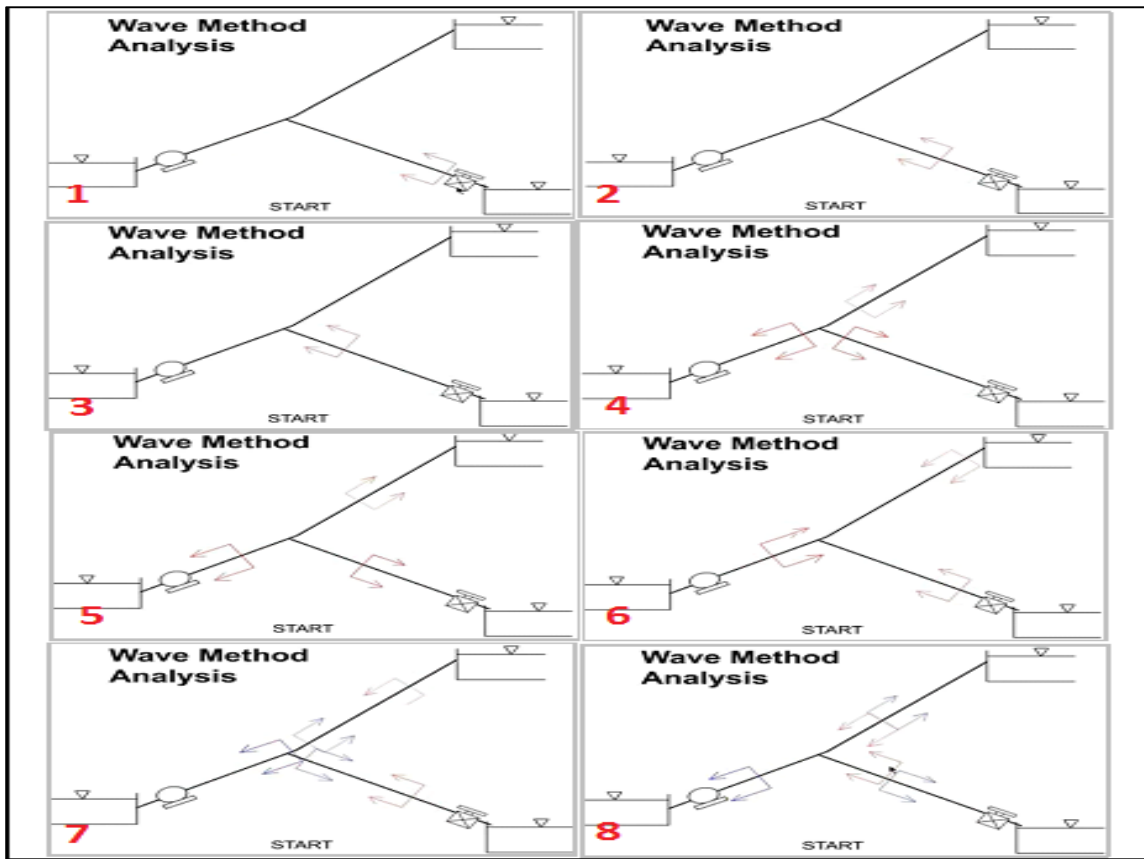


Figure 5-3 Pressure/surge wave movement and reflection through a pipe segments [20]

Table 5-1 Physical pipe characteristics

Pipe Line	Material	Dia	Length	Wave Speed	Nominal Pressure	C
		(mm)	(m)	(m/s)	(bar)	
KFUPM	UPVC	400	1,268	352	16	140
Doha-3	UPVC	200	446	485	16	140
Doha-1	UPVC	200	292	485	16	140
Doha-2	FRP	300	1010	702	16	130
Dana	DI	400	255	1,265	16	130
Palace	FRP	300	285	702	16	130
Dist-537	FRP	300	740	702	16	130
Main Line	CCP	700	18,055	1,124	24	110

5.2 Scenario 1: Power Failure and Pump Sudden Shutdown

When the water pump suddenly shuts down at Yarmouk station, the high water inertia will keep it running, causing a water column separation and cavitation. The cavitation will cause the water to vaporize and thus vapor pockets are created. When these pockets collapse water will travel rapidly generating pressure spikes that might damage the pipeline, pump or any other water network component. Figure 5.4 shows few examples of the damages that might be caused by the water hammer.

For any pipeline system similar to the KDRL, in case of power failure, then it is expected that a high negative pressure wave will develop and travel downstream to the pump station causing pressure drop along the whole pipeline up to its end. This pressure wave may be reflected backwards as a positive pressure wave up to the pump station. If a fast closing check valve is installed at the pump discharge, the high-pressure wave is normally eliminated. In case of severe negative pressures are allowed to occur along the pipeline, the cement mortar lining can breakdown. Therefore, no negative pressure shall be allowed along the KDRL.

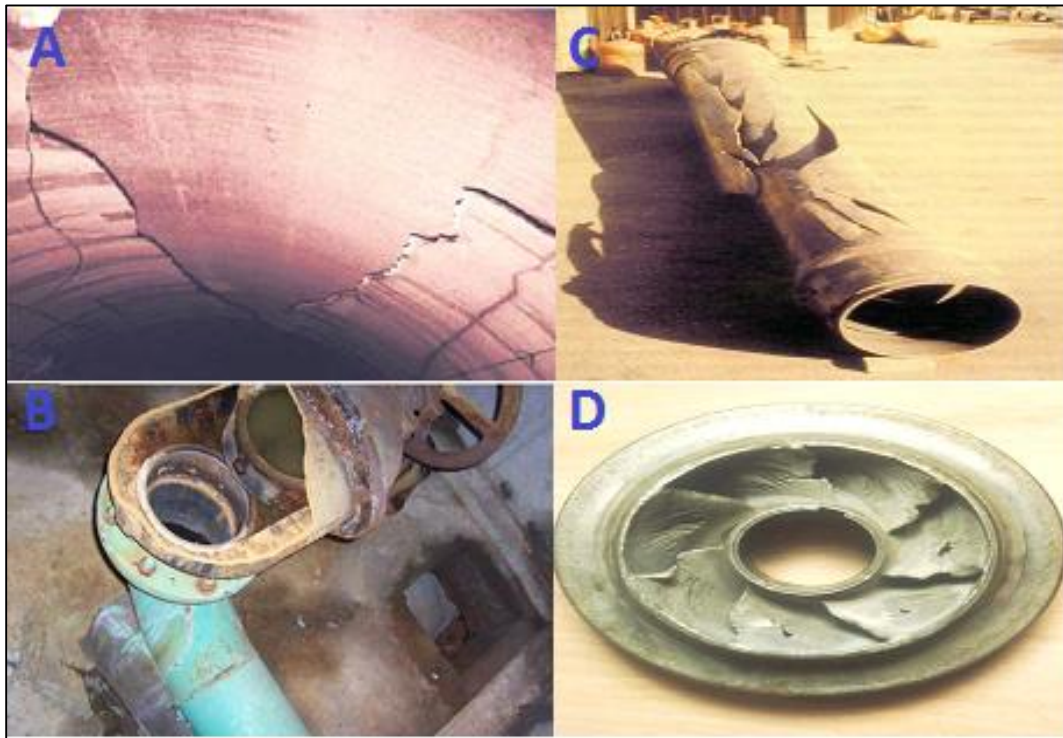


Figure 5-4 Sample effects of water hammer: (A) internal pipeline damage due to negative pressure, (B) pipeline collapse due to negative pressure, (C) and (D) pump parts damage

The constructed transient model of the KDRL executed considering power failure and pump sudden shutdown at Yarmouk. The variation of the HGL along the KDRL and selected branches' pipelines during the water hammer is displayed in Figures 5.5 to 5.8, showing the behavior of the system as a result of the transient conditions developed due to the pump shutdown without any protection devices installed along the KDRL or its branches.

The figures indicate that the major effect of the power failure is the initiation of a high negative pressure wave that travels downstream to the pump station and causes pressure drop along the pipeline up to the highest point of the pipeline. Thus, the first two branches (KFUPM and Doha-3) are severely affected by the down-surge compared to the other branches that are far away from the pump. As revealed from the figures, the pressure decreases until it reaches (-1 bar) in some locations. As a result, the water hammer analysis for this scenario clearly proves the development of a huge severe negative pressure which requires close attention and deep investigation for a surge protection to resolve this serious problem.

Note: color coding in all graphs of water hammer analysis results, is as follows:

Green : Pipeline profile elevation from sea level.

Black : Steady-State operation hydraulic grade line HGL.

Blue : Minimum pressure (max down-surge).

Red : Maximum pressure (max up-surge).

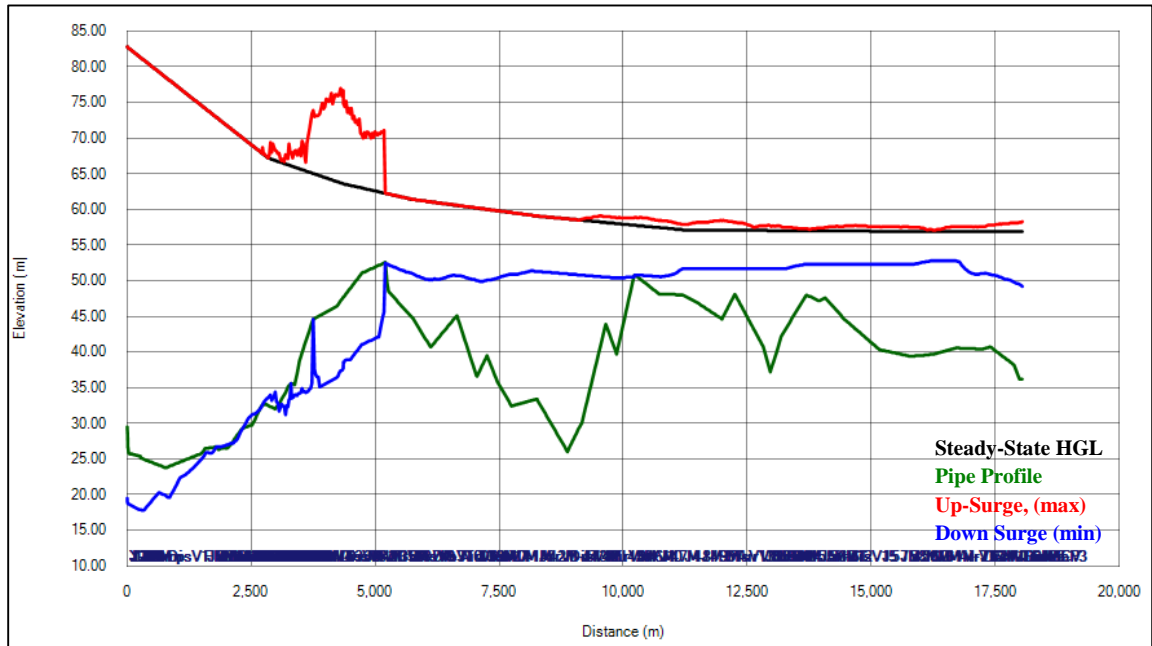


Figure 5-5 Surge wave effect along KDRL due to pump sudden shut down

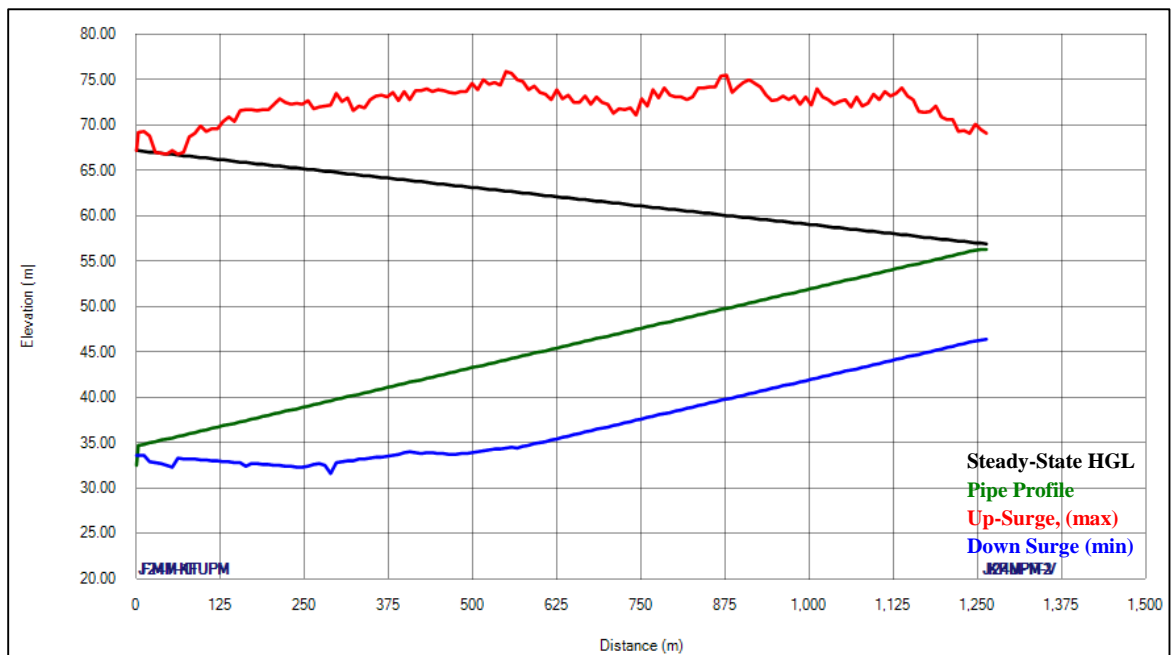


Figure 5-6 Surge wave effect along KFUPM branch due to pump sudden shut down

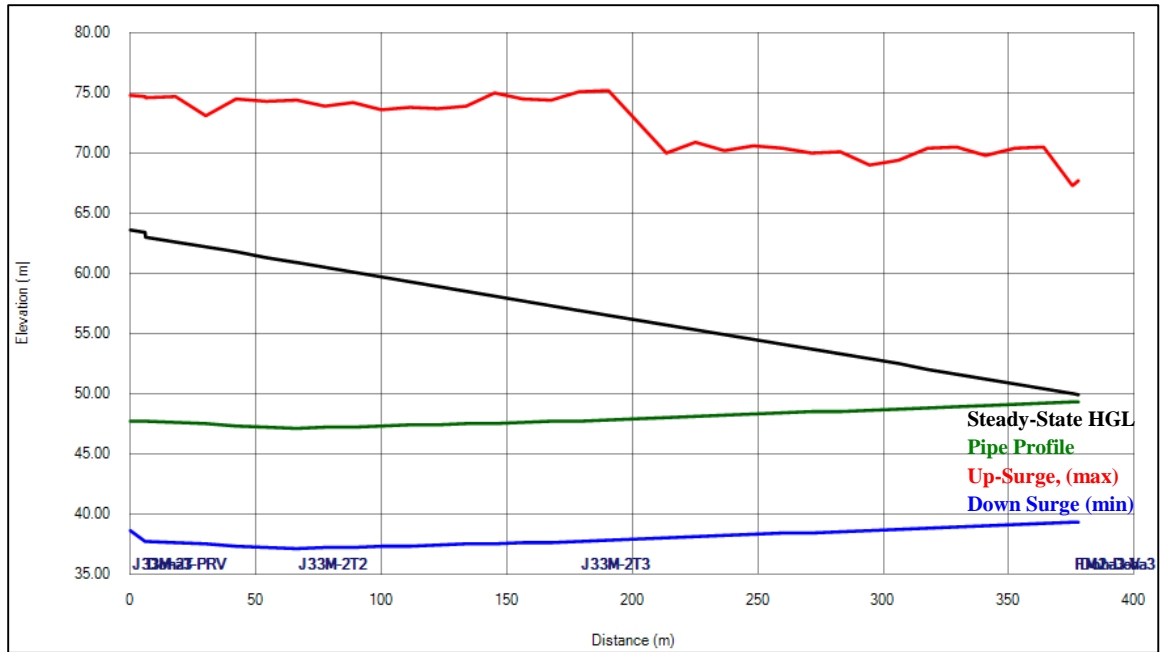


Figure 5-7 Surge wave effect along Doha3 branch due to pump sudden shut down

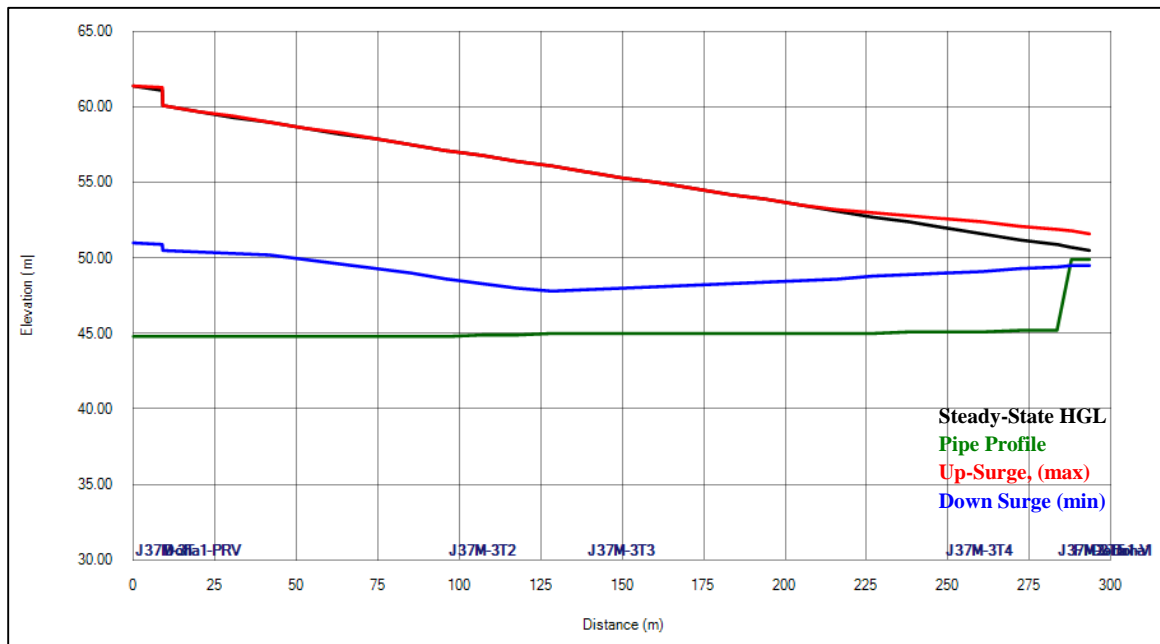


Figure 5-8 Surge wave effect along Doha1 branch due to pump sudden shut down

5.3 Scenario 2: Sudden Closure of All Valves

The second possible worst scenario that might occur is the case when all main valves installed in the branches along KDRL are closed suddenly while the pump is still operating. Such an action would cause the following:

- Decrease in the amount of the water pumped to the system.
- Pump goes back in its curve and produces more head pressure
- High energy consumption

If all valves are closed simultaneously, then maximum pressure will be created within the KDRL. This scenario represents the worst maximum up-surge pressure that could be generated in the system. The following sections present the analysis and simulation of the two situations:

- A) A single valve closure (KFUPM valve and Doha3 valve), and
- B) Simultaneous closure of all branches' main valves installed along the KDRL.

5.3.1 Sudden Closure of KFUPM Valve

One possible scenario for the development of a water hammer is the case when one of the valves installed along the KDRL is closed suddenly. For example, the sudden closure of KFUPM valve. Such incidents have occurred frequently in the past. Figures 5.9 to 5.11 show the system transient behavior at selected locations. As revealed from the figures that the main pipeline and all other branches are severely affected by the generated surge wave.

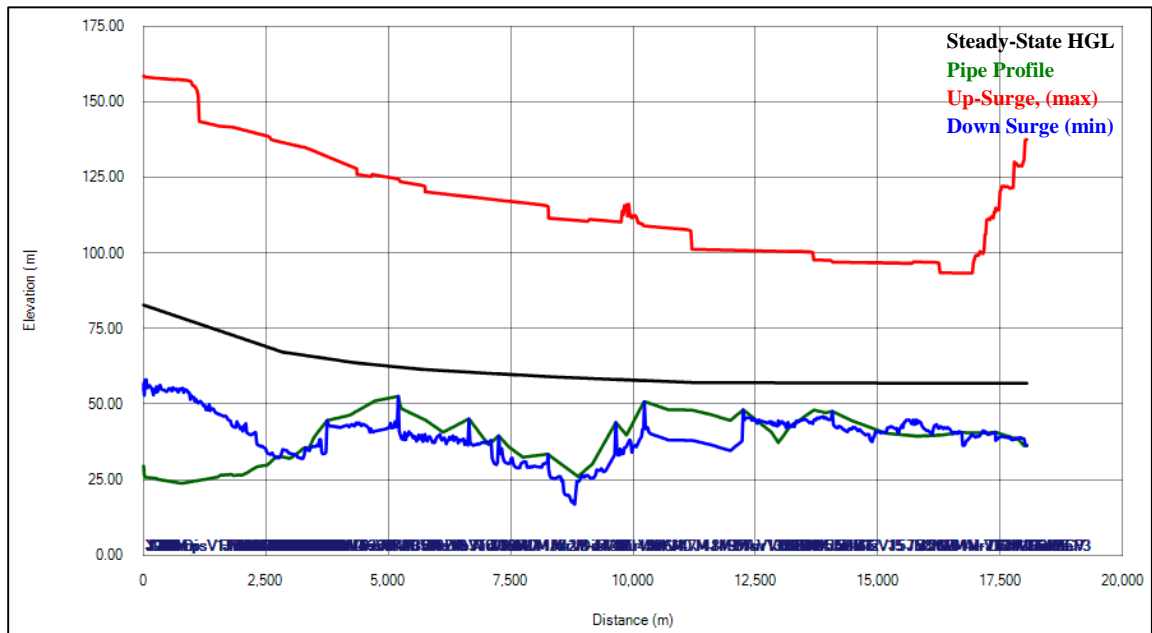


Figure 5-9 Surge wave variation along KDRL due to the sudden valve closure at KFUPM

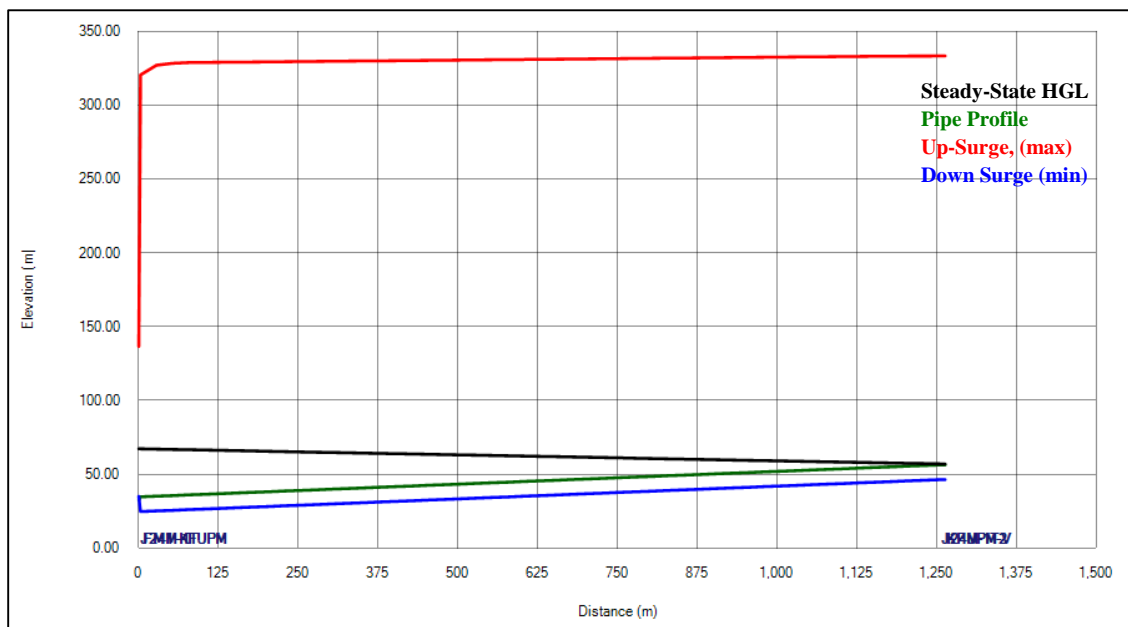


Figure 5-10 Surge wave variation along KFUPM branch due to the sudden valve closure at KFUPM

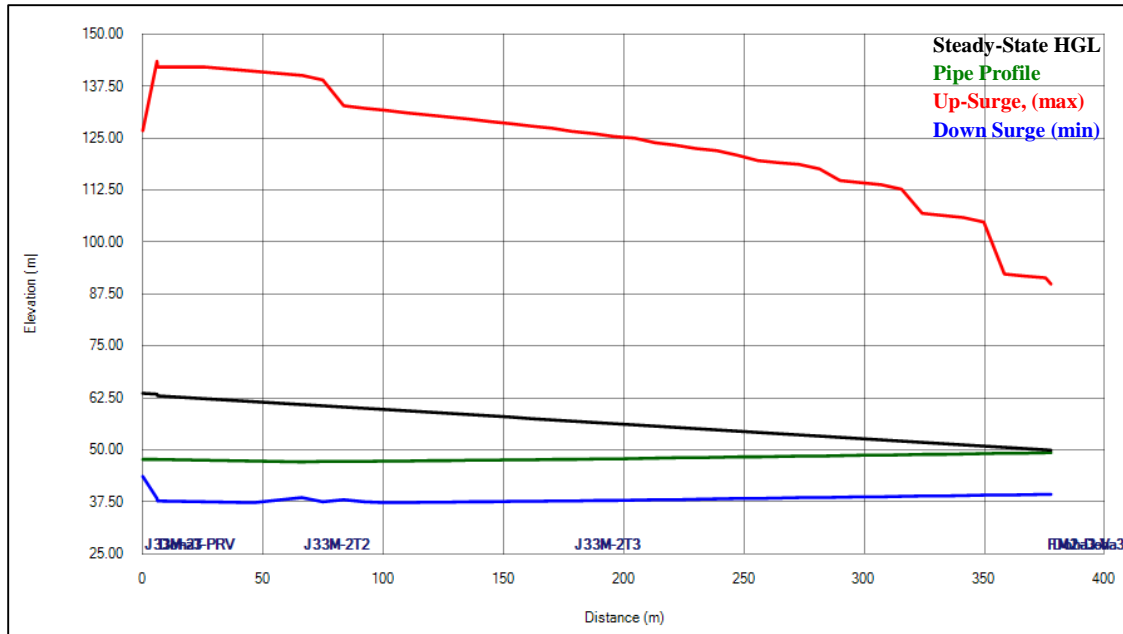


Figure 5-11 Surge wave variation at Doha3 due to the sudden valve closure at KFUPM

The figures also show that the pressure decreases until it reaches (-1 bar) at some locations. Thus, a surge protection is essential for this case. Moreover, corrections to the system setup maybe required to eliminate or minimize the effect from the branches on the network, including the main pipeline and the other branches' pipeline.

5.3.2 Sudden Closure of Doha3 Valve

Another example for a single valve closure is the case when the valve at Doha3 is suddenly closed. Figures 5.12 to 5.14 show the system behavior and the HGL variations at selected locations along the KDRL. The development of huge pressure acting on the pipelines is evident. Negative pressure is also clear at certain sections of the pipeline.

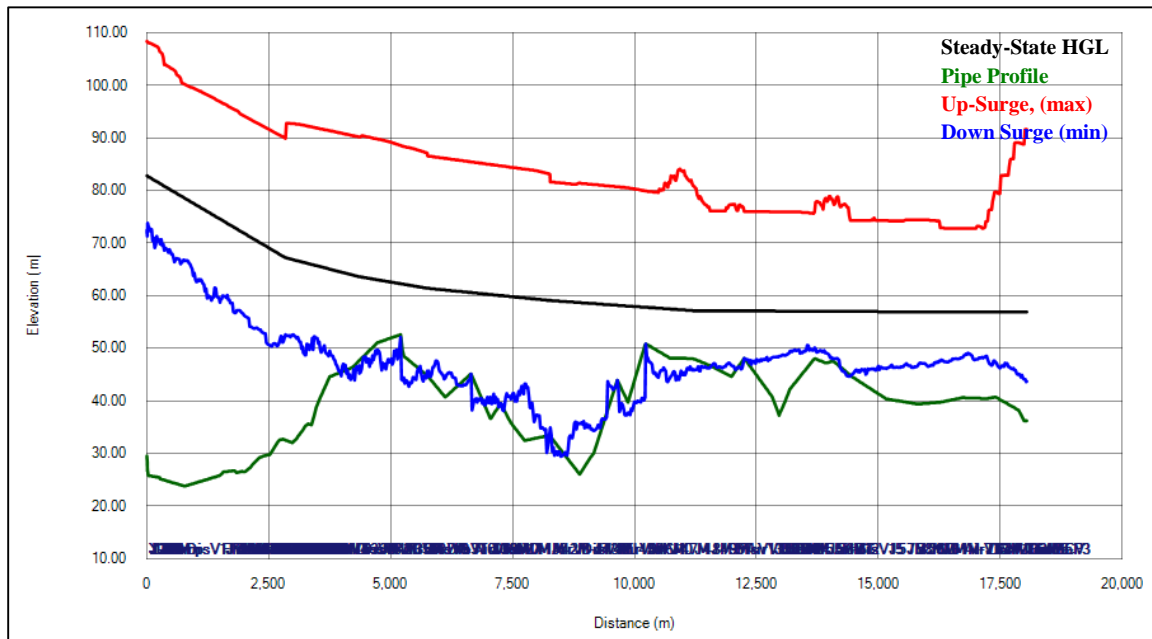


Figure 5-12 Surge wave variation along KDRL due to sudden valve closure at Doha3

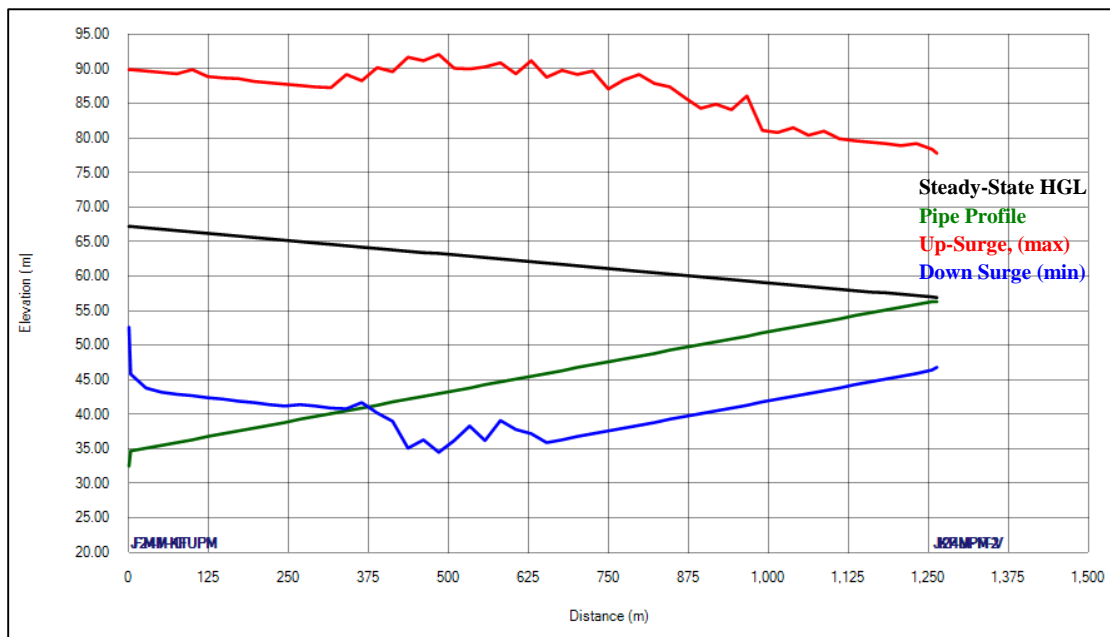


Figure 5-13 Surge wave variation at KFUPM due to sudden valve closure at Doha3

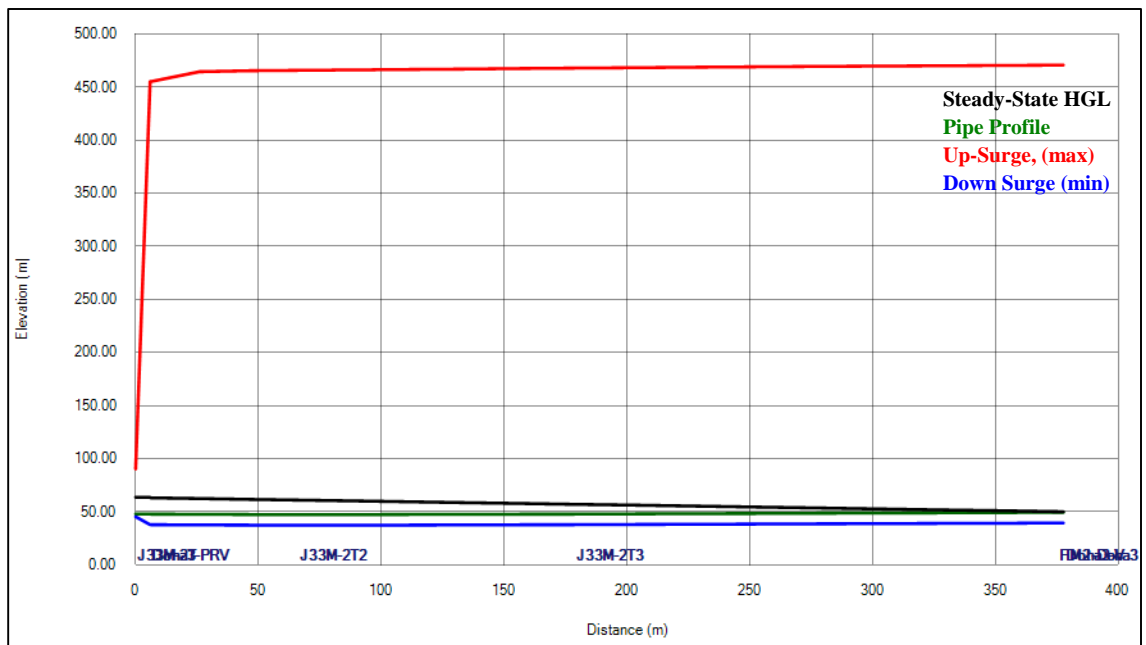


Figure 5-14 Surge wave variation at Doah3 branch due to sudden valve closure at Doha3

The effect of a sudden closure of Doha3 valve will propagate to the main pipeline and all other branches. However, the effect due to Doha3 valve closure is less than the effect of KFUPM valve closure but it is still unacceptable. Such incidents have occurred frequently in the past, which requires an immediate action to protect the main line as well as the branched pipelines from water hammer.

5.3.3 Sudden Closure of All Valves

Another possible scenario is the case when all valves installed in the branches along the DKRL are closed suddenly at the same time. As expected a huge surge wave will develop which will propagate upstream/downstream along the pipeline. Figures 5.15 to 5.17 show the surge wave variation at selected locations. It is obvious that an action should be taken to control this huge pressure; otherwise, the pipeline or the installed devices along the pipeline will be damaged.

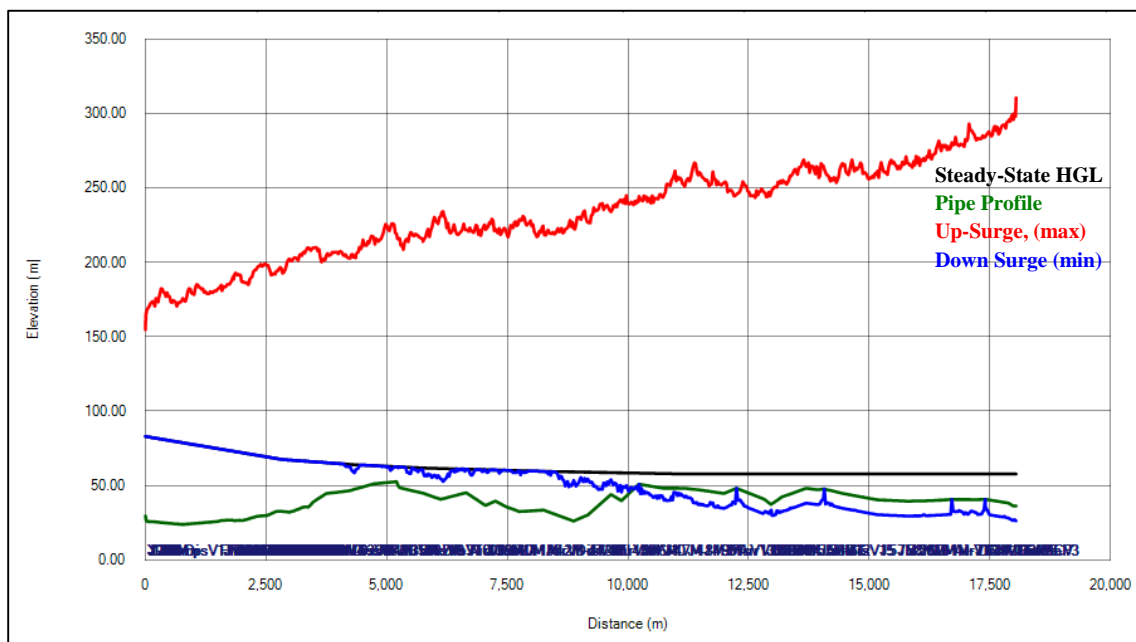


Figure 5-15 Surge wave variation along DKRL due to sudden closure of all valves

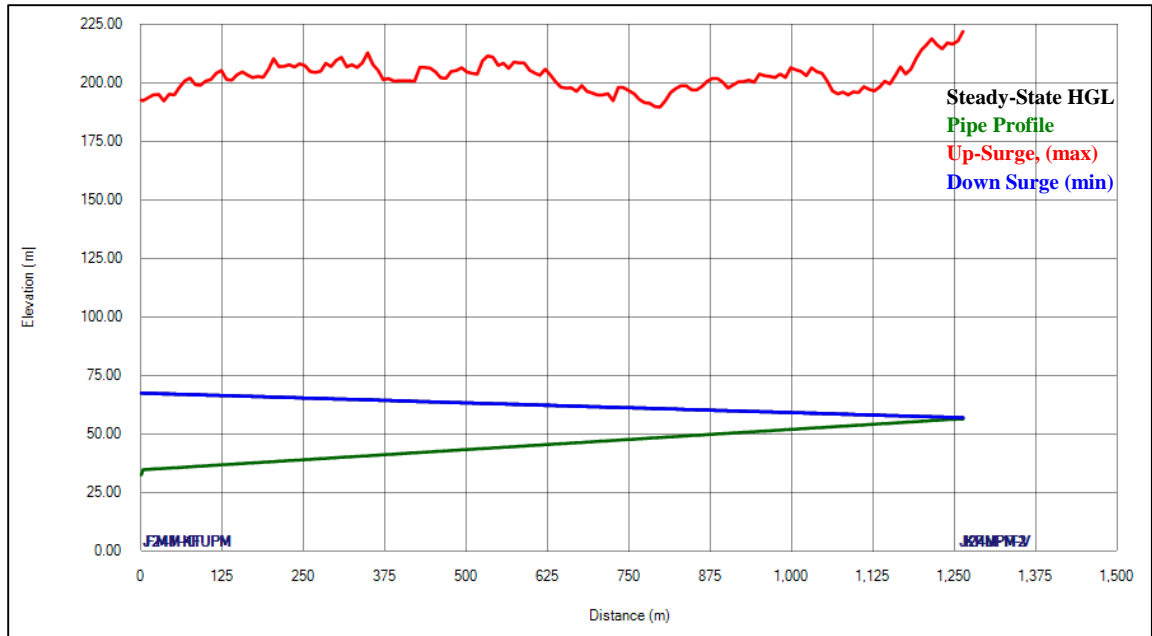


Figure 5-16 Surge wave variation at KFUPM due to sudden closure of all valves

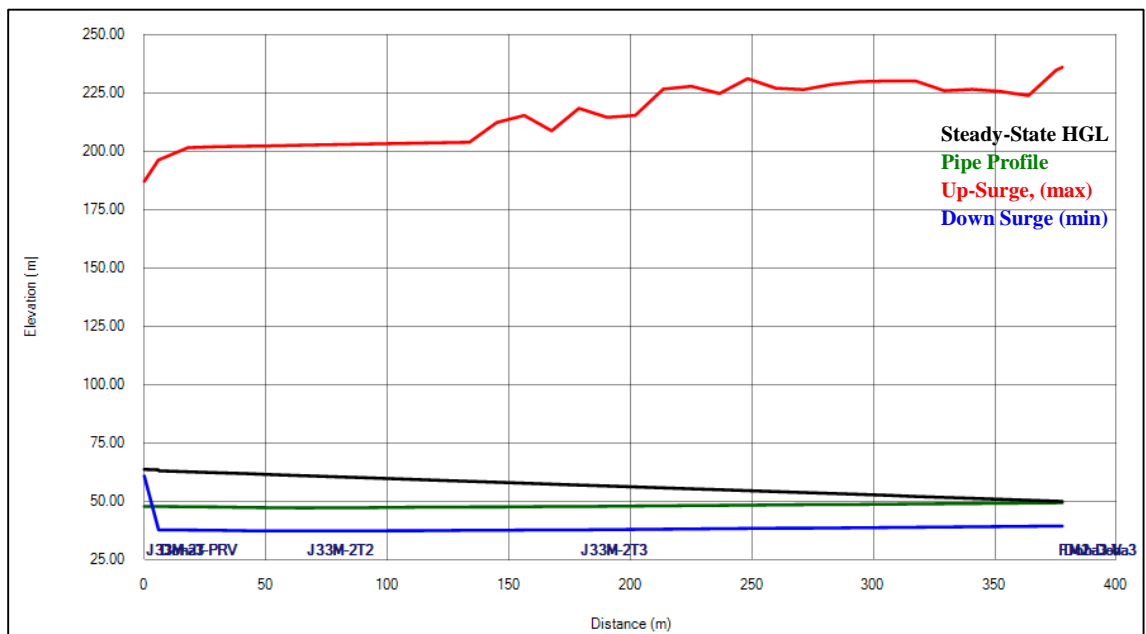


Figure 5-17 Surge wave variation at Doah3 due to sudden closure of all valves

CHAPTER 6

WATER HAMMER CONTROL

6.1 Background

Water hammer protection is not only about installation of surge protection devices to resolve the water hammer issue. It is more about preventing any potential or minimize the probability of a water hammer occurrence by controlling the system setup and operation. Therefore, the operational procedures and controls of the system need to be optimized first. Then, water hammer mitigation devices should be installed to absorb upsurge and down-surge waves in extreme cases, e.g. power outage.

6.2 Isolating Branched Pipes from KDRL

As mentioned previously, branch pipelines, with the current setup of placing the isolation and check valve at the far end of the branch pipeline (prior to the sub tank), are affecting the KDRL hydraulics even when they are closed. This is due to the surge waves and water column returning from the branch pipeline back to the system. For example, in the KFUPM branch, which is 1,268 meter long with an elevation difference between the tank base and the branch connection point to the KDRL is about 24 meter, the backflow from the branch during the water hammer is large enough to severely affect the system. To resolve this problem, the branches' effects to the main line should be eliminated by

installing an isolation valve and a check valve just upstream of the branching point. Figures 6.1 to 6.3 shows a schematic diagram of the existing and proposed setups.

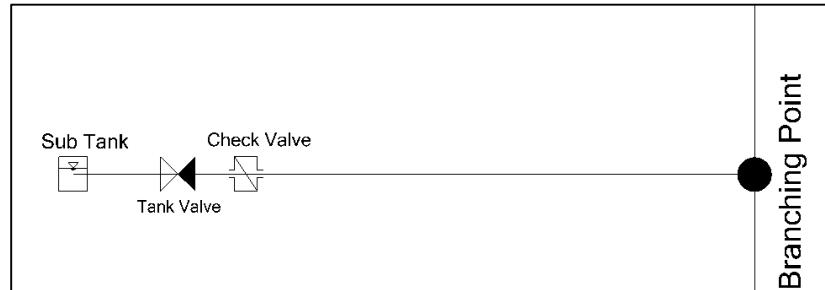


Figure 6-1 Existing system setup, tank valve and check valve in the upstream (case A)



Figure 6-2 Proposed setup, tank valve upstream and check valve downstream (case B)



Figure 6-3 Proposed setup, tank valve and check valve downstream the pipe (case C)

The following sections will discuss the effect of the valve closure on the surge wave development when isolating the branch from its connection point with the main pipeline.

The analysis is performed for the following cases of operational controls:

- a) Closure of the valve upstream of the tank with no check valve installed in the branching point (current practice).
- b) Closure of the valve upstream of the tank with a check valve installed in the branching point.
- c) Closure of the valve at the branching point.

Figures 6.4 to 6.6 show the results of the HAMMER for the above-mentioned cases. The figures represent the situation when KFUPM valve is suddenly closed while the other valves were still open. Figure 6.4 shows the effect of KFUPM valve closure for the above-mentioned cases on the main pipeline. The figure indicates that the down-surge extreme effect on KDRL will occur for case A when the valve is closed upstream of the branched pipeline. On the other hand, the effect is minimal in the case of isolating the KFUPM branch pipeline from the main pipeline by either placing a check valve at the branching point (case B) or closing the valve at downstream of the branch pipeline (case C). The figure also indicates that case C has the minimum up-surge effect.

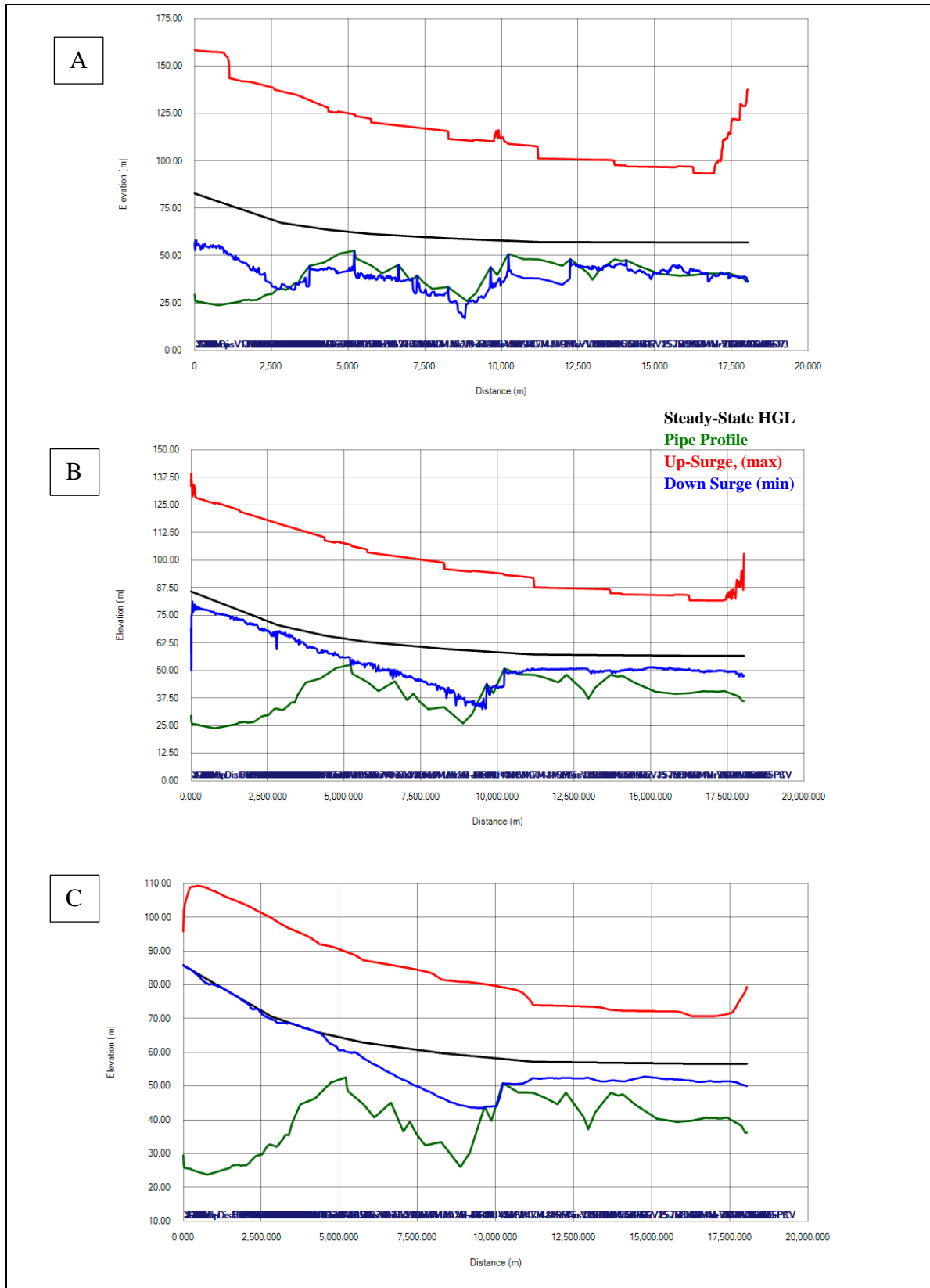


Figure 6-4 Water hammer analysis results comparison for cases A, B, and C– main pipeline

Figure 6.5 shows the effect of KFUPM closure for the above-mentioned cases on the KFUPM branch pipeline, it is clearly shown that case A is the worst for both up-surge and down-surge wave development in the system. On the other hand, case B has no risk of down-surge, and the developed upsurge is less than (case A). Finally, case C shows a risk of down-surge development whereas, the up-surge development is minimal. For the effect on KFUPM branch case C is acceptable, even with the risk of down-surge development, because the effect could be controlled easier when there is no outside effect. Figure 6.6 shows the effect of KFUPM closure for the above-mentioned cases on the Doha-3 branch pipeline. The figure reveals that case A is the worst for both up-surge and down-surge wave development in the system. On the other hand, case C seems to be the best which shows that the developed up-surge is minimal and there no risk of down-surge. Moreover, case B is still accepted and could be mitigated within the branch pipeline without transferring the effect back to the main pipeline.

Similar analysis can be performed to all branches. Therefore, according to the above analysis, the branch pipeline is recommended to be isolated from the main pipeline at the branching point (downstream of the branch pipeline) which will minimize the surge waves that could propagate from the branched pipes to the KDRL. Even in the case where a worse situation in the branch pipeline takes place, it will be easier to be resolved. Moreover, it will be less costly and risky if it fails and takes less time to be retrieved from a failure where only one part of the system will be out of service. The out-of-service part can still be served with raw water pumped from groundwater wells. However, if KDRL fails, all communities will be out of service.

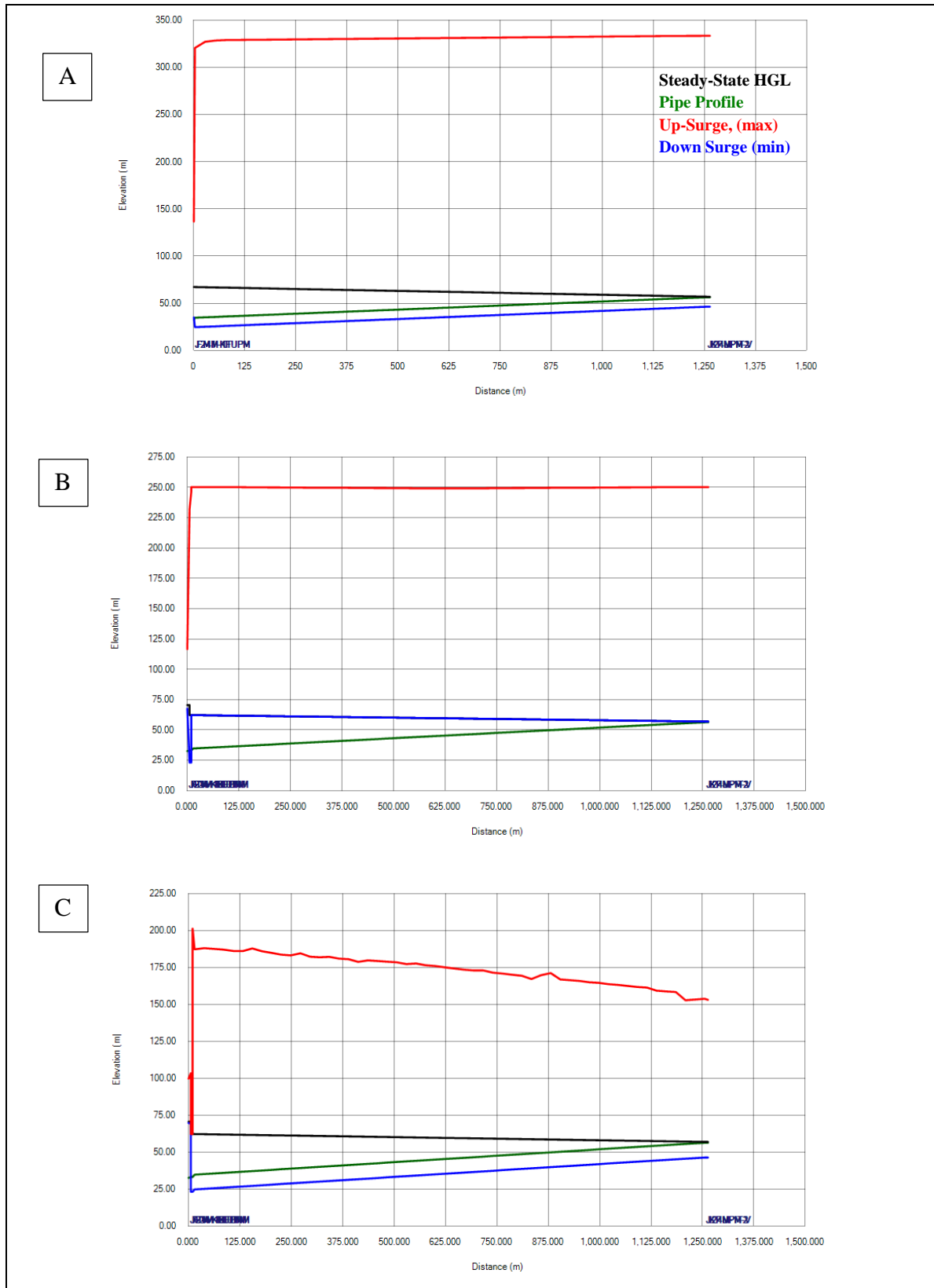


Figure 6-5 Water hammer analysis results comparison for cases A, B, and C – KFUPM branch

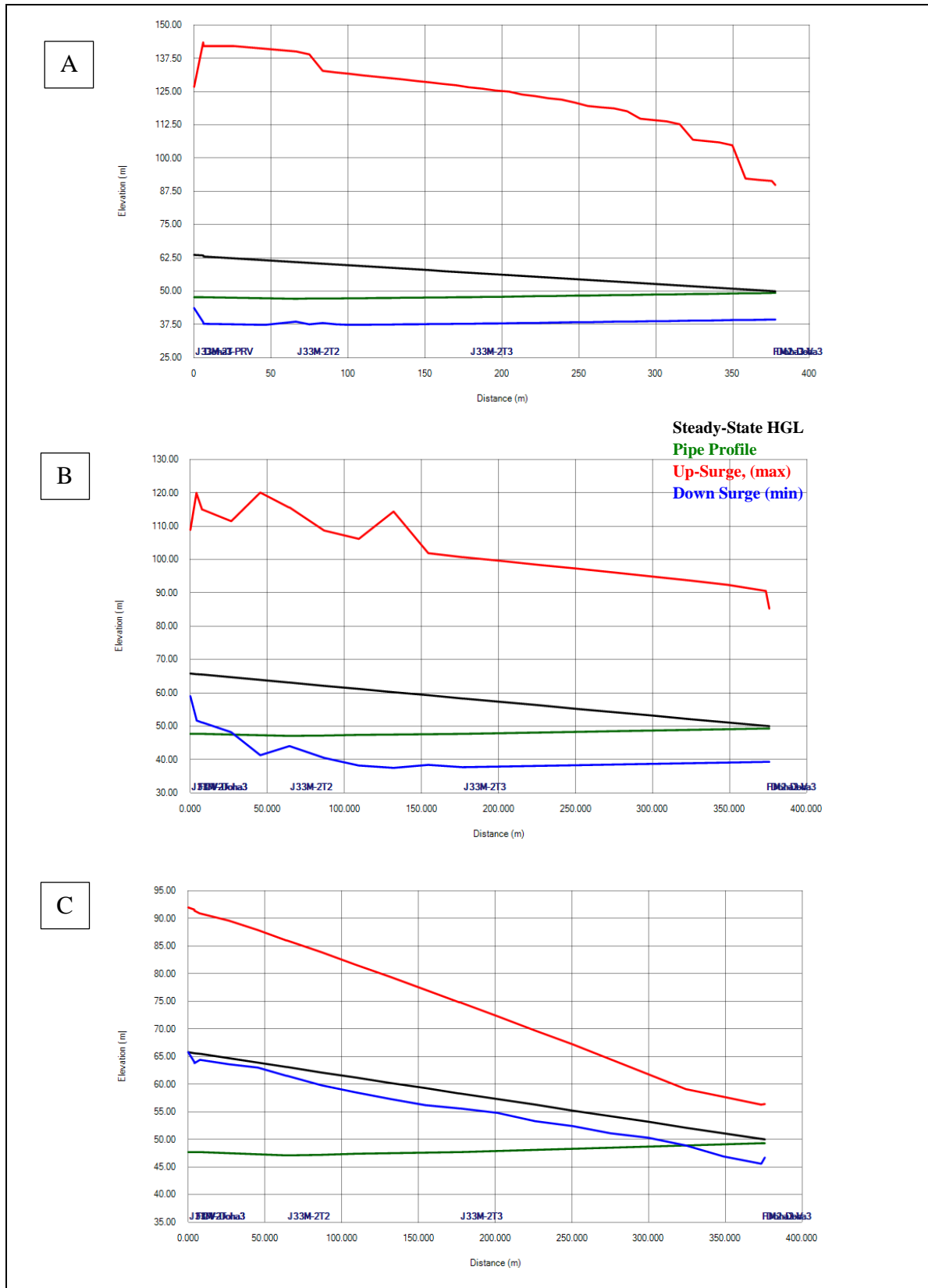


Figure 6-6 Water hammer analysis comparison for cases A, B, and C – Doha3

6.3 Power Failure Protection

The power failure has also been studied. For this scenario, several model simulations have been performed in order to identify the best surge preventive solution. As the water hammer action causes a negative pressure in the pipeline, the most effective ways to handle this situation is by using surge vessels downstream the pump. The surge vessels and air valves are particularly effective when there is a loss of power and a negative pressure (down-surge) wave develops. The residual pressure in the surge vessel reduces the liquid column, compensates for the loss of the pressure due to the pumps shutdown, and accordingly prevents the negative pressure. Air valve settings were optimized to ensure their effectiveness for the surge wave resistance as vacuum breakers, where all air valves were set to intake air fast but release it slowly.

After several runs of the model, it has been observed that using a surge vessel and air valves with the following specifications will solve the problem of the negative pressure:

- A) Surge vessel with an effective volume of 13m^3 and a maximum working pressure of 8 bars.
- B) Existing air valves with an inlet orifice of 150mm and an Outlet orifice of 50mm.

The effect of the surge preventing equipment on the KDRL and the selected branches are presented in Figures 6.7, 6.8 and 6.9.

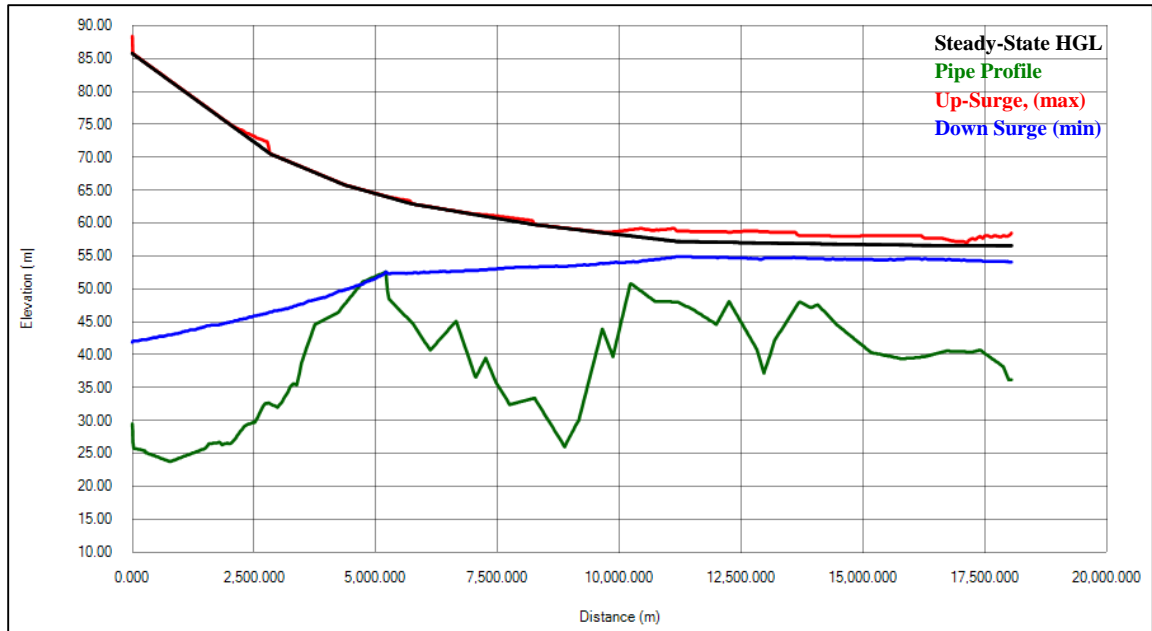


Figure 6-7 Surge protection using surge vessel – main pipeline

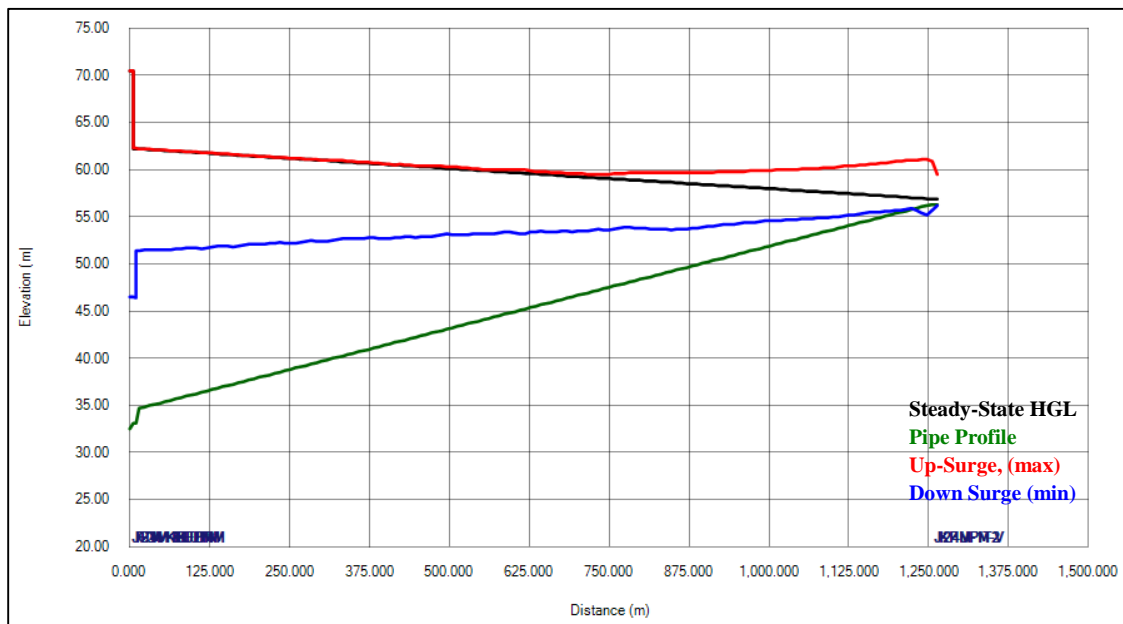


Figure 6-8 Surge protection using surge vessel – KFUPM

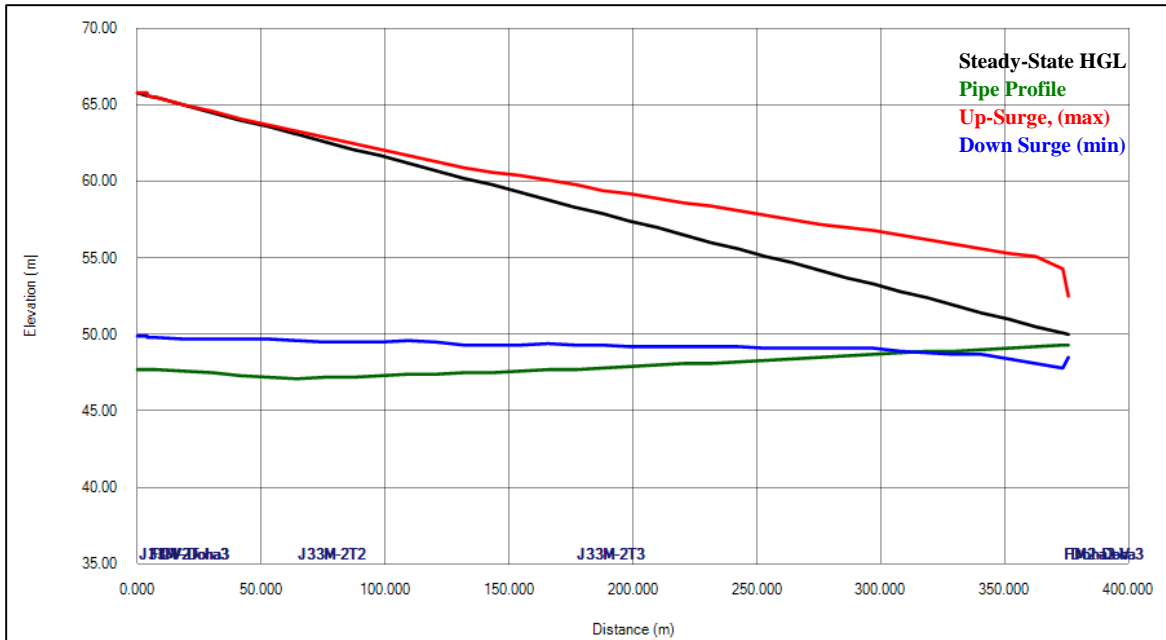


Figure 6-9 Surge protection using surge vessel – Doha3

As revealed from the figures the wave pressure due to the transient condition drops dramatically indicting the efficiency of the installing surge vessel and air valves along the pipeline.

6.4 All Valves Sudden Closure Protection

The water hammer action of a rapid valve closure of the water supply branches causes a high pressure along the pipeline. The following solutions are the common solutions to eliminate the effect of the high pressure:

- Installation of a pressure relief valve
- Installation of a surge vessel
- Extension of the closure time of the valves
- Installation of a rigid pipeline that can sustain high pressure

As stated earlier, changing the route of the KDRL is not an option. Moreover, any operational correction policy is eliminated keeping in mind the worst case of having a non-skilled operator. Thus, installation of a pressure relief valve is suggested since there is already a surge vessel installed at Khobar PS. Also, it might be an option to install another surge vessel at Dammam PS. Pressure Relief Valves (PRVs) installations at different locations along the KDRL were tested. These locations are proposed at sites where washout chambers already installed and the available space can accommodate for additional valve installation. After several model runs (details are available in Appendix D) an optimized solution was achieved. This model was achieved while monitoring the change in the maximum and minimum surge pressure and the amount of water expelled out from the system at each point.

According to water hammer simulation, the proposed solution is to install three Pressure Relief Valves with the following specifications:

- Threshold Pressure = 6 bars
- Diameter = 600 mm
- Spring Constant = 150 lb/in

The proposed PRVs are recommended to be installed at the following locations:

- Yarmouk station and connected with an overflow pipe to the tank to assure no water wasted (the over flow from the PRV = 41 m³)
- Chamber of washout valve No 5. (overflow = 2 m³)
- Chamber of washout valve No 13. (overflow = 4 m³)

Figure 6.10 shows the effect of surge preventing equipment on the KDRL. In addition, after resolving the water hammer problem in the KDRL, it has been noticed that all water hammer/transient problems in the branches were also resolved. Figure 6.11 depicts the protected model results for the KFUPM branch, where there is no suction pressure at any point along the pipeline and the maximum pressure is within the nominal pressure of the pipeline.

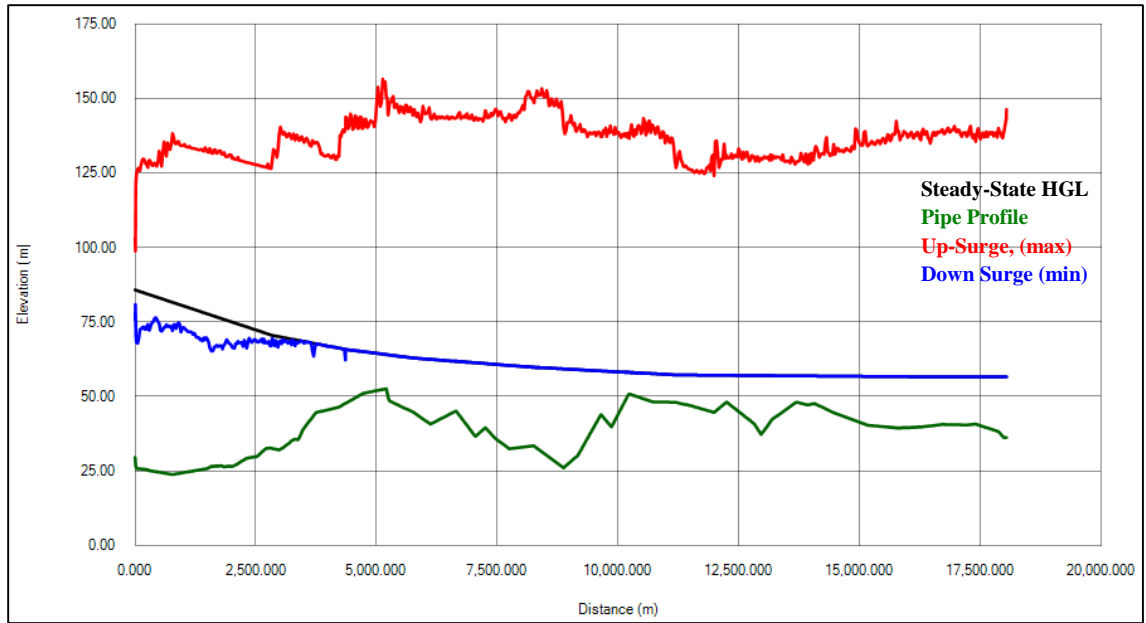


Figure 6-10 Optimized protection considering sudden closure of all pipes – main pipeline

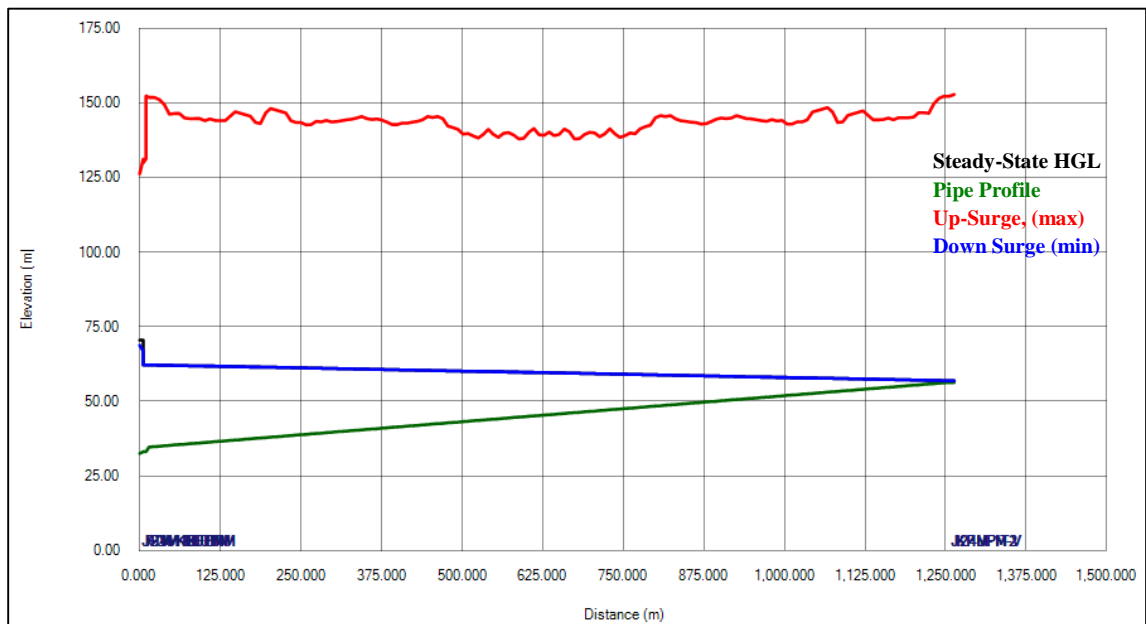


Figure 6-11 Optimized protection considering sudden closure of all pipes – KFUPM

CHAPTER 7

CONCLUSION AND RECOMMENDATIONS

Khobar-Dammam Ring Line (KDRL) is of great importance to the water supply network of Khobar as well as Dammam cities. Two main potential problems associated with water hammer that need to be mitigated to keep this water network operational: the up-surge and the down-surge because they can cause pipe rupture and backflow of dirty water into the water distribution system. The main cause of the two phenomenon is a sudden change in flow condition such as during the daily startup or shutdown of a pump or closing a valve, leading to a pressure spike forming a surge wave that travels with a supersonic speed through the system. Thus, the control of these two phenomenon is essential not only to keep the water running but also to provide a safe water supply to two highly populated cities in the eastern region.

The current practice for protection of the KDRL from the water hammer are:

- 1- A soft startup/shutdown of the pump
- 2- Main valve closure 10 second before the pump shutdown.

These operational constraints are of no value in case of power failure.

To mitigate the water hammer problems, a model was constructed for the KDRL network. The model was reliable and representative to the real operation conditions as it was calibrated with field data.

Water hammer has been investigated in KDRL for two cases:

- 1- Power failure in pumping station.
- 2- Rapid close of actuator valves at 5 tank at the same time, assuming other two branches are closed.

The calculations of the surge wave for water hammer show the following effects:

1. During the power failure: negative water pressure along the pipeline goes up to the point where the pipeline is at a maximum elevation.
2. During the rapid valves closure: high water pressure along the KDRL was observed to increase from the normal working pressure of 6-7.5 bar to a surge pressure of >20 bar.

From the water surge study results, the following recommendations were made to solve the surge problem:

- 1- A 13 m³ surge vessel with a maximum working pressure of 8 bar be installed downstream of the pumping station.

- 2- Pressure Relief Valves with the following specifications be installed at three locations: downstream of the pump station, and at washout chambers number five and thirteen.
 - a- Diameter if 600 mm
 - b- Spring Constant of 150 lb/in.
 - c- Threshold pressure of 6 bars.
- 3- Configure Air Valves to slowly release air, outlet orifice should not exceed 2-3”.

In addition, the following actions were recommended to protect the KDRL network:

- 1- A standby pump be added to operate in emergency cases (during the primary pump failure).
- 2- A non-return flow control valve be installed at the branching point to prevent back flow to main pipeline and eliminate the effect of branches on the main pipeline.
- 3- Valves be installed, in the same place, to isolate all branches from the main KDRL at the branching point close to the served water tank. These valves better to be as pressure control valves or flow control valve to control the amount of water delivered to the tank and to maintain the delivering pressure to the branch pipe.
- 4- Enforce a policy of time delay in start-up/shutdown of a pump, or closing and opening of a valve.

References

- [1] D. J. Wood, S. Lingireddy and P. F. Boulos, Pressure Wave Analysis of Transient Flow in Pipe Distribution System, Pasadena, California USA: MWHsoft, 2005.
- [2] Haested-Methods, T. M. Walski, D. V. Chase, D. A. Savic, W. Grayman, S. Beckwith and E. Koelle, Advanced Water Distribution Modeling and Analysis, Exton, Pennsylvania USA: Bentley Institute Press, 2007.
- [3] B. S. Jung, B. W. Karney, P. F. Boulos and D. J. Wood, "The Need for Comprehensive Transient Analysis of Distribution Systems," AWWA, vol. 99, no. 1, 2007.
- [4] P. F. Boulos, K. E. Lansey and B. W. Karney, Comprehensive Water Distribution Analysis Handbook for Engineers and Planners, Pasadena, California USA: MWHsoft, 2006.
- [5] B. E. Larock, R. W. Jeppson and G. Z. Watters, Hydraulics of Pipeline Systems, USA: CRC Press, 2000.
- [6] Haested Methods Inc., WaterGEMS for ArcGIS, Waterbury, USA: Haested Methods Inc., 2003.
- [7] Bentley, "E-Doc," Bentley, 2004. [Online]. Available: www.bentley.com. [Accessed 2013].

- [8] A. Bergant, A. R. Simpson and E. Sijamhodzic, *Water Hammer Analysis of Pumping Systems for Control of Water in Underground Mines*, Ljubljana, Slovenia, Yugoslavia: Pro, 1991.
- [9] E. B. Wylie and V. L. Streeter, *Fluid Transient*, USA: McGraw-Hill, 1978.
- [10] A. Lohrasbi and R. Attarnejad, "Water Hammer Analysis by Characteristic Method," *American J. of Engineering and Applied Sciences*, vol. 1, no. 4, pp. 287-294, 2008.
- [11] K. H. Asli, A. K. Haghi, H. H. Asli and E. S. Eshghi, "Water Hammer Modeling and Simulation by GIS," *Modelling and Simulation in Engineering*, vol. 2012, 2012.
- [12] A. Bergant and A. Tijsseling, *Parameters Affecting Water Hammer Wave Attenuation, Shape and Timing*, Technische Universiteit Eindhoven, 2001.
- [13] B. S. Jung, P. F. Boulos, D. J. Wood and C. M. Bros, "A Lagrangian Wave Characteristic Method for Simulating Transient Water Column Separation," *AWWA*, vol. 101, no. 6, 2009.
- [14] D. Ramalingam, S. Lingireddy and D. J. Wood, "Using The WCM for Transient Modeling of Water Distribution Networks," *AWWA*, vol. 101, no. 2, 2009.
- [15] A. R. Simpson, *Large Water Hammer Pressures Due to Column Separation in Sloping Pipes (Transient)*, ProQuest Dissertation & Thesis, 1986.

- [16] B. S. Jung, P. F. Boulos and D. J. Wood, "Effect of Pressure-Sensitive Demand on Surge Analysis," *AWWA*, vol. 101, no. 4, 2009.
- [17] Z. Y. Wu and T. M. Walski, "Pressure Dependent Hydraulic Modeling for Water Distribution Systems under Abnormal Conditions," in *IWA World Water Congress*, 2006.
- [18] Y. W. Zheng, R. H. Wang, T. M. Walski, S. Y. Yang, D. Bowdler and C. Baggett, "Efficient Pressure Dependent Demand Model for Large Water Distribution System Analysis," in *8th Annual International Symposium on Water Distribution System Analysis*, Cincinnati, Ohio, 2006.
- [19] B. S. Jung, P. F. Boulos and D. J. Wood, "Pitfalls of Water Distribution Model Skeletonization for Surge Analysis," *AWWA*, vol. 99, no. 12, 2007.
- [20] KYPipe LLC, "Learning about KYPipe," KYPipe LLC, [Online]. Available: www.KYPipe.com. [Accessed 2013].
- [21] P. F. Boulos, B. W. Karney, D. J. Wood and S. Lingireddy, "Hydraulic Transient Guidelines for Protecting Water Distribution System," *AWWA*, vol. 97, no. 5, 2005.

APPENDICES

Appendix A

Field Survey Results

Table A-1: Survey elevation Vs as-built elevations

CODE	STATION	ELEV	ELEV (ABD)	DIFF	Notice
TANK	0	29.323	29.5	-0.177	Yarmouk Tank
DisV1	776.833	23.427	23.76	-0.333	G-ELEVATION
FM-Yar	1503.463	27.002	25.78	1.222	G-ELEVATION - Main FM
AirV1	1797.863	27.214	26.7	0.514	P3
xxx	1883.413	27.339	25.98	1.359	ROAD CROSSING
J11M	1952.813	28.177	26.6	1.577	ROAD CROSSING
DisV4	2013.123	27.822	26.45	1.372	
AirV2	2799.213	35.17	32.68	2.49	
J25M-1T	2846.333	34.643	31	3.643	KFUPM FM
DisV6	2986.453	34.291	32.05	2.241	
AirV3	3305.273	37.855	35.59	2.265	
J30M	3318.113	37.771	35.59	2.181	PLUG
DisV8	3379.883	37.471	35.4	2.071	
AirV4	3752.903	46.791	44.58	2.211	
DisV10	4225.793	48.33	46.36	1.97	G-ELEVATION
DisV12	4362.753	50.139	47.7	2.439	Doha-3 FM
AirV5	5208.543	57.415	52.57	4.845	G-ELEVATION
J38M-3T	5758.153	47.745	44.77	2.975	Doha-1 FM
DisV16	6121.673	43.543	40.68	2.863	
AirV6	6649.143	48.182	45.13	3.052	
DisV18	7057.323	40.098	36.6	3.498	
AirV7	7255.393	43.025	39.51	3.515	
J41M	7452.043	39.332	35.8	3.532	PLUG
xxx	7576.863	36.005	32.44	3.565	G-ELEVATION
AirV8	8273.213	37.142	33.44	3.702	G-ELEVATION

CODE	STATION	ELEV	ELEV (ABD)	DIFF	Notice
J44M-4T	8279.873	37.059	33.24	3.819	Doha-2 FM
DisV19	8884.313	30.619	26.03	4.589	
AirV9	9655.153	48.045	43.93	4.115	
AirV10	10226.363	50.748	50.85	-0.102	G-ELEVATION
48M	10723.363	51.283	49.11	2.173	PLUG
xxx	10734.473	51.18	49.09	2.09	PLUG
J49M-5T	11209.773	50.008	48.02	1.988	Dana FM
J50M	11536.753	48.679	46.77	1.909	
DisV23	11998.783	46.561	44.61	1.951	
xxx	12013.643	46.702	44.63	2.072	PLUG
AirV11	12257.923	49.968	48.08	1.888	
DisV23	12971.923	39.387	37.25	2.137	
J53M	12990.923	40.29	37.36	2.93	ROAD CROSSING
J54M	13092.953	39.786	37.65	2.136	ROAD CROSSING
J57M-6T	13699.843	48.761	48.06	0.701	Palace FM
AirV12	14077.223	49.204	47.61	1.594	
DisV25	14475.053	46.27	44.54	1.73	G-ELEVATION
J58M	15177.783	37.974	40.31	-2.336	
J65M-7T	15611.783	42.23	40	2.23	Dist-537 FM
J66M	16709.783	43.95	40.57	3.38	
DisV27	17230.033	40.49	40.4	0.09	
AirV14	17412.713	41.2	40.68	0.52	FM
Dm55-P3	18039.713	36.25	33.16	3.09	P3

Table A-2: Air valve locations

SN	NODE_ID	DIA	X_COO	Y_COO	ELEVATION
1	AIR-1	150	417214.706	2909167.53	27.214
2	AIR-2	150	416421.541	2909410.18	35.17
3	AIR-3	150	416257.4968	2909886.09	37.855
4	AIR-4	150	416046.712	2910274.32	46.791
5	AIR-5	150	415644.701469	2911569.59	50.24
6	AIR-6	150	416923.539	2912041.75	48.182
7	AIR-7	150	417239.98	2912436.52	43.025
8	AIR-8	150	416998.123732	2913166.14	24.7
9	AIR-9	150	415587.422	2913190.4	50.748
10	AIR-10	150	416043.732	2913529.15	48.045
11	AIR-11	150	414289.238	2914748.06	49.968
12	AIR-12	150	413395.51	2915744.2	49.204
13	AIR-13	150	412503.3859	2917338.51	40.985
14	AIR-14	150	411392.737	2917769.27	39.601

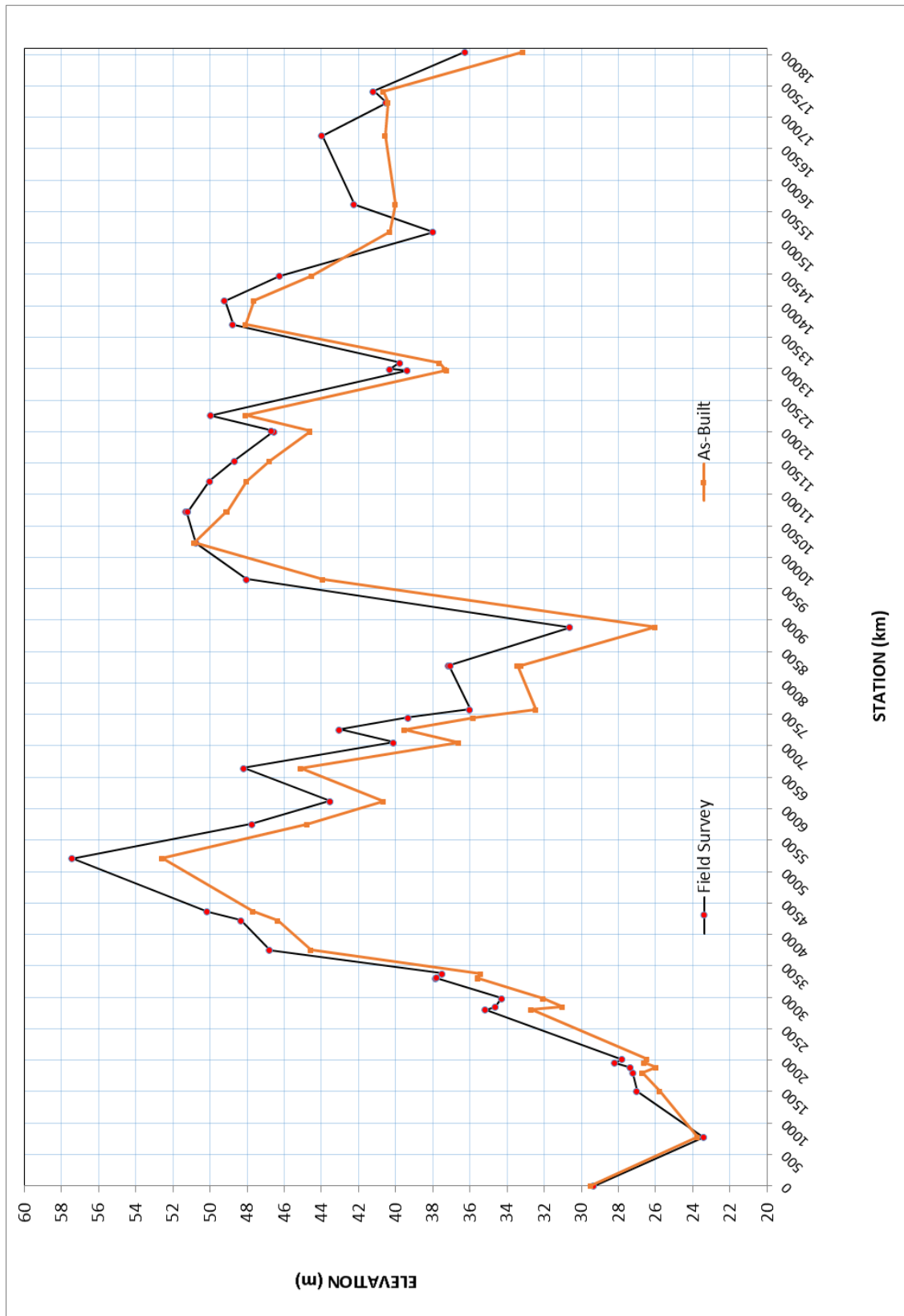


Figure A-1: Survey elevation Vs as-built elevation

Appendix B

Sample Input Data & Sample Hydraulic Analysis Results

Table B-1: Sample hydraulic analysis results - tanks

Label	Dia (m)	Elev (m)	Level (m) (Initial)	Flow In (L/s)	Level (m)	Status
Dammam-55	40	36.25	5	8	5.4	Filling
Dana	7	56	2.4	7	1.49	Filling
Doha-1	18	49.87	8.64	-47	4.02	Emptying
Doha-2	18	59	2	-13	3.62	Emptying
Doha-3	11	49.28	9.2	-23	2.67	Emptying
KFUPM	40	56.35	2.3	26	3.71	Filling
Yarmouk-Tank	40	29.5	13	-1,819	18	Emptying

Table B-2: Sample hydraulic analysis results - pump

Label	Elev (m)	HGL (Suction) (m)	HGL (Discharge) (m)	Flow (Total) (L/s)	Pump Head (ft)
Y-Pump	29.5	47.42	108.7	560	201.07

Table B-3: Sample hydraulic analysis results – air valve

ID	Label	Elev (m)	Air Valve Type	Dia (mm) (Inflow)	Dia (mm) (Outflow)	HGL (m)
325	AirV1	26.7	Double Acting	150	150	92.24
326	AirV2	32.68	Double Acting	150	150	83.14
327	AirV3	35.59	Double Acting	150	150	80.72
328	AirV4	44.58	Double Acting	150	150	78.78
329	AirV6	45.13	Double Acting	150	150	69.47
330	AirV7	39.51	Double Acting	150	150	68
331	AirV10	50.85	Double Acting	150	150	62.34
332	AirV11	48.1	Double Acting	150	150	60.63
333	AirV12	47.61	Double Acting	150	150	60.39
334	AirV14	40.7	Double Acting	150	150	60.06
5266	AirV5	52.57	Double Acting	150	150	73.41
5269	AirV8	33.44	Double Acting	150	150	65.55

Table B-4: Sample hydraulic analysis results - pipes

Label	Length (m)	Start Node	Stop Node	Dia (mm)	Mat.	Vel. (ft/s)	Flow (L/s)	HL (ft)
L1	4	J1M	J2M	600	DI	6.19	534	0.2
L2	13	J2M	J3M	700	CCP	4.55	534	0.34
L3	48	J3M	J4M	700	CCP	4.55	534	1.3
L32	80	J26M	J27M	700	CCP	2.92	343	0.96
L33	48	J27M	J28M	700	CCP	2.92	343	0.57
L34	61	J28M	AirV3	700	CCP	2.92	343	0.74
L66	218	AirV9	J45M	700	CCP	1.83	215	1.1
L67	349	J45M	J46M	700	CCP	1.83	215	1.77
L68	16	J46M	AirV10	700	CCP	1.83	215	0.08
L69	494	J47M	AirV10	700	CCP	1.83	-215	2.5
L70	477	J47M	J48M-5T	700	CCP	1.83	215	2.41
L71	327	J48M-5T	J49M	700	CCP	0.43	50	0.11
L72	461	J49M	DisV13	700	CCP	0.43	50	0.16
L84	704	DisV15	J57M	700	CCP	0.43	50	0.24
L85	364	J57M	J58M	700	CCP	0.43	50	0.12
L86	254	J58M	J59M	700	CCP	0.43	50	0.09
L90	457	AirV13	J62M	700	CCP	0.29	34	0.08
L91	52	DisV16	J62M	700	CCP	0.29	-34	0.01
L97	11	Dm55-P3	Dam-CV	600	DI	0.4	34	0
LT1-1	3	J24M-1T	FM1-KFUPM	400	DI	4.98	191	0.17
LT1-2	1,253	FM1-KFUPM	J24M-1T2	400	DI	4.98	191	77.54
LT2-1	5	J33M-2T	Doha3-PRV	200	UPVC	3.54	34	0.19
LT2-2	60	Doha3-PRV	J33M-2T2	200	UPVC	3.54	34	2.39
LT3-1	9	J37M-3T	Doha1-PRV	200	UPVC	2.3	22	0.16
LT3-2	87	Doha1-PRV	J37M-3T2	200	UPVC	2.3	22	1.56
LT4-1	4	J42M-4T	Doha2-PRV	300	FRP	3.35	72	0.08
LT4-2	4	Doha2-PRV	J42M-4T2	300	FRP	3.35	72	0.07
LT5-1	89	J48M-5T	FM5-Dana	400	DI	4.3	165	4.21
LT5-2	35	FM5-Dana	J48M-5T2	400	DI	4.3	165	1.64
LT6-1	4	J55M-6T	FM6-Khaleej	300	FRP	0	0	0
LT6-2	285	FM6-Khaleej	KhaleejPalace	300	FRP	0	0	0
LT7-1	60	J61M-7T	FM7-p537	300	FRP	0.74	16	0.06
LT7-2	734	FM7-p537	Dist-537	300	FRP	0.74	16	0.78

Table B-5: Sample hydraulic analysis results - junctions

Label	Elev (m)	Demand (L/s)	HGL (m)	Max HGL (m)	Min HGL (m)
Dana-D	55	0	57.98	59.58	55
Dist-537	41.87	16	60.85	114.24	56.71
Dm55-D	36	0	41.25	43.17	41.25
Dm55-P3	36.25	0	61.01	114.13	57.14
Doha1-D	49	1	58.51	58.66	49
Doha2-D	58	1	61	65.34	58
Doha3-D	49	1	58.48	59.32	49
FM-Tank55	40.7	0	61.05	114.24	57.17
FM-Yarmouk	25.78	0	93.74	127.2	93.74
FM1-KFUPM	34.68	0	82.53	124.17	81.79
FM2-Doha3	49.29	0	58.56	59.45	49.52
FM3-Doha1	49.87	0	58.56	58.78	50.23
FM4-Doha2	59	0	61.17	65.54	59.16
FM5-Dana	49	0	60.35	115.65	57.49
FM6-Khaleej	48.04	0	61.38	115.05	57.51
FM7-p537	39.89	0	61.09	114.42	57.18
J1M	26.6	0	106.14	130.55	106.14
J2M	26.6	0	106.08	130.54	106.08
J32M	41	0	79.89	122.52	78.4
J33M-2T	47.7	0	77.01	120.75	74.59
J34M	51.07	0	75.89	120.18	73.27
J36M	48.5	0	74.27	119.35	71.36
J37M-3T	44.77	0	72.8	118.6	69.63
J38M	37	0	69.45	117.46	66.5
J41M	32.44	0	67.54	116.82	64.71
J42M-4T	33.24	0	66.16	116.35	63.42
J43M	29.27	0	64.88	116.15	62.17
J47M	48.12	0	62.37	115.76	59.48
J48M-5T	48.02	0	61.64	115.65	58.51
J49M	46.77	0	61.6	115.57	58.38
J54M	42.18	0	61.43	115.17	57.72
J55M-6T	48.05	0	61.38	115.05	57.52
J56M	47.15	0	61.35	114.99	57.49
J60M	39.5	0	61.14	114.5	57.25
J61M-7T	39.72	0	61.11	114.44	57.22
J62M	40.43	0	61.06	114.28	57.18
KFUPM-D	20	0	58.65	66.36	58.65

Appendix C

Model Calibration

Table C-1: Calibration result table field observed reading Vs model calculated data

Field Data Snapshot	Pipe	Observed Flow (L/s)	Simulated Flow (L/s)	Difference (L/s)
28/Oct Yar 1:00PM	L7	589	593	4
28/Oct Yar 1:15PM	L7	586	590	4
28/Oct Yar 1:30PM	L7	593	598	4
28/Oct Yar 1:45PM	L7	613	618	5
28/Oct Yar 2:00PM	L7	618	623	5
28/Oct Yar 2:15PM	L7	612	617	5
28/Oct Yar 2:30PM	L7	595	600	4
28/Oct Yar 2:45PM	L7	590	594	4
28/Oct Yar 3:00PM	L7	335	338	3
28/Oct Yar 3:15PM	L7	0	0	0
28/Oct Yar 3:30PM	L7	0	0	0
28/Oct Yar 3:45PM	L7	0	0	0
28/Oct Yar 4:00PM	L7	389	392	3
28/Oct Yar 4:15PM	L7	538	542	4
28/Oct Yar 4:30PM	L7	539	543	4
28/Oct Yar 4:45PM	L7	541	545	4
28/Oct Yar 5:00PM	L7	549	553	4
28/Oct Yar 5:15PM	L7	515	519	4
28/Oct Yar 5:30PM	L7	548	552	4
28/Oct Yar 5:45PM	L7	540	544	4
28/Oct Yar 6:00AM	L7	0	0	0
28/Oct Yar 6:00PM	L7	540	544	4
28/Oct Yar 6:15AM	L7	0	0	0
28/Oct Yar 6:15PM	L7	530	534	4
28/Oct Yar 6:30AM	L7	32	32	0
28/Oct Yar 6:30PM	L7	527	531	4
28/Oct Yar 6:45AM	L7	547	551	4
28/Oct Yar 6:45PM	L7	524	528	4
28/Oct Yar 7:00AM	L7	549	553	4
28/Oct Yar 7:00PM	L7	532	536	4
28/Oct Yar 7:15AM	L7	596	600	4
28/Oct Yar 7:15PM	L7	522	526	4
28/Oct Yar 7:30AM	L7	611	615	5

Field Data Snapshot	Pipe	Observed Flow (L/s)	Simulated Flow (L/s)	Difference (L/s)
28/Oct Yar 7:30PM	L7	537	541	4
28/Oct Yar 7:45AM	L7	595	600	4
28/Oct Yar 7:45PM	L7	522	526	4
28/Oct Yar 8:00AM	L7	614	619	5
28/Oct Yar 8:00PM	L7	500	503	4
28/Oct Yar 8:15AM	L7	604	608	5
28/Oct Yar 8:15PM	L7	505	509	4
28/Oct Yar 8:30AM	L7	616	621	5
28/Oct Yar 8:30PM	L7	530	534	4
28/Oct Yar 8:45AM	L7	620	624	5
28/Oct Yar 8:45PM	L7	527	531	4
28/Oct Yar 9:00AM	L7	620	624	5
28/Oct Yar 9:00PM	L7	524	528	4
28/Oct Yar 9:15AM	L7	627	631	5
28/Oct Yar 9:15PM	L7	532	536	4
28/Oct Yar 9:30AM	L7	630	634	5
28/Oct Yar 9:30PM	L7	515	519	4
28/Oct Yar 9:45AM	L7	609	614	5
28/Oct Yar 9:45PM	L7	519	523	4
28/Oct Yar 10:00AM	L7	625	629	5
28/Oct Yar 10:00PM	L7	521	524	4
28/Oct Yar 10:15AM	L7	625	630	5
28/Oct Yar 10:15PM	L7	498	502	4
28/Oct Yar 10:30AM	L7	614	618	5
28/Oct Yar 10:30PM	L7	477	480	4
28/Oct Yar 10:45AM	L7	604	608	5
28/Oct Yar 10:45PM	L7	57	58	0
28/Oct Yar 11:00AM	L7	608	613	5
28/Oct Yar 11:00PM	L7	0	0	0
28/Oct Yar 11:15AM	L7	601	605	5
28/Oct Yar 11:15PM	L7	0	0	0
28/Oct Yar 11:30AM	L7	609	613	5
28/Oct Yar 11:30PM	L7	0	0	0
28/Oct Yar 11:45AM	L7	599	603	4
28/Oct Yar 11:45PM	L7	0	0	0
28/Oct Yar 12:00PM	L7	612	617	5
28/Oct Yar 12:15PM	L7	598	603	4
28/Oct Yar 12:30PM	L7	598	603	4
28/Oct Yar 12:45PM	L7	606	610	5

Field Data Snapshot	Pipe	Observed Flow (L/s)	Simulated Flow (L/s)	Difference (L/s)
29/Oct Yar 1:00AM	L7	379	382	3
29/Oct Yar 1:00PM	L7	595	600	4
29/Oct Yar 1:15AM	L7	498	502	4
29/Oct Yar 1:15PM	L7	578	583	4
29/Oct Yar 1:30AM	L7	503	506	4
29/Oct Yar 1:30PM	L7	598	602	4
29/Oct Yar 1:45AM	L7	487	491	4
29/Oct Yar 1:45PM	L7	590	595	4
29/Oct Yar 2:00AM	L7	474	478	4
29/Oct Yar 2:00PM	L7	585	590	4
29/Oct Yar 2:15AM	L7	476	480	4
29/Oct Yar 2:15PM	L7	574	578	4
29/Oct Yar 2:30AM	L7	471	475	4
29/Oct Yar 2:30PM	L7	565	569	4
29/Oct Yar 2:45AM	L7	463	467	3
29/Oct Yar 2:45PM	L7	0	0	0
29/Oct Yar 3:00AM	L7	461	464	3
29/Oct Yar 3:00PM	L7	0	0	0
29/Oct Yar 3:15AM	L7	468	471	4
29/Oct Yar 3:15PM	L7	0	0	0
29/Oct Yar 3:30AM	L7	453	457	3
29/Oct Yar 3:30PM	L7	0	0	0
29/Oct Yar 3:45AM	L7	458	461	3
29/Oct Yar 3:45PM	L7	407	410	3
29/Oct Yar 4:00AM	L7	452	456	3
29/Oct Yar 4:00PM	L7	503	507	4
29/Oct Yar 4:15AM	L7	436	439	3
29/Oct Yar 4:15PM	L7	523	527	4
29/Oct Yar 4:30AM	L7	359	362	3
29/Oct Yar 4:30PM	L7	508	512	4
29/Oct Yar 4:45AM	L7	376	379	3
29/Oct Yar 4:45PM	L7	507	510	4
29/Oct Yar 5:00AM	L7	426	429	3
29/Oct Yar 5:00PM	L7	507	510	4
29/Oct Yar 5:15AM	L7	413	416	3
29/Oct Yar 5:15PM	L7	497	500	4
29/Oct Yar 5:30AM	L7	395	398	3
29/Oct Yar 5:30PM	L7	510	513	4
29/Oct Yar 5:45AM	L7	405	408	3

Field Data Snapshot	Pipe	Observed Flow (L/s)	Simulated Flow (L/s)	Difference (L/s)
29/Oct Yar 5:45PM	L7	513	517	4
29/Oct Yar 6:00AM	L7	423	426	3
29/Oct Yar 6:00PM	L7	511	515	4
29/Oct Yar 6:15AM	L7	393	396	3
29/Oct Yar 6:15PM	L7	506	510	4
29/Oct Yar 6:30AM	L7	465	468	3
29/Oct Yar 6:30PM	L7	521	525	4
29/Oct Yar 6:45AM	L7	488	491	4
29/Oct Yar 6:45PM	L7	519	522	4
29/Oct Yar 7:00AM	L7	497	501	4
29/Oct Yar 7:00PM	L7	501	505	4
29/Oct Yar 7:15AM	L7	550	554	4
29/Oct Yar 7:15PM	L7	510	514	4
29/Oct Yar 7:30AM	L7	586	590	4
29/Oct Yar 7:30PM	L7	516	520	4
29/Oct Yar 7:45AM	L7	570	575	4
29/Oct Yar 7:45PM	L7	520	524	4
29/Oct Yar 8:00AM	L7	575	579	4
29/Oct Yar 8:00PM	L7	528	532	4
29/Oct Yar 8:15AM	L7	570	575	4
29/Oct Yar 8:15PM	L7	532	536	4
29/Oct Yar 8:30AM	L7	576	580	4
29/Oct Yar 8:30PM	L7	535	539	4
29/Oct Yar 8:45AM	L7	557	562	4
29/Oct Yar 8:45PM	L7	500	504	4
29/Oct Yar 9:00AM	L7	554	558	4
29/Oct Yar 9:00PM	L7	503	506	4
29/Oct Yar 9:15AM	L7	535	539	4
29/Oct Yar 9:15PM	L7	505	509	4
29/Oct Yar 9:30AM	L7	551	555	4
29/Oct Yar 9:30PM	L7	497	500	4
29/Oct Yar 9:45AM	L7	553	557	4
29/Oct Yar 9:45PM	L7	476	480	4
29/Oct Yar 10:00AM	L7	550	554	4
29/Oct Yar 10:00PM	L7	450	453	3
29/Oct Yar 10:15AM	L7	562	566	4
29/Oct Yar 10:15PM	L7	447	450	3
29/Oct Yar 10:30AM	L7	563	567	4
29/Oct Yar 10:30PM	L7	456	459	3

Field Data Snapshot	Pipe	Observed Flow (L/s)	Simulated Flow (L/s)	Difference (L/s)
29/Oct Yar 10:45AM	L7	591	596	4
29/Oct Yar 10:45PM	L7	464	468	3
29/Oct Yar 11:00AM	L7	588	592	4
29/Oct Yar 11:00PM	L7	334	336	3
29/Oct Yar 11:15AM	L7	587	591	4
29/Oct Yar 11:15PM	L7	0	0	0
29/Oct Yar 11:30AM	L7	609	614	5
29/Oct Yar 11:30PM	L7	0	0	0
29/Oct Yar 11:45AM	L7	607	612	5
29/Oct Yar 11:45PM	L7	0	0	0
29/Oct Yar 12:00AM	L7	0	0	0
29/Oct Yar 12:00PM	L7	595	600	4
29/Oct Yar 12:15AM	L7	0	0	0
29/Oct Yar 12:15PM	L7	600	604	4
29/Oct Yar 12:30AM	L7	0	0	0
29/Oct Yar 12:30PM	L7	606	611	5
29/Oct Yar 12:45AM	L7	0	0	0
29/Oct Yar 12:45PM	L7	595	599	4
30/Oct Yar 1:00AM	L7	0	0	0
30/Oct Yar 1:15AM	L7	404	407	3
30/Oct Yar 1:30AM	L7	467	471	4
30/Oct Yar 1:45AM	L7	479	482	4
30/Oct Yar 2:00AM	L7	473	477	4
30/Oct Yar 2:15AM	L7	480	483	4
30/Oct Yar 2:30AM	L7	487	491	4
30/Oct Yar 2:45AM	L7	477	481	4
30/Oct Yar 3:00AM	L7	469	473	4
30/Oct Yar 3:15AM	L7	469	472	4
30/Oct Yar 3:30AM	L7	474	477	4
30/Oct Yar 3:45AM	L7	466	470	3
30/Oct Yar 4:00AM	L7	460	464	3
30/Oct Yar 4:15AM	L7	450	454	3
30/Oct Yar 4:30AM	L7	461	465	3
30/Oct Yar 4:45AM	L7	455	459	3
30/Oct Yar 5:00AM	L7	388	391	3
30/Oct Yar 5:15AM	L7	0	0	0
30/Oct Yar 5:30AM	L7	0	0	0
30/Oct Yar 5:45AM	L7	0	0	0

Table C-2: Field flow meter reading for all metering points 28th to 30th Oct, 2013

Date	TIME	Yar	UPM	Doha3	Doha1	Doha2	Dana	palace	P537	Dm55
28th	6:00AM	0.00	0.00	0.00	0.00	0.00	0.00	0.00	37.89	-46.78
	6:15AM	0.00	0.00	0.00	0.00	0.00	0.00	0.00	40.98	-48.23
	6:30AM	32.04	0.00	0.00	0.00	0.00	0.00	0.00	41.86	-49.29
	6:45AM	547.06	0.00	89.67	78.51	89.54	158.51	0.00	61.64	-2.05
	7:00AM	548.90	0.00	104.18	89.92	110.66	194.61	0.00	53.74	20.12
	7:15AM	595.72	126.83	90.00	78.51	73.06	140.46	0.00	51.44	17.13
	7:30AM	610.51	159.50	86.04	73.97	50.78	137.53	46.34	47.51	8.07
	7:45AM	595.11	138.85	83.62	79.22	39.94	137.53	73.77	48.09	-0.03
	8:00AM	614.21	162.50	83.40	79.12	41.96	135.82	73.19	46.37	16.07
	8:15AM	603.73	162.50	83.18	79.02	43.55	136.56	73.12	46.94	13.57
	8:30AM	616.05	138.47	81.09	75.99	29.38	183.88	71.38	45.79	7.01
	8:45AM	619.75	141.85	80.65	75.79	25.62	196.08	71.02	46.10	-0.03
	9:00AM	619.75	149.36	81.75	77.20	34.01	169.00	72.03	47.21	8.07
	9:15AM	626.53	145.23	81.53	77.30	32.13	173.39	71.82	46.63	2.00
	9:30AM	629.61	141.47	82.63	78.11	39.21	152.17	72.75	46.10	12.02
	9:45AM	609.28	131.71	80.98	75.29	24.90	193.88	71.02	46.10	-0.03
	10:00AM	624.68	136.97	82.52	77.71	36.61	160.71	71.96	46.10	8.55
	10:15AM	625.29	156.49	81.20	75.79	25.76	191.93	70.66	45.79	12.60
	10:30AM	613.59	151.99	82.52	77.71	34.73	197.79	53.19	46.37	15.11
	10:45AM	603.73	145.23	85.82	81.44	57.29	193.88	0.00	45.22	19.06
	11:00AM	608.05	142.60	85.71	81.04	58.30	194.37	0.00	39.88	21.57
	11:15AM	600.65	164.76	85.49	80.53	59.32	192.91	0.00	44.38	20.12
	11:30AM	608.66	159.12	85.27	80.13	59.75	198.03	0.00	44.95	19.06
	11:45AM	598.80	148.98	85.16	79.83	60.33	195.35	0.00	44.95	18.58
	12:00PM	612.36	145.60	86.15	81.14	67.56	174.37	0.00	46.63	19.06
	12:15PM	598.19	156.49	87.14	82.15	74.36	154.85	0.00	47.21	20.60
	12:30PM	598.19	158.75	86.81	81.64	73.06	156.31	0.00	45.79	22.14
	12:45PM	605.58	159.12	86.59	81.44	73.20	158.51	0.00	45.79	20.12
	1:00PM	588.95	159.50	86.48	81.24	73.49	158.02	0.00	45.22	21.57
	1:15PM	585.87	156.87	86.48	81.14	74.65	155.83	0.00	44.95	20.60
	1:30PM	593.26	150.11	85.27	79.63	70.16	175.83	0.00	44.11	20.60
	1:45PM	612.97	155.74	83.95	78.11	64.67	196.08	0.00	42.97	18.58
	2:00PM	617.90	153.49	83.84	77.91	65.25	197.05	0.00	42.13	21.08
	2:15PM	612.36	134.71	83.73	77.71	65.82	195.10	0.00	44.38	20.60
	2:30PM	595.11	151.61	86.04	81.34	74.50	160.22	0.00	46.63	21.08
	2:45PM	589.56	167.38	89.34	84.07	86.94	107.53	0.00	45.79	25.13

	3:00PM	335.13	125.33	59.33	48.54	50.64	92.65	0.00	41.29	14.05
	3:15PM	0.00	0.00	6.01	0.00	0.00	0.00	0.00	39.88	-17.57
	3:30PM	0.00	0.00	0.00	0.00	0.00	0.00	0.00	37.32	-44.28
	3:45PM	0.00	0.00	0.00	0.00	0.00	0.00	0.00	37.32	-47.26
	4:00PM	389.35	0.00	61.86	61.96	64.38	105.09	0.00	55.42	-17.09
	4:15PM	537.82	0.00	105.28	101.32	116.01	183.88	0.00	55.42	22.14
	4:30PM	539.05	0.00	105.50	102.03	118.47	173.39	0.00	53.74	21.57
	4:45PM	540.90	0.00	104.40	101.02	115.57	182.90	0.00	53.43	21.57
	5:00PM	548.90	0.00	104.84	101.93	117.45	172.66	0.00	55.15	22.14
	5:15PM	515.02	0.00	104.73	101.93	118.47	172.66	0.00	55.99	21.08
	5:30PM	547.67	0.00	103.19	100.62	113.26	190.22	0.00	56.56	19.64
	5:45PM	539.66	0.00	102.97	100.52	112.97	188.76	0.00	57.67	17.61
	6:00PM	540.28	0.00	102.97	100.52	114.13	185.34	0.00	57.13	18.58
	6:15PM	530.42	0.00	102.75	100.21	113.40	186.32	0.00	55.42	18.10
	6:30PM	526.73	0.00	102.53	99.91	113.84	187.30	0.00	55.15	18.58
	6:45PM	524.26	0.00	102.20	99.51	113.40	189.73	0.00	53.16	21.57
	7:00PM	531.65	0.00	101.98	99.10	113.26	188.27	0.00	53.74	21.08
	7:15PM	521.80	0.00	101.76	98.80	113.55	191.93	0.00	51.44	21.08
	7:30PM	537.20	0.00	101.54	98.29	112.83	191.93	0.00	51.44	23.11
	7:45PM	522.41	0.00	102.31	99.41	116.88	177.29	0.00	51.44	23.11
	8:00PM	499.62	0.00	105.94	103.14	130.18	115.33	0.00	51.44	27.16
	8:15PM	505.16	0.00	104.62	101.12	125.99	132.65	0.00	49.76	27.16
	8:30PM	529.81	0.00	100.77	96.88	113.55	189.73	0.00	47.78	25.62
	8:45PM	526.73	0.00	100.33	96.28	112.25	194.37	0.00	44.95	26.10
	9:00PM	524.26	1.41	100.00	95.77	112.39	194.37	0.00	45.22	28.12
	9:15PM	531.65	0.00	99.67	93.55	112.25	195.10	0.00	44.95	30.15
	9:30PM	515.02	0.00	100.88	72.86	116.30	207.30	0.00	44.95	28.70
	9:45PM	519.33	0.00	100.44	72.66	116.01	207.79	0.00	45.79	28.70
	10:00PM	520.57	0.00	95.60	72.96	117.17	209.49	0.00	44.95	28.70
	10:15PM	498.39	0.00	90.11	76.80	132.06	159.49	0.00	48.35	30.15
	10:30PM	476.83	0.00	91.32	77.81	136.40	134.12	0.00	47.78	30.63
	10:45PM	57.29	0.00	18.66	10.40	25.04	32.15	0.00	22.62	-14.10
	11:00PM	0.00	0.00	0.00	0.00	0.00	0.00	0.00	28.00	-45.72
	11:15PM	0.00	0.00	0.00	0.00	0.00	0.00	0.00	28.27	-43.70
	11:30PM	0.00	0.00	0.00	0.00	0.00	0.00	0.00	29.99	-45.24
	11:45PM	0.00	0.00	0.00	0.00	0.00	0.00	0.00	28.00	-45.72
29th	12:00AM	0.00	0.00	0.00	0.00	0.00	0.00	0.00	27.70	-45.24
	12:15AM	0.00	0.00	0.00	0.00	0.00	0.00	0.00	28.58	-47.75
	12:30AM	0.00	0.00	0.00	0.00	0.00	0.00	0.00	28.58	-48.23

	12:45AM	0.00	3.66	0.00	0.00	0.00	0.00	0.00	28.84	-52.28
	1:00AM	378.87	0.00	59.77	43.19	67.56	60.45	0.00	47.51	-9.09
	1:15AM	497.77	0.00	110.22	75.49	135.53	129.97	0.00	46.10	34.19
	1:30AM	502.70	0.00	109.78	74.88	133.80	131.43	0.00	43.27	31.69
	1:45AM	487.30	1.78	109.34	67.31	132.93	132.90	0.00	41.29	31.21
	2:00AM	474.36	0.00	112.31	24.42	142.76	150.95	0.00	39.57	35.64
	2:15AM	476.21	0.00	112.31	16.15	141.90	155.10	0.00	36.75	38.73
	2:30AM	471.28	0.00	112.09	10.80	143.34	158.02	0.00	37.05	42.20
	2:45AM	463.27	0.00	111.87	5.95	143.78	158.02	0.00	36.75	42.20
	3:00AM	460.81	0.00	111.54	3.23	143.63	162.41	0.00	37.62	43.74
	3:15AM	467.59	0.00	111.10	3.23	143.63	161.19	0.00	36.75	42.20
	3:30AM	453.42	0.00	110.44	3.23	142.04	162.90	0.00	36.75	43.74
	3:45AM	457.73	0.00	110.00	3.13	142.04	163.39	0.00	35.64	46.24
	4:00AM	452.18	0.00	105.72	3.23	141.90	164.12	0.00	35.91	43.26
	4:15AM	435.75	0.00	73.18	3.28	147.83	174.07	0.00	35.63	43.70
	4:30AM	358.85	0.00	78.74	3.17	177.42	42.51	0.00	38.73	49.76
	4:45AM	376.14	0.00	78.52	3.28	174.39	45.19	0.00	37.59	48.30
	5:00AM	425.61	0.00	73.96	5.58	150.51	147.76	0.00	39.29	44.77
	5:15AM	413.09	0.00	74.52	8.54	137.14	148.03	0.00	42.98	41.25
	5:30AM	394.62	0.00	76.52	21.34	103.99	146.15	0.00	45.23	41.74
	5:45AM	405.35	0.00	74.52	57.67	99.18	135.41	0.00	47.22	37.24
	6:00AM	423.23	0.00	78.41	69.60	96.15	134.87	0.00	50.62	34.69
	6:15AM	392.83	0.00	83.52	77.37	53.01	139.70	0.00	54.86	31.66
	6:30AM	464.96	1.10	80.52	96.08	0.00	268.85	0.00	52.02	30.19
	6:45AM	487.61	0.00	83.97	92.80	23.07	273.41	0.00	50.88	28.62
	7:00AM	497.14	0.00	79.63	71.90	108.62	225.35	0.00	48.36	25.10
	7:15AM	550.20	74.38	75.85	68.07	40.89	206.56	0.00	48.92	24.61
	7:30AM	585.96	179.37	71.18	63.03	0.00	150.44	60.19	46.37	24.61
	7:45AM	570.46	164.56	70.73	63.03	0.00	139.17	81.27	45.52	23.14
	8:00AM	574.64	181.84	70.96	63.36	0.00	136.75	81.27	46.67	23.63
	8:15AM	570.46	164.94	71.18	63.69	0.00	135.68	81.19	47.78	21.09
	8:30AM	575.83	174.43	71.51	64.02	0.00	136.75	81.19	49.21	22.16
	8:45AM	557.35	170.63	71.62	64.35	0.00	134.60	80.96	49.47	19.62
	9:00AM	553.77	165.89	82.86	66.86	24.67	159.03	60.83	49.47	22.65
	9:15AM	534.70	44.96	96.31	68.62	107.20	180.25	0.00	48.36	24.12
	9:30AM	550.79	73.05	93.98	67.30	101.14	164.14	0.00	47.22	23.63
	9:45AM	552.58	75.33	93.76	67.41	101.14	162.79	0.00	47.22	25.59
	10:00AM	550.20	73.62	93.53	67.41	100.60	165.48	0.00	46.93	24.61
	10:15AM	561.52	76.66	93.42	67.74	100.78	166.55	0.00	47.52	24.12
	10:30AM	562.71	75.14	93.09	67.30	100.42	166.55	0.00	46.67	25.10

	10:45AM	591.33	138.36	89.75	65.99	95.79	92.18	0.00	43.53	27.64
	11:00AM	587.75	168.93	85.19	60.85	76.01	158.50	0.00	45.52	21.09
	11:15AM	586.56	150.13	82.52	58.98	65.31	200.65	0.00	45.82	20.11
	11:30AM	609.21	155.64	82.41	59.09	66.38	201.99	0.00	46.37	18.05
	11:45AM	607.42	152.98	82.41	59.20	66.74	199.85	0.00	46.08	18.64
	12:00PM	595.50	153.93	82.41	59.31	67.45	196.62	0.00	45.82	19.13
	12:15PM	599.67	163.99	82.41	59.42	68.16	198.77	0.00	46.08	20.60
	12:30PM	606.23	157.35	79.96	59.64	69.77	198.77	0.00	44.68	20.60
	12:45PM	594.90	167.98	79.41	59.75	70.30	199.85	0.00	44.38	20.60
	1:00PM	595.50	152.60	79.41	59.86	70.48	197.70	0.00	43.27	22.65
	1:15PM	578.21	153.74	79.41	59.86	71.73	198.50	0.00	42.42	22.16
	1:30PM	597.88	156.02	79.41	59.97	71.73	197.43	0.00	41.84	22.65
	1:45PM	590.14	158.29	80.41	61.17	76.72	182.66	0.00	41.57	24.12
	2:00PM	585.37	160.38	82.41	63.03	86.52	146.15	0.00	42.68	25.10
	2:15PM	574.04	148.80	82.41	63.14	86.70	144.27	0.00	42.68	25.59
	2:30PM	564.50	159.05	81.30	80.32	81.00	140.78	0.00	39.88	25.10
	2:45PM	0.00	48.18	5.45	0.66	0.00	13.24	0.00	25.45	-30.69
	3:00PM	0.00	0.72	0.00	0.00	0.00	0.08	0.00	34.20	-48.21
	3:15PM	0.00	0.00	0.00	0.00	0.00	0.00	0.00	36.48	-49.78
	3:30PM	0.00	0.00	0.00	0.00	0.00	0.08	0.00	36.74	-50.27
	3:45PM	406.54	0.00	65.17	75.73	85.27	67.75	0.00	58.81	-13.07
	4:00PM	503.11	0.00	101.65	111.84	135.89	114.46	0.00	55.97	22.16
	4:15PM	522.78	0.00	106.88	111.29	132.51	113.39	0.00	55.71	22.16
	4:30PM	507.87	0.00	106.99	111.08	130.90	114.46	0.00	54.01	23.63
	4:45PM	506.68	0.00	106.77	110.86	131.26	114.20	0.00	54.57	24.61
	5:00PM	506.68	0.00	106.43	110.64	130.90	114.20	0.00	54.86	22.16
	5:15PM	496.55	0.00	106.10	110.31	130.37	115.27	0.00	56.26	21.09
	5:30PM	509.66	0.00	105.77	109.98	130.37	113.93	0.00	56.56	20.60
	5:45PM	513.24	0.00	105.54	109.76	130.55	115.00	0.00	55.71	22.16
	6:00PM	511.45	0.00	105.43	109.32	129.83	115.27	0.00	54.86	22.65
	6:15PM	506.09	0.00	105.32	108.89	128.94	115.27	0.00	53.16	22.65
	6:30PM	520.99	0.00	105.10	108.34	129.30	116.34	0.00	54.57	22.16
	6:45PM	518.60	0.00	105.10	107.90	128.94	117.69	0.00	55.42	22.65
	7:00PM	501.32	0.00	104.88	107.35	129.65	116.08	0.00	53.42	23.63
	7:15PM	510.26	0.00	104.65	106.81	128.23	117.15	0.00	52.87	24.12
	7:30PM	516.22	0.00	102.21	103.31	120.74	152.05	0.00	51.17	25.59
	7:45PM	519.80	0.00	99.21	99.91	110.05	195.55	0.00	49.47	24.12
	8:00PM	527.55	0.00	98.98	99.37	110.05	196.36	0.00	48.36	24.12
	8:15PM	531.72	0.00	98.76	98.82	109.69	194.48	0.00	47.52	24.61

	8:30PM	535.29	0.00	98.54	98.93	110.76	196.62	0.00	45.82	25.59
	8:45PM	500.12	0.00	103.10	103.74	128.59	118.49	0.00	46.93	29.70
	9:00PM	502.51	0.00	102.76	103.20	127.69	119.57	0.00	45.82	30.68
	9:15PM	505.49	0.00	98.54	103.20	128.59	121.44	0.00	44.68	32.15
	9:30PM	496.55	0.00	78.41	104.40	131.26	129.23	0.00	44.68	32.64
	9:45PM	476.28	0.00	74.63	84.92	136.78	132.45	0.00	45.23	33.22
	10:00PM	450.05	0.00	52.38	58.66	148.90	150.17	0.00	43.83	37.24
	10:15PM	447.07	0.00	52.38	58.77	147.48	149.64	0.00	45.52	35.67
	10:30PM	456.01	0.00	52.49	58.77	146.94	150.71	0.00	45.23	34.20
	10:45PM	464.36	0.00	52.49	58.88	148.01	151.52	0.00	45.52	35.67
	11:00PM	333.81	0.00	44.15	35.02	122.35	131.38	0.00	32.24	32.64
	11:15PM	0.00	0.00	0.00	0.00	0.00	0.08	0.00	32.79	-39.21
	11:30PM	0.00	0.00	0.00	0.00	0.00	0.08	0.00	31.68	-41.75
	11:45PM	0.00	0.00	0.00	0.00	0.00	0.08	0.00	30.25	-41.26
30th	12:00AM	0.00	0.00	0.00	0.00	0.00	0.08	0.00	30.25	-41.75
	12:15AM	0.00	0.00	0.00	0.00	0.00	0.08	0.00	30.25	-40.67
	12:30AM	0.00	0.00	0.00	0.00	0.00	0.08	0.00	28.29	-45.76
	12:45AM	0.00	0.00	0.00	0.00	0.00	0.08	0.00	28.84	-50.27
	1:00AM	0.00	0.00	0.00	0.00	0.00	0.08	0.00	27.14	-49.29
	1:15AM	403.56	0.00	69.51	15.98	81.35	51.10	0.00	47.52	-3.48
	1:30AM	467.34	0.00	113.66	24.73	143.02	148.03	0.00	44.12	33.71
	1:45AM	478.67	0.00	112.66	24.62	141.95	152.05	0.00	39.58	32.64
	2:00AM	473.30	0.00	109.88	24.08	133.58	185.62	0.00	37.04	34.69
	2:15AM	479.86	0.00	109.10	24.08	134.29	186.69	0.00	35.63	38.21
	2:30AM	487.01	0.00	102.76	24.19	134.11	190.72	0.00	32.79	41.74
	2:45AM	477.47	0.00	92.64	24.19	136.43	195.82	0.00	32.53	42.23
	3:00AM	469.13	0.00	92.31	24.08	135.36	196.62	0.00	31.68	44.28
	3:15AM	468.53	0.00	92.09	24.08	135.71	196.89	0.00	32.24	43.21
	3:30AM	473.90	0.00	91.64	24.08	134.82	198.50	0.00	32.53	43.70
	3:45AM	466.15	0.00	91.86	15.65	136.07	198.50	0.00	33.64	43.70
	4:00AM	460.19	0.00	92.20	6.13	138.03	200.92	0.00	33.64	42.72
	4:15AM	450.48	0.00	91.93	6.13	137.20	199.10	0.00	35.07	44.74
	4:30AM	461.47	0.00	91.71	6.13	137.34	199.10	0.00	35.61	42.19
	4:45AM	455.36	0.17	91.49	6.13	136.78	200.29	0.00	37.02	42.19
	5:00AM	388.22	0.00	88.69	5.47	129.38	197.11	0.00	30.83	41.17
	5:15AM	0.00	0.00	0.64	0.00	0.00	1.38	0.00	22.05	-22.15
MAX		629.61	181.84	113.66	111.84	177.42	273.41	81.27	61.64	49.76
AVG		442.68	47.03	76.42	57.93	83.01	136.83	7.39	43.80	14.58

Appendix D

PRV Optimization

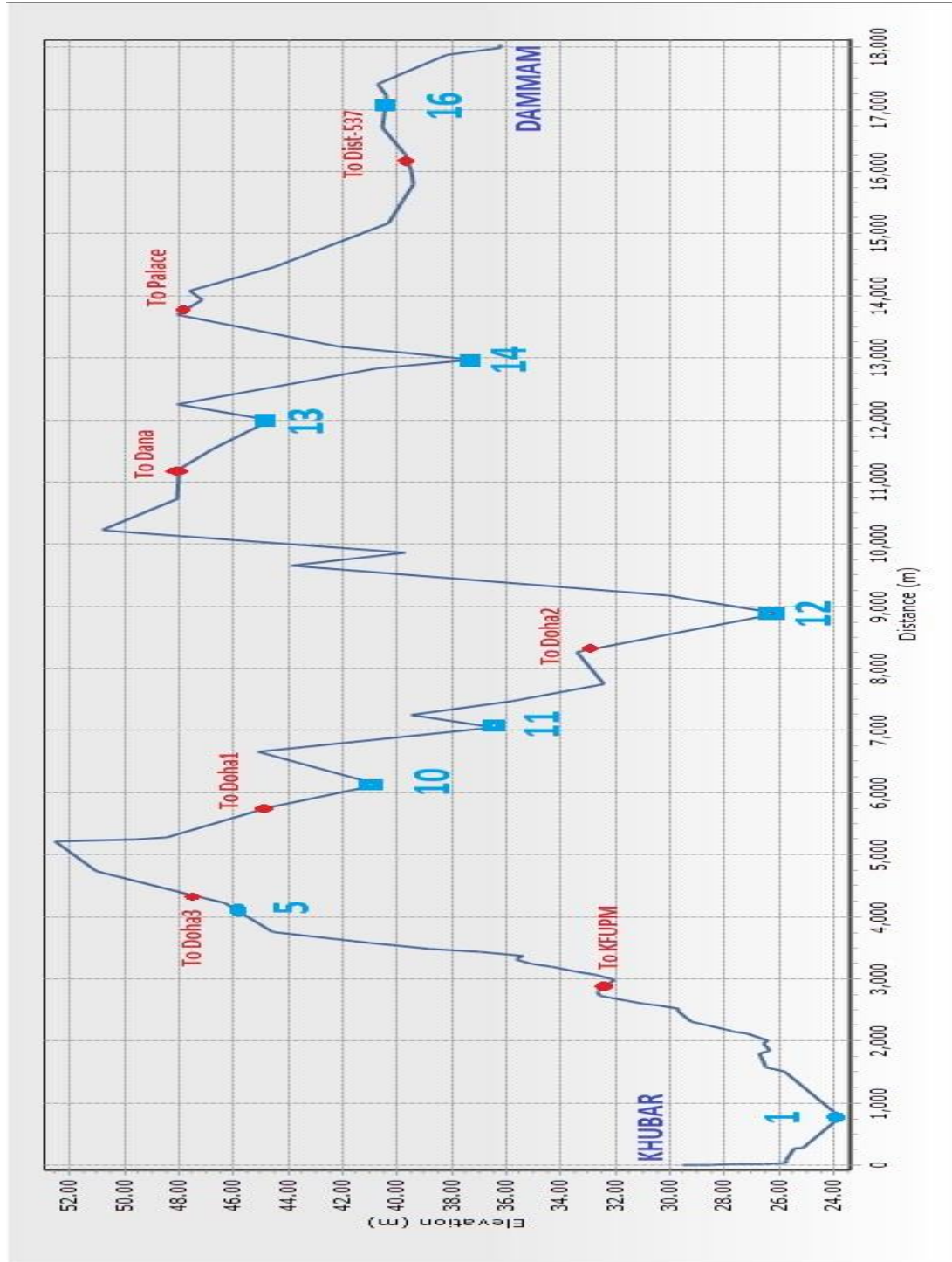


Figure D-1: Possible locations for PRVs at the washout chambers

Table D-1: PRV optimization trials

	Trial 1		Trial 2		Trial 3		Trial 4		Trial 5		Trial 6		Trial 7		Trial 8	
	Set	V (m3)	Set	V (m3)	Set	V (m3)	Set	V (m3)	Set	V (m3)	Set	V (m3)	Set	V (m3)	Set	V (m3)
Yar-PS	8	0	6	35	6	36	6	31	6	40	6	39	6	X	6	X
WC-1	6	32	8	0.1	8	0.2										
WC-5	6	0.5	6	0.6	6	0.6	6	0.7	6	1.3	6	2			6	X
WC-10	6	0.1	6	0.2												
WC-11	6	0.4	6	2.7	6	6	6	7	7	1.5						
WC-12	6	13	7	3.8												
WC-13	6	0	6	1.4												
WC-14	6	0	6	0	6	0.3	6	1.1	6	3.2	6	4	6	X		
WC-16	6	0.2	6	0	6	1.7										

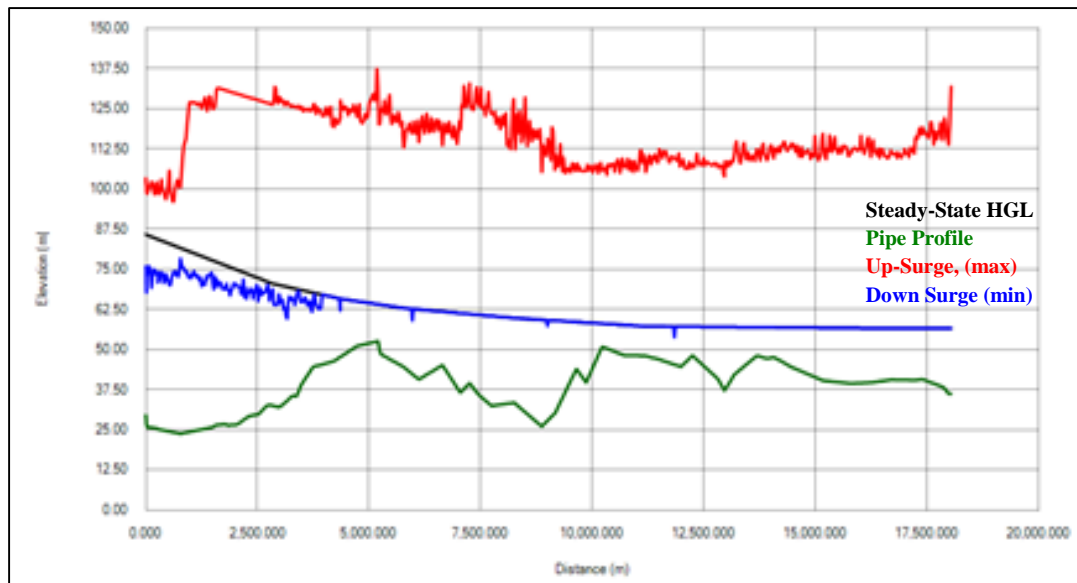


Figure D-2: PRV trial 1 resulted protection

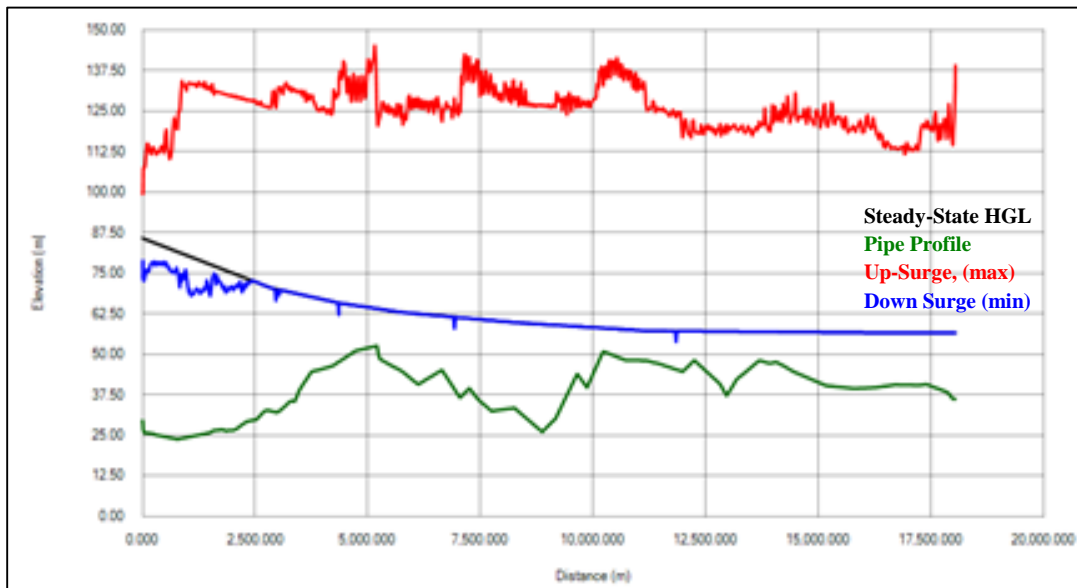


Figure D-3: PRV trial 3 resulted protection

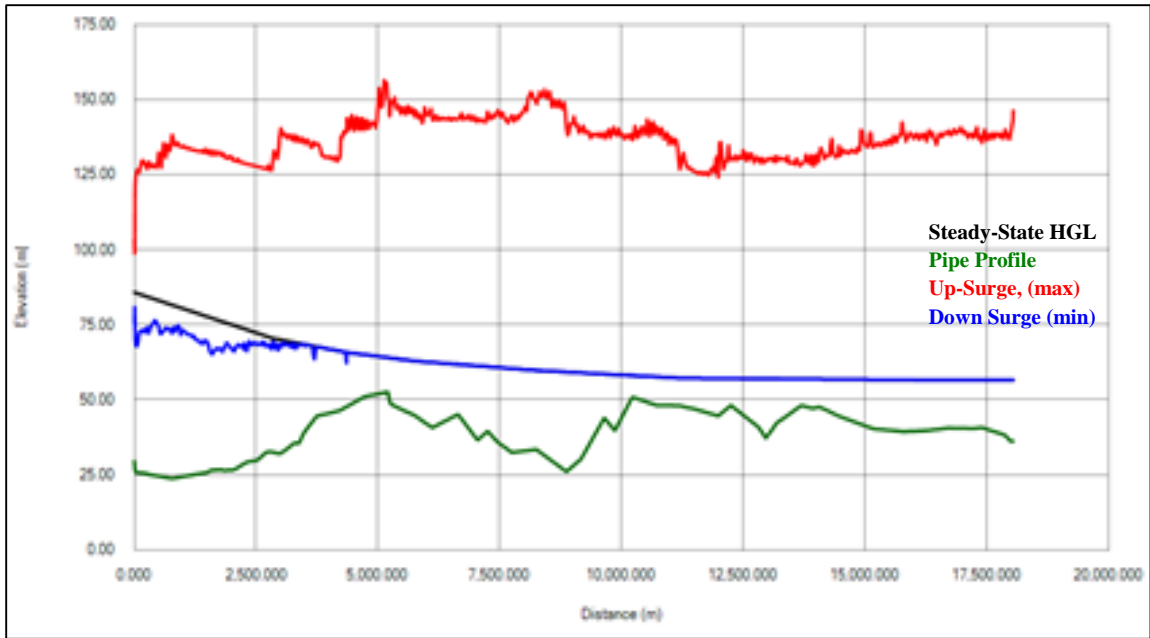


Figure D-4: PRV trial 6 resulted protection (proposed solution)

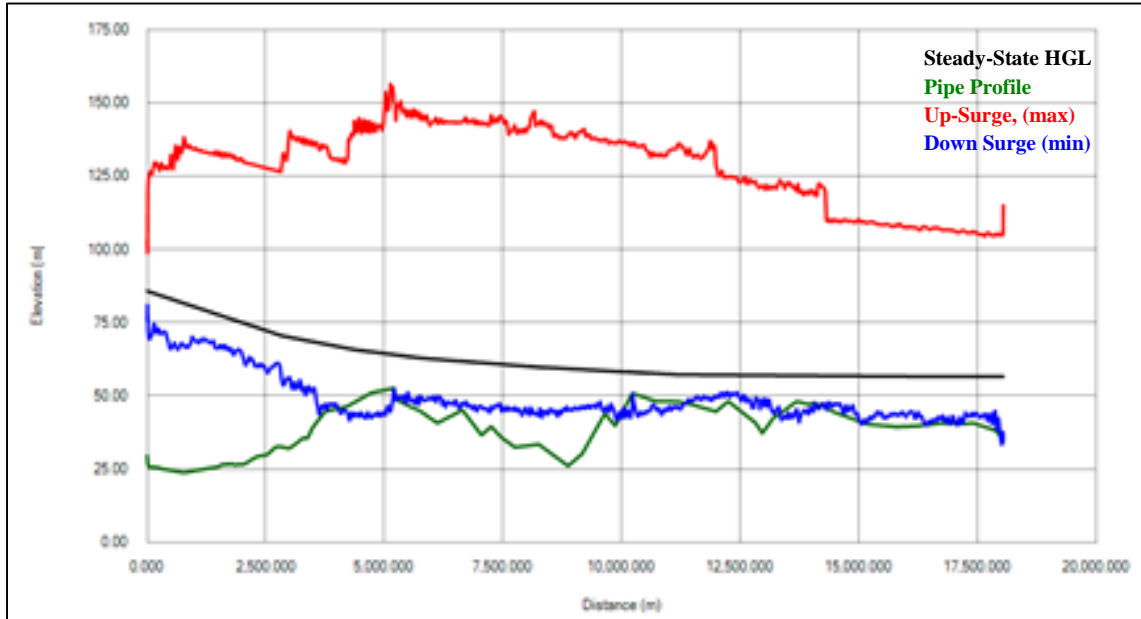


Figure D-5: PRV trial 7 resulted protection

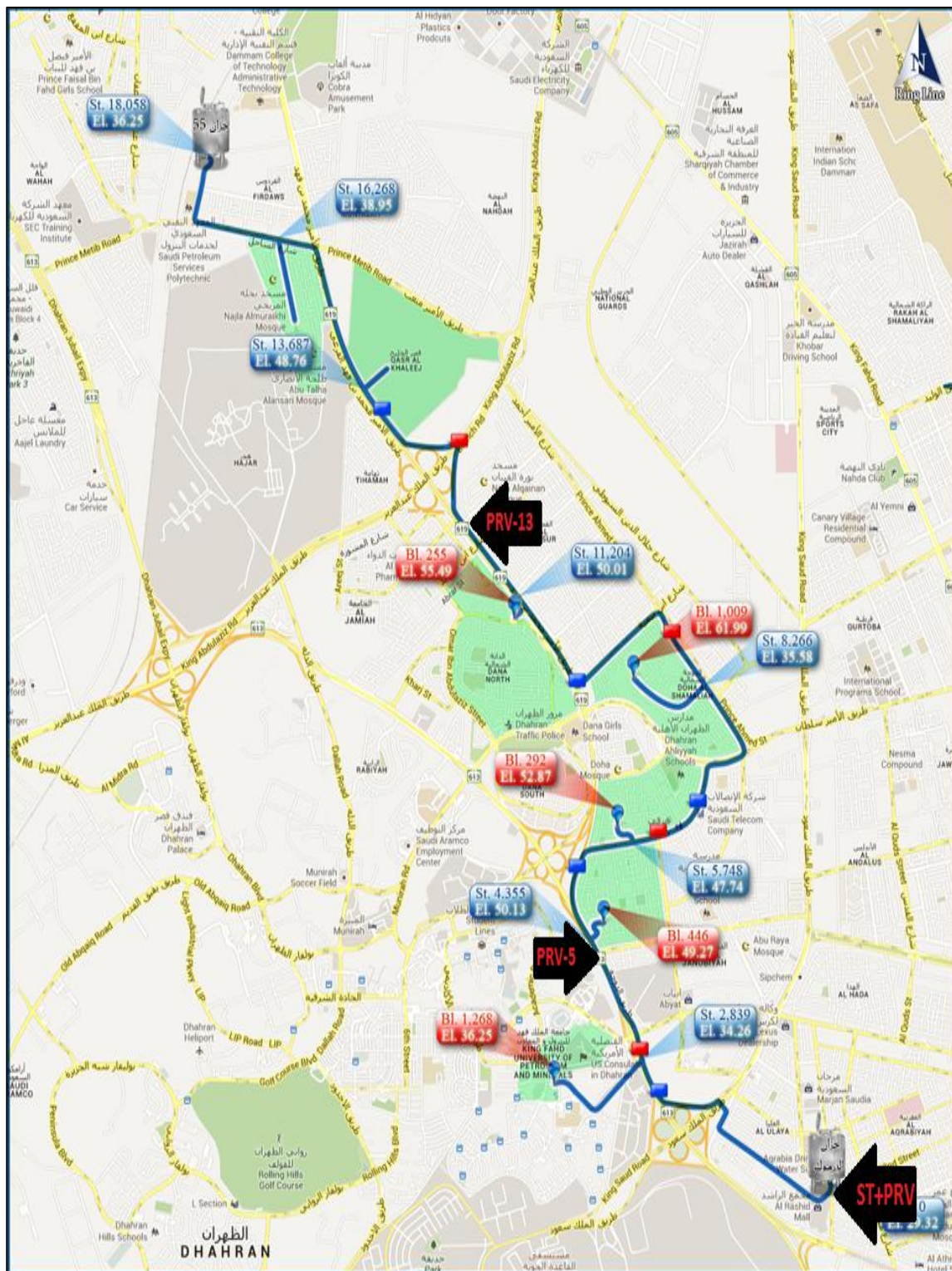


Figure D-6: Final proposed combination of surge protection devices

Vitae

Name	:Hussain Taleb Ammar
Nationality	:Saudi Arabia
Date of Birth	:11/23/1981
Email	:ammar_ht@hotmail.com
Address	:Dammam, Saudi Arabia.
Academic Background	:B.Sc (Civil Engineering), May 2005 King Fahd University of Petroleum and Minerals Saudi Arabia.